ITMO University

Bagmutov Aleksandr Sergeevich

Spectral analysis of systems with interactions on sets of zero measure

Speciality 1.3.3. Theoretical physics

Dissertation is submitted for the degree of Candidate of Physical and Mathematical Sciences

Translation from Russian

Scientific advisor:
Popov Igor Yurievich
Dr. Sci. (Phys.-Math), Prof.,

Saint-Petersburg
2023

Contents

Introduction

In this work, we consider a number of quantum mechanical systems that contain interactions on sets of measure zero. For such systems, we study the dependence of various spectral characteristics on the parameters of the system, in particular, the existence of bound states, their energies, and the position of the continuous spectrum. The study uses both analytical and numerical methods.

The object of the dissertation research are the spectral properties of a number of quantum mechanical systems with singular interactions in two and three dimensions. The subject of research is mathematical models describing the systems.

The purpose of the dissertation research is to conduct a spectral analysis of Laplace operators with singular interactions for a number of systems with different geometries, both two-dimensional and three-dimensional.

To achieve this goal, the following tasks were formulated and solved in the dissertation:

1. Limiting boundary conditions are found for the wave function in a region with a border corrugated by strips, as well as for a region with a semitransparent barrier of corrugated strips. (Hereinafter, corrugated boundaries are refer to boundary perturbation in the form of attachment through small holes of many small Helmholtz resonators.)

2. Numerical confirmation of the results for these systems is obtained and the character of the convergence is found.

3. For two systems of quantum leaky wires with a variation in the intensity of the potential, several analytical theorems about the spectrum, including theorems on the existence of bound states, are obtained.

4. For a system of two conducting layers, the dependence of the system's own energies on its parameters, including the hole shape, is numerically studied. A classification of bound states according to the number and location of constant-sign domains has been created.

Theoretical and practical significance of the work. The physical effects that arise during the transition to the nano-scale are radically different from the phenomena of the macrocosm and are very interesting from the point of view of both fundamental physics and applications of microelectronic devices.

In this paper, a number of analytical statements are proved: for systems with leaky quantum wires (Chapter 2), the existence of bound states and a limitation on their number, and for regions with a corrugated boundary and a barrier, convergence to a specific limiting boundary condition is proved.

The considered systems should be further used in the development of nanosystems as models. We confirm the analytical results with numerical calculations and give the form of the eigenfunctions of the systems, which allows us to build the intuition necessary for further practical activities.

Methods of research. In this paper, we apply both classical and newer methods of the theory of linear operators. For numerical calculations, we use the FreeFEM++ package, as well as the Wolfram Mathematica system.

Relevance. The topic of the work is very relevant, since the systems under consideration are models for physical systems of the conductive type, such as nano-waveguides, conductive layers, etc., as well as a model of interacting DNA molecules. The spectrum of operators that describe the models studied in the work is the most important characteristic of the system, which determines the set of possible states of the system and their energy levels.

The results obtained can be useful in solving various physical problems related to the behavior of charged particles in low-dimensional systems such as nanotubes, nanowires, and also in conducting layers. Another physical system that can be modeled using singular potentials is a system of two interacting linear molecules (such systems are discussed in Chapter 2).

Scientific novelty. The paper considers systems with a new geometry, such as a region with a boundary and a barrier formed by a system of open resonators and non-constant potentials concentrated on lines, for which new results are obtained. For a system of parallel conducting layers, a new classification of eigenstates is proposed, related to the Courant nodal theorem.

Degree of reliability of the results of this work is provided with analytical proof using generally accepted mathematical methods. Many of the proposed

results are verified numerically.

Approbation of the results of the work. The main results of the dissertation research were presented at 7 scientific conferences, of which 4 are international and 3 are Russian:

1. XI Congress of Young Scientists (YSC) (04/04/2022 - 04/06/2022)
2. Analytic and Algebraic Methods in Physics XVIII (09/01/2021 - 09/03/2021)
3. XV International Scientific Conference "Differential Equations and Their Applications in Mathematical Modeling" (07/15/2021 - 07/18/2021)
4. X Congress of Young Scientists (YSC) (04/14/2021 - 04/17/2021)
5. IX Congress of Young Scientists (YSC) (04/15/2020 - 04/18/2020)
6. 17th International Conference of Numerical Analysis and Applied Mathematics. ICNAAM 2019 (09/23/2019 - 09/28/2019)
7. Mathematical Challenge of Quantum Transport in Nanosystems, "Pierre Duclos Workshop" (09/19/2019 - 09/20/2019)

Publications.

On the topic of the dissertation research, 11 papers have been published in journals, of which 8 publications are indexed in the scientometric databases Web of Science and Scopus, 3 publications - in the lists of the Higher Attestation Commission or the RSCI.

Publications included only in the lists of HAC, RSCI:

1. Багмутов А.С., Попов И.Ю. Вольт-амперные характеристики для двух систем квантовых волноводов с присоединенными квантовыми резонаторами // Научно-технический вестник информационных технологий, механики и оптики [Scientific and Technical Journal of Information Technologies, Mechanics and Optics] - 2016. - Т. 16. - № 4(104). - С. 725-730.
2. Bagmutov A.S., Popov I.Y. Bound states for two delta potentials supported on parallel lines on the plane // Physics of Complex Systems - 2022, Vol. 3, No. 1, P. 37-42.

3. Багмутов А.С., Попов И.Ю. Спектр лапласиана в области с границей и барьером, составленными из малых резонаторов // Математическая физика и компьютерное моделирование - 2022. - Т. 25. - № 4. - С. 29-43.

Publications indexed in Web of Science / Scopus scientometric databases:

1. Vorobiev A.M., Bagmutov A.S., Popov A.I. On formal asymptotic expansion of resonance for quantum waveguide with perforated semitransparent barrier // Nanosystems: Physics, Chemistry, Mathematics - 2019, Vol. 10, No. 4, P. 415-419.

2. Bagmutov A.S., Popov I.Y. Window-coupled nanolayers: window shape influence on one-particle and two-particle eigenstates // Nanosystems: Physics, Chemistry, Mathematics - 2020, Vol. 11, No. 6, P. 636-641.

3. Popov I.Y., Bagmutov A.S., Melikhov I.F., Najar H. Numerical analysis of multi-particle states in coupled nano-layers in electric field // AIP Conference Proceedings - 2020, Vol. 2293, P. 360006.

4. Smolkina M.O., Popov I.Y., Bagmutov A.S., Blinova I.V. The electron transmission properties in a non-planar system of two chained rings // Journal of Physics: Conference Series - 2021, Vol. 2086, No. 1, P. 012211.

5. Bagmutov A.S. Bound states for laplacian perturbed by varying potential supportedby line in R3 // Nanosystems: Physics, Chemistry, Mathematics - 2021, Vol. 12, No. 5, P. 549-552.

6. Bagmutov A.S., Najar H., Melikhov I.F., Popov I.Y. On the discrete spectrum of a quantum waveguide with Neumann windows in presence of exterior field // Nanosystems: Physics, Chemistry, Mathematics - 2022, Vol. 13, No. 2, P. 156-164.

7. Trifanova E.S., Bagmutov A.S., Katasonov V.G., Popov I.Yu. Asymptotic Expansions of Resonances for Waveguides Coupled through Converging Windows //Chelyabinsk Physical and Mathematical Journal - 2023. - Vol. 8. - № 1. - P. 72-82.

8. Trifanova E.S., Bagmutov A.S., Popov I.Yu. Resonator with a Corrugated Boundary: Numerical Results // Physics of Particles and Nuclei Letters - 2023, Vol. 20, No. 2, P. 96-99.

Participation in research projects.

This dissertation research was prepared with the support of the following research projects:

1. Grant of Committee for Science and Higher Education of St. Petersburg 2020, project: "Multi-particle problems in quantum waveguides".

2. Grant "Postgraduate students" RFBR 2020 project No. 20-31-90050, "Spectral analysis of systems with interactions concentrated on sets of zero measure".

Statements submitted for defense:

1. For a Hamiltonian with Neumann boundary conditions, a geometric perturbation of the domain boundary by connecting N Helmholtz resonators of fixed length through small holes in the $N \to \infty$ limit leads to an energy-dependent Robin-type boundary condition.

2. Under a geometric perturbation of the Neumann Hamiltonian by means of a barrier of N Helmholtz resonators of a fixed length, connected to the regions to be separated through small holes, in the $N \to \infty$ limit, the boundary condition on the barrier converges to the energy-dependent conditions obtained in this research, which relate boundary values of functions and their normal derivatives.

3. For a two-dimensional quantum system with a delta potential concentrated on two parallel lines and having a constant intensity over the entire length, except for a finite region on each line, there is at least one point of the discrete spectrum below the boundary of the continuous spectrum, which is the solution of the transcendental equations.

4. For a three-dimensional quantum system with constant intensity delta potential concentrated on a straight line and intensity variation on a finite

segment, there is at least one point of the discrete spectrum and the number of points of the discrete spectrum is bounded from above by an integral depending on the parameters of the system.

5. When considering the bound states of a system of two parallel conductive layers in 3D, connected through windows located in a bounded area, functions with a similar number and location of constant-sign domains in the cross section along the window plane undergo a continuous change with a continuous change in the shape of the window, with a stable and predictable for each type changing of energy levels.

The scope and structure of the work. The dissertation consists of an introduction, three chapters and a conclusion, contains 34 figures. The list of references contains 117 titles.

The work is divided into three chapters, each of which considers a separate class of systems with some geometric features. Quantum mechanics is taken as a natural context for the differential equations under consideration, and the operator is interpreted as the Hamiltonian of some quantum system, but most of the results extend to the general case of wave media.

In the first chapter, a certain geometric perturbation of the region boundary is considered in the form of several Helmholtz resonators connected through small holes. Specifically, we are interested in the case when the number of connected resonators tends to infinity, and the area of each of them tends to zero. This type of perturbation is called "corrugated boundary". As a result of such limit, the boundary condition of the problem turns into some (generally energy-dependent) boundary condition resembling a singular delta potential.

For these systems, the main task is to derive the limit problem using the zero-width slits approximation and carry out a numerical analysis corresponding to the results. We also propose the use of the concept of corrugated boundaries in the design of a semitransparent barrier, using the example of a system with a barrier of resonator strips.

In the second chapter, we turn to the consideration of more classical pertur-

bations of systems in the form of delta potentials concentrated on one-dimensional sets in the spaces $\mathbb{R}^2$ and $\mathbb{R}^3$. Such systems are often referred to in sources as leaky quantum wires. Here the task is to prove a number of statements about the spectrum of the operator, in particular, we are interested in the existence and number of bound states of the system.

The last chapter is focused on numerical studies of a family of systems with the following geometry: in three-dimensional space there are two parallel unbounded conducting layers with a common boundary, in which there is a set of holes of some shape. In addition, the case with the application of an external transverse electric field is considered. For such systems, we solve single-particle and many-particle eigenfunction problems. When solving the many-particle problem, the approximation of the many-particle Hartree-Fock wave function is used, in which each particle is represented for other particles as an external field with a delta potential. Using the numerical finite element method, we construct the operator's eigenfunctions and analyze the dependence of the characteristics of bound states on the parameters of the system. Based on the results, a classification of bound states for such systems is proposed, based on the number and mutual arrangement of constant-sign domains of functions.

Chapter 1. Corrugated boundary perturbation

This chapter considers the eigenvalue problem for the Laplace operator with Neumann boundary conditions for some two-dimensional domain, part of whose boundary undergoes an irregular perturbation, as a result of which the Neumann boundary condition on this part of the boundary effectively changes to the energy-dependent Robin condition. The introduction briefly describes the problem to be solved and methods, then the necessary context from the existing results will be presented, followed by our results.

Problems related to the influence of geometric perturbations of the domain boundaries on the spectrum of an operator are widely covered in the literature [6, 7, 11, 12, 13, 14]. Specifically, perturbations with the help of Helmholtz resonators attract interest due to the resonance effects of the cavity, the simplicity of description, the possibility of physical implementation, and the developed methods for studying such systems. The results are obtained using variational methods or direct analysis of the asymptotics [23, 24, 25, 26, 1, 9, 4], as well as the approximate model of zero-width slits [15, 16, 17, 18, 19, 20, 21, 22]. Systems containing an infinitely increasing number of resonators connected to one of the boundaries were considered in the works [8, 27, 9, 10]. The boundaries of the area with such perturbations are called **corrugated** boundaries. The results presented in this paper are published in [3, 5].

There are many practical applications of Helmholtz resonator perturbation theory, such as nanoelectronics using nanometer-scale waveguides, which exhibit quantum effects, or acoustic devices for problems such as noise reduction [30], etc. In particular, surfaces of interest to us, filled with large numbers of resonators that create special boundary conditions, are currently being actively studied in the field of metamaterials [28, 29].

1.1 Resonator with corrugated boundary

1.1.1 Description of the general task

Consider a simply connected domain Ω_0 on the plane $\mathbb{R}^2$, $\partial\Omega$ is the boundary of this domain. Denote a part of the domain boundary $\Gamma \subseteq \partial\Omega_0$ - the perturbation of the boundary will occur on this part. On the domain Ω_0, the Laplace operator with the Neumann boundary conditions is defined:

$$-\Delta_0 u = -\frac{\partial^2 u}{\partial x^2} - \frac{\partial^2 u}{\partial y^2}$$

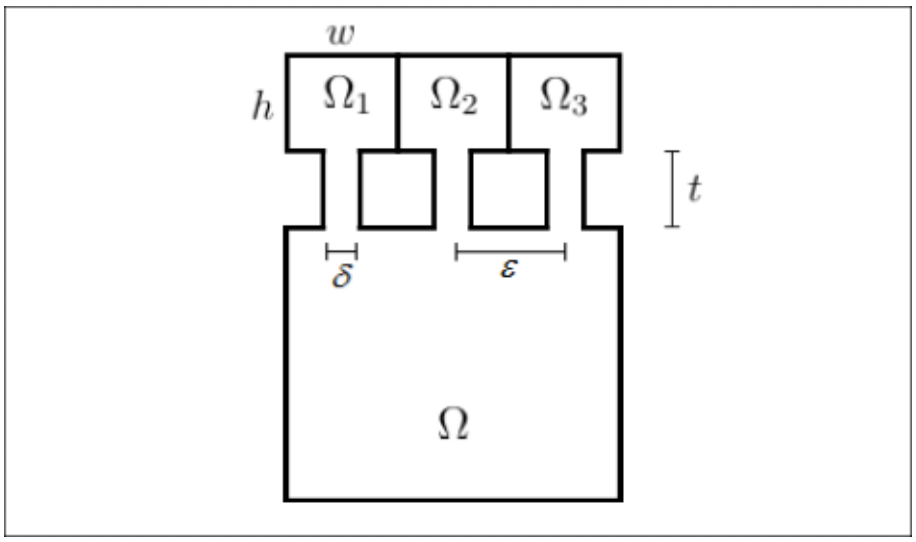

Figure 1 – Example of system geometry with corrugated boundary

The perturbed system is described below, an example of which is shown in Fig.1. Let us introduce a family of domains Ω_ϵ, where a parametrization by a small parameter ϵ is introduced. These regions coincide with the original region everywhere, except for the Γ boundary, where small Helmholtz resonators Ω_i are connected through corridors (holes). The ϵ parameter characterizes the distance between adjacent holes in the Γ boundary leading to the Helmholtz resonators. In the domains Ω_ϵ, Laplace operators with Neumann boundary conditions are defined.

Also, when describing the existing results, we will use the following notation for identical system parameters: w and h denote the width and height of the Helmholtz resonator, in cases where rectangular resonators are considered, δ -

denotes the width of the hole or the width of the tunnel connecting the resonator with the main area, in cases where it is constant throughout the tunnel. The length of the tunnel is denoted by t, the volume (area) of the resonator - $|R|$, the area of the tunnel section or the area (width) of the hole - $|T|$. The eigenvalues with ordinal number n of the operators $-\Delta_\epsilon$ and $-\Delta_0$ are denoted by λ_n^ϵ and λ_n^0 respectively, and their eigenfunctions by $\psi_n^\epsilon(x)$ and $\psi_n^0(x)$ (Here and in what follows, x denotes a variable vector in the considered space $\mathbb{R}^\bullet$). $\frac{\partial}{\partial n}$ is the derivative in the direction of the outward normal to the domain.

Systems of the described type are encountered in a number of works, in different variations, both with a finite and infinite number of resonators, various restrictions on the form and relationships between the system parameters, as well as variations in the operators themselves acting in the region. One of the main goals is to reveal the influence of such perturbations of the boundary on the spectrum of the operator, in particular, on the eigenvalues and eigenfunctions of the original operator.

1.1.2 Results from the variational calculus theory

The effect of boundary perturbations on the spectrum varies greatly, depending on the type of perturbation. For example, in the case of sufficiently regular perturbations, the eigenvalues λ_n^ϵ of the operator Ω_ϵ, at $\epsilon \to 0$, continuously transform into the eigenvalues λ_n^0 of the original operator. This section provides theorems on the influence of boundary perturbations on the continuity of eigenvalues, from the first volume of Methods of Mathematical Physics by Courant and Hilbert [6], chapter VI, §2. The theorems in this chapter refer to the following eigenvalue problem λ:

$$\frac{\partial}{\partial x}\left(p\frac{\partial}{\partial x}u\right) + \frac{\partial}{\partial y}\left(p\frac{\partial}{\partial y}u\right) - qu + \lambda\rho u = 0 \tag{1}$$

Here we introduce a parametric function of the coordinates $\rho(x)$, the mass density, which will be considered below, as well as the parameters $p > 0$, $q \geq 0$, which in further considerations are equal to $p = 1$, $q = 0$. We introduce the following definition:

Definition 1.1.1. *The boundary Γ'_ϵ is deformed into the boundary Γ* ***strongly***

continuously *if the points of the boundary* Γ'_ϵ *are expressed in terms of the points of the boundary* Γ *as follows:*

$$x' = x + g(x, y);$$
$$y' = y + h(x, y);$$

And the functions $g(x, y), h(x, y)$ *are continuous functions of two variables, with a piecewise continuous first derivative and, together with their first derivatives, not exceeding* ϵ *in absolute value:*

$$\begin{aligned} \left|g(x, y)\right| &< \epsilon \\ \left|h(x, y)\right| &< \epsilon \\ \left|g'(x, y)\right| &< \epsilon \\ \left|h'(x, y)\right| &< \epsilon \end{aligned} \tag{2}$$

Below, without proof, we give Theorem 10 from [6].

Theorem 1.1.1. *For any boundary conditions of a mixed type (the Neumann or Dirichlet conditions on all boundaries), the eigenvalue of the problem* (1) *with ordinal number* n*, changes continuously if the domain boundary changes strongly continuously.*

Thus, under continuous deformation of the boundary, a sufficient (but not necessary) condition for the continuous change of the Laplacian eigenvalues with the Neumann boundary conditions, in addition to pointwise convergence, is a continuous change in the normal to the boundary of the domain. The theorem can be refined:

Corollary 1.1.1. *If the region border is deformed with* (2)*, when executing*

$$\left|\frac{\partial g}{\partial x}\right| < \epsilon, \left|\frac{\partial g}{\partial y}\right| < \epsilon,$$
$$\left|\frac{\partial h}{\partial x}\right| < \epsilon, \left|\frac{\partial h}{\partial y}\right| < \epsilon,$$

where ϵ *is an arbitrary small positive number, then there exists a number* η *depending on* ϵ *and approaching* 0 *together with* ϵ *such that for any* n *and any boundary condition of the type*

$$A\frac{\partial u}{\partial n} + Bu = 0,$$

the eigenvalues μ_n, μ'_n with order number n of the unperturbed and deformed regions, respectively, satisfy the relation:

$$\left|\frac{\mu'_n}{\mu_n} - 1\right| < \eta$$

The following is Theorem 11 from [6].

Theorem 1.1.2. *If the problem boundary condition* (1) *is a pure Dirichlet condition*

$$u|_{\partial\Omega} = 0,$$

then under deformation (2) *of the domain boundary, for the continuity of the eigenvalue λ_n with ordinal number n, a sufficient condition is only the continuity of the functions $g(x, y)$ and $h(x, y)$.*

In addition to these theorems, the statement about the mass density is further used - Theorem 7 from [6]:

Theorem 1.1.3. *If in the differential equation* (1)*, the coefficient $\rho(x)$ varies at each point in the same direction (increases everywhere or decreases everywhere), then for any boundary condition, each eigenvalue λ_n of the problem, with ordinal number n, changes in the opposite direction (decreases or increases accordingly).*

If one of the coefficients p, q varies in this equation, then each eigenvalue λ_n of the problem, with ordinal number n, changes in the same direction.

Thus, by increasing the "mass" of the wave function in the region, one can decrease the energy of the system's eigenstates.

1.1.3 Survey of existing results

1.1.3.1 System with one resonator

The case with the perturbation of the boundary by a single rectangular Helmholtz resonator, with a finite length of a rectangular tunnel, occurs in [6] as an example of discontinuity of eigenvalues under a deformation that has weak continuity at $\epsilon \to 0$ (i.e., pointwise convergence) .

Below is a description of the system whose geometry is shown in fig.2. Consider the differential equation ((1), $\rho = 1, p = 1, q = 0$)

$$\Delta u + \lambda \rho u = 0$$

And let Ω be a square with side equal to 1. We attach the resonator R - the second square Ω_ϵ, with side ϵ, oriented parallel to the original one. Tunnel T is a narrow rectangular strip with length ϵ and width δ perpendicular to both rectangles. The region with deformed boundary Ω_ϵ is the union of these three regions: $\Omega_\epsilon = \Omega \cup R \cup T$.

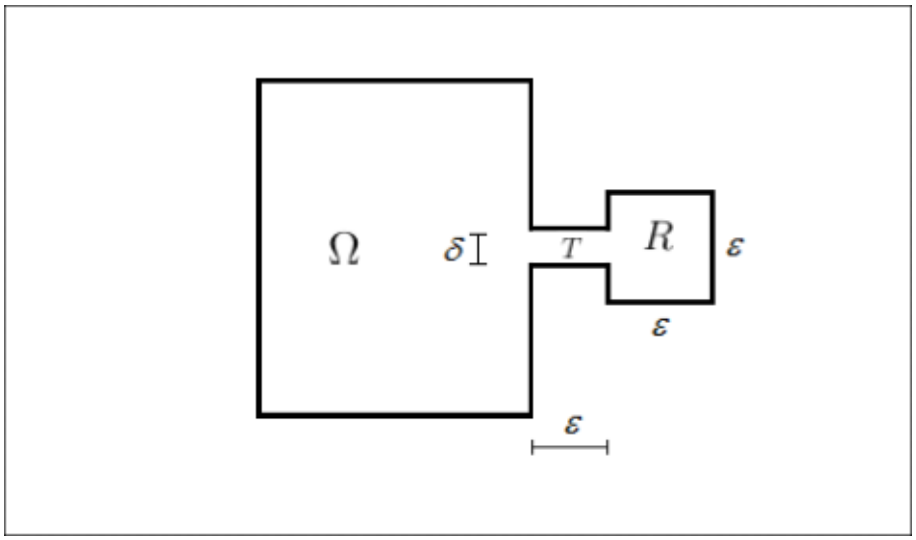

Figure 2 – Geometry of the system with one attached resonator.

Imposing the Neumann boundary condition $\frac{\partial u}{\partial n} = 0$ over the entire boundary, we obtain the first eigenvalue equal to zero, which corresponds to a constant eigenfunction:

$$\lambda_1^\epsilon = 0$$
$$\psi_1^\epsilon = const$$

Further, if the width of the tunnel δ is chosen sufficiently small, then the second eigenvalue can be approached indefinitely to zero. Let us prove this using the following test function: let the function ϕ take two constant values in Ω and R,

and in the tunnel T go linearly between them, preserving continuity:

$$\phi(x) = \begin{cases} c, & x \in \Omega \\ -\frac{1}{\epsilon}(x_0 - x_t^1)/\epsilon + c(x_t^2 - x_0)/\epsilon, & x \in T \\ -\frac{1}{\epsilon}, & x \in R \end{cases} \tag{3}$$

where x_t^1 and x_t^2 are the horizontal coordinates of the beginning and end of the tunnel.

Next, we choose a constant c so that the integral of ϕ over the region Ω_ϵ becomes 0. If ϵ is small enough, then c is arbitrarily close to zero.

The spectral integral $(\Delta_\epsilon \phi, \phi)$ over the domain Ω_ϵ will be of order $\frac{\eta}{\epsilon^3}$. If we choose $\eta = \epsilon^4$, then this integral is arbitrarily small, while the norm ϕ is arbitrarily close to unity. Thus, due to the minimizing property of eigenfunctions, the second eigenvalue of the perturbed operator is arbitrarily small.

As ϵ approaches zero, the second eigenvalue converges to zero if $\frac{\eta}{\epsilon^3} \to 0$. But the second eigenvalue of the original operator is strictly positive. This means that it is not the limit of the second eigenvalue of the perturbed operator, despite the fact that the boundary of the perturbed domain converges pointwise to the boundary of the original one.

1.1.3.2 System with a finite number of resonators

This section presents results from the article by H. Arrieta, D. Hale, C. Hahn, Eigenvalue problems for non-smoothly perturbed domains [7]. This paper considers systems with one attached resonator and extends the results to the case of a finite number of resonators. Resonators and tunnels have a generalized form and the number of dimensions of the considered space is $\mathbb{R}^N, n \geq 2$. In essence, the system parameters used here, when translated into terms of other works, are equivalent to the system proportions from [6], i.e.

$$w \approx h \approx \epsilon$$

$$t \approx \epsilon$$

$$\delta = \epsilon^\eta, \eta > 3$$

The main result is the demonstration of the behavior of eigenvalues and eigenfunctions of perturbed systems in the limit. The authors emphasize the fact that when describing the limiting spectrum, it is not the specific features of the shape of the joined regions that are important, but their relative change in area in the process of decreasing the parameter ϵ.

Let us describe the considered system with one resonator shown in Fig.3. Let Ω_0 be the original region, Ω_1 be the join region that does not intersect with the original region, such that the following conditions are satisfied:

$$\begin{aligned}
&\exists \alpha, \beta > 0 : \\
&\{(x,y) \in \mathbb{R}^2 : |x| < \alpha, |y| < \beta\} \cap \Omega_0 = \{(x,y) : -\alpha < x < 0, |y| < \beta\} \\
&\{(x,y) \in \mathbb{R}^2 : 0 < x < 2\alpha, |y| < \beta\} \cap R_1 = \{(x,y) : \alpha < x < 2\alpha, |y| < \beta\}
\end{aligned} \tag{4}$$

$$\Omega_0 \cap R_1 = \emptyset.$$

Let also

$$T_1 \subset \{(x,y) \in \mathbb{R}^2 : 0 \leq x \leq \alpha, |y| \leq \beta\}$$

- some simply connected set, such that $\Omega_0 \cup T_1 \cup R_1$ is a bounded, simply connected set with a smooth boundary.

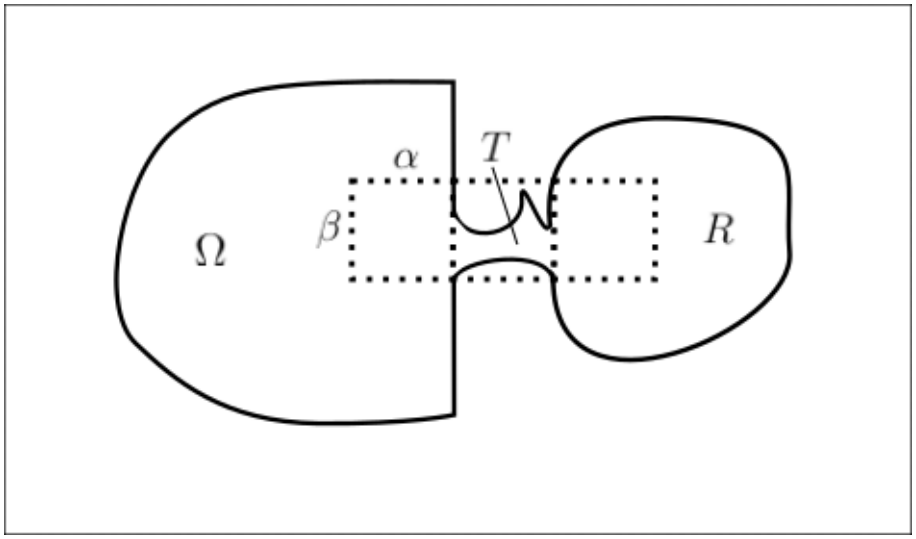

Figure 3 – Geometry of a system with one resonator and an arbitrary shape tunnel.

The above conditions describe regions Ω_0, R_1 large enough to completely

contain the tunnel T_1 reflected with respect to its left and right boundaries. (dotted line on Fig.3)

Next, the dependence of the attached regions on the ϵ parameter is determined. This dependence is determined similarly to other works, and is reduced to multiplication by a scaling factor, which is different for each of the regions T_ϵ and R_ϵ. Specifically, the Resonator scales as ϵR_1 and the tunnel as $\epsilon^\eta T_1, \eta > 0$.

The paper considers various boundary conditions. Here we present the results that are essential for us for the Neumann boundary conditions. It is worth noting that it is precisely when considering the Neumann boundary conditions that restrictions are imposed on the parameter η, in particular, for a two-dimensional space, $\eta > 3$. Let λ_k^ϵ be the k-th eigenvalue for the domain with parameter ϵ, then the eigenvalues of the original operator are λ_k^0.

So, for the case with one attached generalized resonator of the described type in two-dimensional space and Neumann boundary conditions, the following theorem holds for the second eigenvalue and second eigenfunction:

Theorem 1.1.4. *Let $\eta > 3$ then:*

1. $$\lim_{\epsilon \to 0} \lambda_0^\epsilon = 0$$

2. *Convergence of the second eigenfunction in H^1. For $\epsilon \to 0$, it converges as follows:*

$$\psi_2^\epsilon \to 0 \ \ (in\ H^1(\Omega_0)) \tag{5}$$

$$||\psi_2^\epsilon||_{H^2(T)} \to 0, \tag{6}$$

$$||\psi_2^\epsilon||_{L^2(R)} \to 1. \tag{7}$$

3. *Convergence of the second eigenfunction in H^L.*

   If the initial region is arbitrarily smooth: $\Omega_0 \subset C^\infty$, then for any $L \geq 1$, for $\epsilon \to 0$,

   $$\psi_2^\epsilon \to 0,$$

   in the sense of the space $H^L(\Omega_0')$, where Ω_0', this is the original region, with the exception of the circle lying in Ω_0, with the center at the perturbation point.

Thus, the second eigenvalue of the limit problem vanishes, and the second eigenfunction, with a sufficiently smooth boundary of the initial domain, vanishes together with its derivatives everywhere, except for the neighborhood of the perturbation point.

The following theorem concerns the rest of the eigenvalues and functions:

Theorem 1.1.5. *Let $\eta > 3$ and $m \geq 3$, then:*

1. $$\lim_{\epsilon \to 0} \lambda_m^\epsilon = \lambda_{m-1}^0$$

2. *For any positive sequence $\{\epsilon_k\}_{k=1}^\infty$ that converges to zero, there exists a subsequence $\{\delta_k\}_{k=1}^\infty$ and a complete system orthogonal eigenfunctions $\{\psi_m^0\}_{m=1}^\infty$, of the original problem, such that for $k \to \infty$, the following holds:*

$$\psi_m^{\delta_k} \to \psi_{m-1}^0 \ \ (in\ H^1(\Omega_0))$$
$$||\psi_2^{\delta_k}||_{H^1(T \cup R)} \to 0,$$

3. *If the initial domain is arbitrarily smooth: $\Omega_0 \subset C^\infty$, then for any $l \geq 1$, for $k \to \infty$,*

$$\psi_m^{\delta_k} \to \psi_{m-1}^0,$$

in the sense of the space $H^l(\Omega_0')$, where Ω_0', this is the original region, with the exception of the circle lying in Ω_0, with the center at the perturbation point.

Now, the result is extended to the case of a finite number of connected resonators $r \geq 1$. Here, in contrast to what follows, each resonator decreases without changing the perturbation point on the boundary of the original region. For the Neumann boundary conditions, we obtain the following statements:

Proposition 1.1.1.

$$\lim_{\epsilon \to 0} \lambda_m^\epsilon = 0, \qquad 2 \leq m \leq r+1$$
$$\lim_{\epsilon \to 0} \lambda_m^\epsilon = \lambda_{m-r}^0, \qquad m \geq r+2$$

That is, each new resonator adds another zero eigenvalue. The eigenfunctions of the limit problem behave in the same way, namely, similarly to the above theorems 1.1.4, 1.1.5, the eigenfunctions corresponding to these eigenvalues also converge to zero together with their derivatives , with sufficient smoothness of Ω_0.

1.1.3.3 System with an infinite number of resonators

In this section, we move on to a sequence of systems with an indefinitely increasing number of attached resonators, which is the goal of our study. In such systems, some subset of Γ is selected on the boundary of the initial region, which will be filled with periodically located resonators. The dimensions of the resonators and tunnels tend to zero along with the ϵ parameter. The small parameter ϵ itself is chosen as the period. As a result of this process, a certain limiting set of values (which may include infinity) is obtained, to which the eigenvalues of the perturbed problems converge. In some cases, this set may coincide with the discrete spectrum of some differential operator, in which case we will call this operator the limit operator.

Such systems were first analyzed in the book by E. Sanchez-Palencia, Inhomogeneous Media and the Theory of Vibrations [8], in chapter XII, §4. This work describes the systems depicted in Fig.1, with the Neumann boundary conditions. Here, the attached resonators are squares with side ϵ, the tunnels are ϵ long and $\delta = \epsilon^4$ wide, as in the previous two papers.

The main results are the following two statements:

Proposition 1.1.2. *The second eigenvalue of the perturbed problem tends to zero as $\epsilon \to 0$, while the second eigenvalue of the original problem is strictly greater than zero.*

$$\lambda_2^0 > 0$$
$$\lambda_2^\epsilon \searrow 0; \epsilon \to 0$$

Proposition 1.1.3. *Each eigenvalue of the original problem is a limit point for some sequence of eigenvalues of perturbed problems, i.e.*

$$\lambda^0 \in \sigma(\Omega_0) \Rightarrow \exists \{\delta_i\}_{i=1}^\infty, \{j_i\}_{i=1}^\infty : \lambda_{j_i}^{\delta_i} \xrightarrow[i\to\infty]{} \lambda^0$$

We will observe the same property of the eigenvalues of the original problem in the case of the system with missing tunnels that we consider.

A recently published article by D. Cardone and A. Khrabustovsky continues the study of strongly corrugated boundaries and considers the problem in detail, generalizing the shapes of resonators, tunnels and the form of the dependence of system parameters on a small parameter, as well as the number of space dimensions: $\mathbb{R}^n,\ n \leq 2$. Here we present only the results for $\mathbb{R}^2$, which are necessary for the present work, but it is worth noting that the results for higher dimensions differ slightly from them.

Let's describe the system shown in Fig.4. As before, Ω is a bounded region in $\mathbb{R}^2$, the part of the boundary of this region that undergoes deformation is denoted by $\Gamma \subseteq \Omega$. Further, $\epsilon > 0$ is a small parameter, and w, δ, t are positive numbers tending to zero as $\epsilon \to 0$, with the following restrictions:

$$\begin{aligned} w &\xrightarrow[\epsilon\to 0]{} 0 \\ \delta &\xrightarrow[\epsilon\to 0]{} 0 \\ t &\xrightarrow[\epsilon\to 0]{} 0 \\ \delta \leq w &\leq \epsilon \end{aligned} \tag{8}$$

which guarantee that the resonators do not intersect geometrically, as well as the restriction on the rate of decrease in the width of the tunnels with decreasing $\epsilon \to 0$:

$$\delta \gg \exp\left(-\frac{a}{\epsilon}\right);\ \ \forall a > 0$$

A set of tunnels with resonators are attached to the Γ boundary, periodically, with a period of ϵ. Each attached area consists of two parts:

- Resonator wB, where B is a fixed region in $\mathbb{R}^2$, then $|B|$ denotes its area,
- Tunnel $\delta * t$, rectangle with sides δ, t.

The total number of connected resonators tends to infinity and is equal to

$$N(\epsilon) = \frac{|\Gamma|}{\epsilon}$$

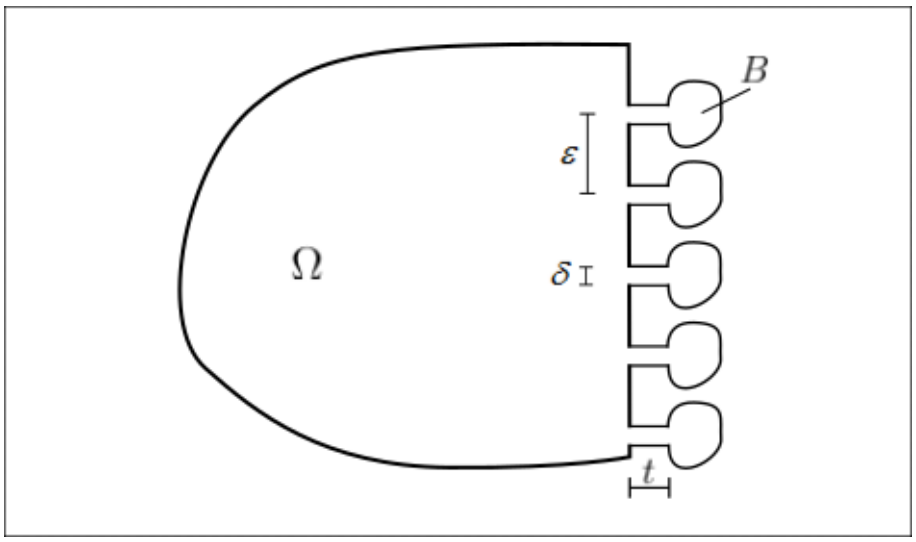

Figure 4 – Geometry of a system with many identical attached arbitrary-shaped resonators.

Also, the parameters must satisfy a number of natural conditions that ensure the geometric isolation of the resonators, such as the boundedness of the B region by a cube with a side equal to one.

The resulting union constitutes the perturbed region Ω_ϵ. In this area, the operator is introduced

$$A^\epsilon = -\frac{1}{\rho}\Delta_\epsilon.$$

This operator, in addition to the Laplace operator, additionally includes the factor ρ, the value of which depends on the coordinates, and which corresponds to the density of the mass of vibrations in a particular area.

Next, two important limiting parameters are introduced that completely characterize the behavior of the spectrum as ϵ decreases:

$$r := \lim_{\epsilon \to 0} \frac{\rho w^2 |B|}{\epsilon} \tag{9}$$

$$q := \lim_{\epsilon \to 0} \frac{\delta}{t \rho w^2 |B|} \tag{10}$$

The following constraints are assumed: $r \in [0, \infty)$ and $q \in [0, \infty]$.

The aim of this paper is to study the behavior of the spectrum of a perturbed operator as $\epsilon \to 0$ passes to the limit. Depending on the parameters of the system, the perturbed operator converges to various eigenvalue problems, including, for some values of the parameters, to the original one. It turns out that the form of the limit problem depends only on two independent factors: whether the limit q

is finite and whether the limit r is equal to zero. The four possible combinations lead to the following four limiting problems:

1. $q < \infty,\ r > 0$. The limit spectrum is the union of the point q and the spectrum of the following problem:

$$\begin{cases} -\Delta u = \lambda u, & x \in \Omega \\ \frac{\partial u}{\partial n} = \frac{\lambda q r}{q-\lambda} u, & x \in \Gamma \\ \frac{\partial u}{\partial n} = 0, & x \in \partial\Omega \setminus \Gamma \end{cases} \tag{11}$$

   The eigenvalues of this problem form two increasing sequences, one of which is unbounded and the other converges to the value q.

2. $q < \infty,\ r = 0$. In this case, the limit spectrum is the union of the point q and the spectrum of the original problem for the operator $-\Delta_0$.

3. $q = \infty,\ r > 0$. Here, the spectrum of the following problem is the limiting one:

$$\begin{cases} -\Delta u = \lambda u, & x \in \Omega \\ \frac{\partial u}{\partial n} = \lambda r u, & x \in \Gamma \\ \frac{\partial u}{\partial n} = 0, & x \in \partial\Omega \setminus \Gamma \end{cases} \tag{12}$$

4. $q = \infty,\ r = 0$. In the latter case, the spectrum converges to the spectrum of the original problem.

The following is an example of the values of the system parameters, with the help of which all values of the limits q, r can be reached.

$$\begin{aligned} \delta &= \epsilon^{\alpha} (\alpha \geq 0), \\ w &= t = \epsilon, \\ \rho &= \epsilon^{\beta} (\beta \geq -1) \end{aligned} \tag{13}$$

Using these values and changing α, β we get all the necessary combinations:

$$\begin{cases} r > 0; & \beta = -1, \\ r = 0; & \beta > -1. \end{cases}$$

$$\begin{cases} q > 0, & \alpha = \beta + 3, \\ q = 0, & \alpha > \beta + 3, \\ q = \infty, & \alpha < \beta + 3. \end{cases}$$

In conclusion, it is important to note that the formulation of the problem in this work does not provide for an independent change in the width and height of the resonators, since their form is specified using the form B and the scaling factor w. In what follows, we will consider systems with long resonators at the boundary (with a fixed length of resonators), which are not described in this way.

1.1.4 Zero-width slit model: Theoretical Part

This section discusses the application of the approximate Zero-width slit model to the study of Helmholtz resonators. This method is used in a number of papers to construct exact solutions to a simplified problem. In the work of the author [2], this method was used when considering a resonator attached to the waveguide from the side and in the middle. The results include the construction of current-voltage characteristics for these systems.

In this paper, we apply it to Ω_ϵ systems, construct exact eigenfunctions, and obtain limit functions that correspond to some "limit problem". The following is a brief description of the method.

Zero-width slit model, this is a common method used when there is a hole in the boundary of an area that is small in diameter relative to the wavelength. The method makes it possible to significantly simplify the geometry of the system, which in many cases leads to the possibility of expressing model solutions in an explicit form. The method is to pass to a system with a geometry in which end holes are replaced by pin holes, and then, the theory of self-adjoint extensions of symmetric operators is used to construct a parameterized operator describing the new system, and the parameter controls the throughput of pin holes and can be

chosen so that in order to most closely match the situation with the final diameter of the holes.

The following notation is used below:

- $D(A)$ - domain of definition of operator A,
- $R(A)$ - set of values of operator A,
- $Ker(A)$ - kernel ($\{u : Au = 0\}$) of operator A,
- $def(A, k)$ is the set of defective elements of the operator A corresponding to a point of regular type k.

Let us briefly describe the process of constructing a model operator using the example of a system with one small hole connecting 2 regions. Let us consider two simply connected domains Ω_1, Ω_2 connected through a small hole of diameter δ in their common boundary. We pass to the geometry in which the hole is replaced by a point x_0 in its center. Now each of the areas can be considered separately. We denote by Ω their totality. We start with the self-adjoint operator H_0 acting as the Laplace operator on functions from $L^2(\Omega)$ whose normal derivative vanishes on the boundary:

$$H_0\psi(x) = -\Delta\psi(x), \qquad \frac{\partial\psi}{\partial n}|_{\partial\Omega} = 0;\ \psi \in L^2(\Omega)$$

Now we restrict the original operator to the set of functions that vanish at the hole point x_0 and construct its closure. The resulting operator will be denoted by H'. This operator is not self-adjoint, but only symmetric. Its defective elements (i.e. the functions $f \in R(H' - k^2)^\perp$ orthogonal to the set of values of the operator $H' - k^2$) can be found using the expression from the classical operator theory

$$Ker(A^*)^\perp = R(A),$$

we obtain an expression for the set of defective elements H':

$$def(H', k) = Ker(H'^* - k^2) = Ker(\Delta + k^2).$$

The desired elements are Green's functions, with a singularity at the hole point, and their number is equal to the number of non-intersecting domains in the prob-

lem:

$$\{f_{def}\} = \begin{pmatrix} G_1(x, x_0, k) \\ 0 \end{pmatrix}, \begin{pmatrix} 0 \\ G_2(x, x_0, k) \end{pmatrix},$$

where $G_i(x, x_0, k)$ is the Neumann Laplacian Green's function in the domain Ω_i. The Green's functions give equal defect numbers $(2, 2)$, and hence the operator H' can be extended to a self-adjoint one.

Note that the set of points of regular type for the considered operator includes the negative semiaxis of real numbers. This fact allows us to apply the Neumann theorem of the theory of Linear operators [32], to express elements from the domain of definition of the adjoint operator H'^*, through elements from the domain of its Friedrichs extension, Δ^F, and its defective elements corresponding to a point of regular type on the real axis:

$$D(H'^*) = D(\Delta^F) \oplus def(H', k_0), \quad k_0^2 < 0.$$

Thus, in each of the isolated regions, the function from the domain of definition of the adjoint operator H'^* has the following form:

$$\psi(x) = a_i G_i(x, x_0, k_0^2) + b_i + o(|x - x_0|), \quad x \in \Omega_i$$

Further, to construct a self-adjoint extension of the symmetric operator H', it is necessary to restrict the domain of definition of its adjoint H'^* so that the following holds:

$$J(u, v) = (Hu, v) - (u, Hv) = 0, \quad u, v \in D(H). \tag{14}$$

Taking into account the well-known asymptotic expression for the Laplacian Green's function near the singularity,

$$G_i(x, x_0, k) = \frac{1}{\pi} \ln \frac{1}{|x - x_0|} + \beta_i + o(|x - x_0|),$$

from (14), we get the integral over the boundary of the region, excluding the hole point:

$$J(u, v) = \lim_{r \to 0} \sum_{i=0}^{2} \int_{\Omega_i \setminus B^r} (-\Delta u \overline{v} + u \overline{\Delta v}) dV,$$

where B^r is a circle of radius r centered at the point of the hole, $B^r = \{x : \left|x - x^0\right| < r\}$.

We apply Green's formula,

$$J(u,v) = \sum_j \int\limits_{\partial B_j^\delta} \left(-\frac{\partial u}{\partial n}\bar{v} + u\frac{\partial \bar{v}}{\partial n} \right) dS,$$

whence, using the asymptotic expression of the Green's functions, we obtain:

$$(H'^* u, v) - (u, H'^* v) = \sum_i a_i^u \overline{C_i^v} - \overline{a_i^v} C_i^u + a_i^u \overline{C_i^v} - \overline{a_i^v} C_i^u,$$

where $C_i = \left[u(x) - \frac{a_i}{\pi} ln|x - x_0|\right]_{x \to x_0}$ is the function value at the hole point minus the singularity , and the "size" of this feature determines the throughput of the hole.

This equation has several solutions. Of these, we choose the one that best corresponds to the physical meaning, namely, we keep the flow through the hole, equating the values of the function without singularity on both sides of the hole. We obtain an expression for functions from the domain of the desired self-adjoint operator that describes the system:

Proposition 1.1.4. *A Zero-width slit model system with the geometry described above is represented by the following statement:*

$$Hu = -\Delta u,$$

$$\begin{aligned} &\forall u \in D(H): \\ &\quad u(x) = \hat{u}_i(x) + a_i G_i(x, x_0, k_0^2), \quad x \in \Omega_i \\ &\quad a_1 = -a_2, \\ &\quad \hat{u}_1(x_0) = \hat{u}_2(x_0), \end{aligned} \tag{15}$$

In conclusion, we note that the constructed operator is parametrized by a real number $k_0^2 < 0$. This parameter determines the throughput of the hole, which is mathematically expressed as the size of the feature that we cut at the point of

the hole using the condition $a_1 = -a_2$. As shown by [16], this parameter most closely matches the final diameter of a real hole δ if it is chosen equal to

$$k_0 = \frac{2i}{\delta} \exp -\gamma, \tag{16}$$

where the Euler constant $\gamma = 0.577$ is involved.

1.1.5 Zero-width slit model: Corrugated Border

This section presents the results for systems with an infinitely increasing number of resonators, obtained using the method, in the work of I.Yu.Popov, I.V.Blinova, A.I.Popov, Model of a boundary consisting of Helmholtz resonators [10]. This work continues the study of such systems without tunnels, using the zero-width slit method.

In this paper, we consider a two-dimensional system shown in Fig.5, in which a square with a side of length 1 is taken as the main region Ω_0, along all the boundaries of which, through small holes, small square-shaped resonators are connected , with side ϵ, with period ϵ. There are no tunnels.

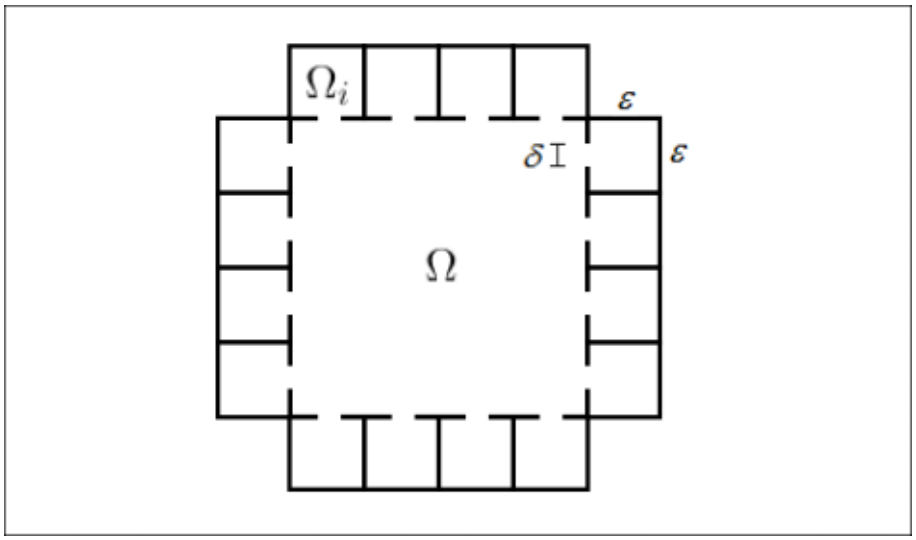

Figure 5 – Example of system geometry with corrugated boundary

The zero-width slit model is applied to this system. The number of connected resonators is $4N$, $N = \lfloor \frac{1}{\epsilon} \rfloor$. Hence the defect indices of the bounded operator H' are equal to $(8N + 2, 8N + 2)$. Further construction is similar to the previous section. As a result, we obtain the following expression for functions from

the domain of the main operator (here and below, i goes over all $4N$ resonator numbers):

$$\begin{pmatrix} u \\ u_1 \\ \vdots \\ u_n \end{pmatrix} = \begin{pmatrix} \tilde{u} \\ \tilde{u}_1 \\ \vdots \\ \tilde{u}_n \end{pmatrix} + \begin{pmatrix} \sum_{i=0}^{n} a_i^{ex} G(x, x_i, k_0) \\ a_1^{in} G_i(x, x_1, k_0) \\ \vdots \\ a_n^{in} G_i(x, x_n, k_0) \end{pmatrix} \tag{17}$$

Now let us construct explicitly the eigenfunctions for the model operators H_ϵ. Given the domain of the operator, the general form for a function from the domain of the model operator corresponding to the eigenvalue k^2 is:

$$u_n(x) = \begin{cases} \sum_{j=1}^{n} \alpha_j^{ex} G(x, x_j, k) & x \in \Omega \\ \alpha_i^{in} G_i(x, x_i, k) & x \in \Omega_i \end{cases}$$

In order to apply restrictions on the coefficients from (15), for each hole point, it is necessary to highlight the features:

$$u_n(x) = \tag{18}$$
$$\begin{cases} \alpha_l^{ex} G(x, x_i, k_0) + \alpha_l^{ex} g(x, x_i, k, k_0) + \sum_{j \neq l}^{n} \alpha_j^{ex} G(x, x_j, k) & x \in \Omega \\ \alpha_l^{in} G_l(x, x_l, k_0) + \alpha_l^{in} g_l(x, x_l, k, k_0) & x \in \Omega_l \\ \alpha_j^{in} G_j(x, x_j, k) & x \in \Omega_{j \neq l} \end{cases}$$

Here and below, g denotes the Green's function, with the singularity removed:

$$g_\bullet(x, z, k, k_0) = G_\bullet(x, z, k) - G_\bullet(x, z, k_0)$$

Applying (15) constraints to the general form of the native function, we get:

$$\alpha_i := \alpha_i^{ex} = -\alpha_i^{in}$$

$$\alpha_i g_i(k, k_0) + \sum_{j \neq i}^{N} \alpha_j G(x_i, x_j, k) = -\alpha_i \hat{g}(k, k_0) \tag{19}$$

The second expression combines all restrictions and is a system of $4N$ equations. This system, in the $N \to \infty$ limit, transforms into an integral equation equivalent to some eigenvalue problem with an energy-dependent Robin-type boundary condition. Conditions of this type are discussed, for example, in [33]. The derivation

of the integral equation will be given in more detail in the results section of this paper. We assume that the hole size δ correlates with the parameter ϵ so that for some function $r(x)$, the following is true:

$$(g_i^{in}(x, x_i, k, k_0) + g^{ex}(x, x_i, k, k_0)) = \frac{1}{r(x_i)k^2\epsilon} \tag{20}$$

In conclusion, we present the main theorem [10]:

Theorem 1.1.6. *For the sequence of operators H_ϵ described above, as $N \to \infty$, the eigenfunctions converge to the functions defined by the following integral equation,*

$$u(x) = -\int_\Gamma u(x_i)G^{ex}(x, x_i, k)[(g_i^{in}(x, x_i, k, k_0) + g^{ex}(x, x_i, k, k_0))dx]^{-1}dx,$$

which, given (20)*, is equivalent to the following problem:*

$$\begin{cases} \Delta u + k^2 u = 0 \\ \frac{\partial u}{\partial n}|_{\partial\Omega} = k^2 r u|_{\partial\Omega} \end{cases}$$

1.1.6 Border of strips

We now turn to the main results of this chapter. The first of the systems we consider, shown in Fig.6, is a square region with side 1 as the initial region Ω_0, the left boundary of the region is perturbed, i.e. $\partial\Omega_0 \supset \Gamma = \{(x_1, x_2) : x_1 = 0, x_2 \in [0, 1]\}$. We do not use the mass density, i.e. $\rho(x) = 1$. The main operator is the Laplacian with the Neumann boundary conditions H_0. The perturbation occurs by Helmholtz resonators Ω_i connected to the left boundary through small holes x_i, without tunnels (Here and below, the counter i runs through all N resonator numbers). The parameter ϵ, as before, corresponds to the period, in this case, to the distance between adjacent holes. Their number N increases indefinitely, while their sizes change as $w = const, h = \epsilon$, and the hole size decreases as $\delta = \epsilon^m$, where different values of $m > 1$ - will be be considered later. Laplace operators with Neumann boundary conditions on domains with N resonators will be denoted by H^N or H_ϵ, and the limit operator by H^{lim}.

To study the system, we move on to the zero-width slit model, similar to [10]. Our goal is to study the limit $\epsilon \to 0$ ($N \to \infty$) by considering the limit problem

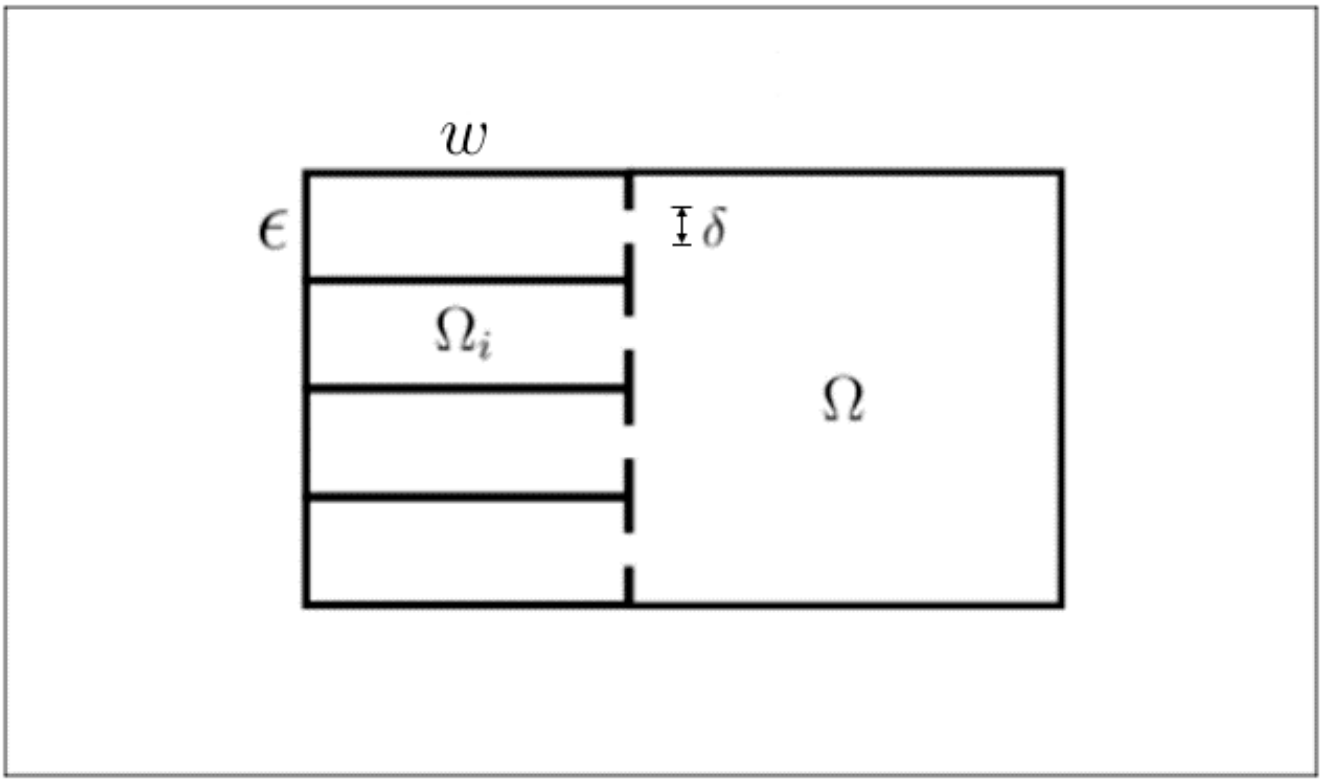

Figure 6 – Example of system geometry with corrugated boundary

whose eigenfunctions converge to the eigenfunctions of perturbed systems. As a result, we obtain the limit problem for the eigenvalues of the differential operator in the domain Ω_0, with the Neumann boundary condition on the unperturbed boundaries and the energy-dependent Robin condition on Γ, expressed explicitly.

We also use numerical methods to construct the eigenfunctions of real systems (with a finite hole diameter), confirming the analytical conclusions and demonstrating the rate of convergence to the eigenfunctions of the limit problem as the number N of resonators increases.

We also introduce the following notation: $G(x, x_i, k), G_i(x, x_i, k)$ - Green's functions with the Neumann conditions in the rectangle, for the domains Ω_0 and Ω_i, respectively, with a singularity at the point holes x_i, as well as $g(x_i, k, k_0), g_i(x_i, k, k_0$ - Green's functions at the points of the holes, with removed singularities, in the same areas.

$$g_\bullet(x_i, k, k_0) = \left[G_\bullet(x, x_i, k) - G_\bullet(x, x_i, k_0)\right]_{x \to x_i}$$

The conditions inside the resonators are the same, so $g_i(x_i, k, k_0)$ actually depends only on the last two parameters and will be written as $\hat{g}(k, k_0)$.

Here is the main analytical result of the section:

Theorem 1.1.7. *Let $\psi_n^N(x), n = 1, 2...$ be the eigenfunctions of the perturbed model operator H^N from the family described above.*

1. *The functions $\psi_n^N(x)$ have the following form:*

$$\psi_n^N(x) = \begin{cases} \sum_{j=1}^N \alpha_j G(x, x_j, k) & x \in \Omega \\ -\alpha_i G_i(x, x_i, k) & x \in \Omega_i \end{cases} \tag{21}$$

where the coefficients satisfy the following system of N conditions:

$$\alpha_i g(x_i, k, k_0) + \sum_{j \neq i}^{N} \alpha_j G(x_i, x_j, k) = -\alpha_i \hat{g}(k, k_0), \qquad i = 1, 2, ...N \tag{22}$$

2. *In the $N \to \infty$ limit, the functions $\psi_n^N(x)$ converge to solutions of the following integral equation:*

$$\begin{aligned} \psi(x) = -\int_\Gamma \psi(y) G(x, y, k) [\hat{g}(k, k_0) dy]^{-1} dy = \\ = -\int_\Gamma \psi(y) G(x, y, k) k \tan[kw] dy, \end{aligned} \tag{23}$$

which corresponds to the following eigenvalue problem for a differential operator:

$$\begin{cases} \Delta u + k^2 u = 0 \\ \frac{\partial u}{\partial n}|_\Gamma = -k \tan(kw) u|_\Gamma \\ \frac{\partial u}{\partial n}|_{\partial\Omega_0 \setminus \Gamma} = 0 \end{cases} \tag{24}$$

The rest of the section is devoted to the proof of the theorem.

First, we describe the zero-width slit model operator (the procedure is described in more detail in sec.1.1.4).

Let us construct for some fixed N (the result extends to all N). Let H' be the closure of the Neumann Laplacian acting in the domain Ω^N to functions that vanish at the points of the holes. According to the Neumann theorem, the domain of the operator H'^* can be represented as:

$$D(A^*) = D(-\Delta^F) \oplus def(H', k_0)$$

And the defective elements are $2N$ elements of the form

$$f_{def} = \begin{pmatrix} G^{\bullet}(x, x_i, k) \\ 0 \\ \vdots \end{pmatrix}$$

where the Green's function acts in one of the regions, with respect to one of the hole points associated with it, and in all other regions the defective element is equal to zero.

We also denote the functions from the domain of the Friedrichs extension of the Neumann Laplacian ($D(-\Delta')$) by $\tilde{u}_{\bullet}$ (the functions act in the region $\Omega_{\bullet}$).

Thus, functions from the domain of the operator H'^{*} have the following general form:

$$\begin{pmatrix} u \\ u_1 \\ \vdots \\ u_n \end{pmatrix} = \begin{pmatrix} \tilde{u} \\ \tilde{u}_1 \\ \vdots \\ \tilde{u}_n \end{pmatrix} + \begin{pmatrix} \sum_{i=0}^{n} a_i^{ex} G(x, x_i, k_0) \\ a_1^{in} G_i(x, x_1, k_0) \\ \vdots \\ a_n^{in} G_i(x, x_n, k_0) \end{pmatrix} \tag{25}$$

The extension parameter k_0 is chosen according to (16) equal to $k_0 = \frac{2i}{\delta} \exp -\gamma$, where $\gamma = 0.577$.

Now, to obtain a self-adjoint operator $\hat{H}$ describing the model system, we restrict $D(H')$ so that the boundary form vanishes

$$J(u, v) = (H'^{*}u, v) - (u, H'^{*}v), \quad u, v \in D(H'^{*}).$$

These functions have singularities at the hole points, so we use the limit transition:

$$J(u, v) = \sum_j \int\limits_{\partial B_j^{\delta}} \left(-\frac{\partial u}{\partial n} \bar{v} + u \frac{\partial v}{\partial n} \right) dS,$$

where B_j^r is the circle with radius r around hole x_j: $B_j^r = \{x : \left|x - x^j\right| < r\}$.

Using Green's formula, (25), and the Neumann boundary conditions, we get:

$$J(u, v) = \sum_j \int\limits_{\partial B_j^{\delta}} \left(-\frac{\partial u}{\partial n} \bar{v} + u \frac{\partial v}{\partial n} \right) dS,$$

We use the well-known expression for the Green's function of the Neumann Laplacian near the singularity

$$G(x, x_j, k) = \frac{1}{\pi} ln\left|x - x_j\right| + \mathcal{O}\left(\left|x - x_j\right|\right),$$

we obtain an expression for the boundary form:

$$(H'^{*}u, v) - (u, H'^{*}v) = \sum_i a_i^{u,in}\overline{C_i^{v,in}} - \overline{a_i^{v,in}}C_i^{u,in} + a_i^{u,ex}\overline{C_i^{v,ex}} - \overline{a_i^{v,ex}}C_i^{u,ex}$$

Here $C_i^{u,in/ex} = \tilde{u}^{in/ex}(x_i)$.

We choose an extension that corresponds to the physical meaning, i.e. maintains flow through the hole:

$$a_i := -a_i^{in} = a_i^{ex}, \tag{26}$$

$$C_i^{in} = C_i^{ex}, \quad i = 1, 2, ...N \tag{27}$$

It is worth noting that the first expression can be interpreted as mutual compensation by features on different sides of the hole.

We write the conditions in the form of a system of N equations:

$$\sum_{j \neq i} a_j G(x_i, x_j, k) + a_i g(x_i, k, k_0) = -a_i \hat{g}(k, k_0), \qquad ; i = 1, 2, ...N \tag{28}$$

The first part of the theorem is proved.

Consider the limit of the constructed functions as $N \to \infty$. In particular, we derive a limit expression for the system of conditions on the coefficients (28). To this end, let us consider the limits of the Green's functions inside the resonators. Let us write the well-known expression for the Green's functions of the Helmholtz equation in a rectangle of dimensions w on h, with the Neumann boundary conditions:

$$G(x, z, k) = \sum_{i=0}^{\infty}\sum_{j=0}^{\infty} \frac{c_{i,j}}{wh} \frac{\cos\frac{\pi i x_1}{w}\cos\frac{\pi j x_2}{h}\cos\frac{\pi i z_1}{w}\cos\frac{\pi j z_2}{h}}{k^2 - (\frac{i^2\pi^2}{w^2} + \frac{j^2\pi^2}{h^2})} \tag{29}$$

$$c_{i,j} = 2^{2-\delta_i-\delta_j}, \delta_i = \begin{cases} 0, & i \neq 0 \\ 1, & i = 0 \end{cases} \text{ - Kronecker delta function}$$

Setting $h = \epsilon$ and passing to the limit $\epsilon \to \infty$, we obtain the coefficients for the limiting conditions $\left(\lambda_{i,j}^{\epsilon} = \frac{i^2\pi^2}{w^2} + \frac{j^2\pi^2}{\epsilon^2}\right)$:

$$\hat{g}_{\epsilon}(k, k_0) = \frac{1}{\epsilon}\sum_{i=0}^{\infty}\sum_{j=0}^{\infty} \frac{c_{i,j}}{w}\cos^2\frac{\pi j}{2} \frac{k_0^2 - k^2}{(k^2 - \lambda_{i,j}^{\epsilon})(k_0^2 - \lambda_{i,j}^{\epsilon})}$$

Noting that $k_0^2 = -\frac{C}{\delta^2}$, we can express the limit $\hat{g}^w(k)dx = \lim_{\epsilon\to 0} \epsilon\, hat g_\epsilon(k, k_0)$:

$$\hat{g}^w(k)dx = \frac{1}{wk^2} + \frac{2}{w}\sum_{i=1}^{\infty} \frac{1}{(k^2 - \frac{i^2\pi^2}{w^2})},$$

using the following formula for a series:

$$\sum_{i=1}^{\infty} \frac{1}{i^2 - a^2} = \frac{1}{2a^2} - \frac{\pi \cot(a\pi)}{2a},$$

When the distance between the holes is $\epsilon \to 0$, the width of the holes is $\delta \to 0$, and given $k_0 = \frac{2i}{\delta} \exp -\gamma$, $k_0^2\ to - \infty$, we can explicitly obtain formulas for the limit:

$$\hat{g}^w(k)dx = \frac{\cot kw}{k} \tag{30}$$

Consider the general form for the eigenfunctions of the model operator H^N corresponding to the eigenvalue k^2:

$$u_n(x) = \begin{cases} \sum_{j=1}^n \alpha_j^{ex} G(x, x_j, k) & x \in \Omega \\ \alpha_i^{in} G_i(x, x_i, k) & x \in \Omega_i \end{cases}$$

Note the difference between this expression and the general form of the elements $D(H)$ (25), where there are arbitrary functions with the Neumann conditions $\tilde{u}$ and the parameter k_0 depends only on the size holes, but not from energy.

Now, in order to correlate $a_\bullet$ and $\alpha_\bullet$, and to express the conditions (28) in terms of $\alpha_i^{in,ex}$, we must extract the singularities of $G_i(x, x_i, k_0)$. For each hole l, do the following:

$$u_n(x) = \tag{31}$$
$$\begin{cases} \alpha_l^{ex} G(x, x_i, k_0) + \alpha_l^{ex} g(x, x_i, k, k_0) + \sum_{j\neq l}^n \alpha_j^{ex} G(x, x_j, k) & x \in \Omega \\ \alpha_l^{in} G_l(x, x_l, k_0) + \alpha_l^{in} g_l(x, x_l, k, k_0) & x \in \Omega_l \\ \alpha_j^{in} G_j(x, x_j, k) & x \in \Omega_{j\neq l} \end{cases}$$

$$g^\bullet(x, z, k, k_0) = G^\bullet(x, z, k) - G^\bullet(x, z, k_0)$$

Comparing this with (25) and using (26) we get

$$\alpha_i^{ex} = a_i, \quad i = 1, ...N$$

and the (28) conditions take the following form:

$$\alpha_i := \alpha_i^{ex} = -\alpha_i^{in}$$

$$\alpha_i g_i(k, k_0) + \sum_{j \neq i}^{N} \alpha_j G(x_i, x_j, k) = -\alpha_i \hat{g}(k, k_0) \tag{32}$$

Let also

$$u_i = u(x_i) = \alpha_i g_i(k, k_0) + \sum_{j \neq i}^{N} \alpha_j G(x_i, x_j, k)$$

The (32) condition can be represented as

$$u_i = -\alpha_i \hat{g}_\epsilon(k, k_0)$$

Multiplying each of these N equations by $G(x, x_i, k)$ and summing, we get

$$\sum_{i=1}^{N} \alpha_i G(x, x_i, k) = -\sum_{i=1}^{N} u_i G(x, x_i, k)[\hat{g}_\epsilon(k, k_0)\epsilon]^{-1}\epsilon$$

The left side of this expression is the original eigenfunction, and the right side contains the values of this function at the hole points, multiplied by the distance between them $dx = \epsilon$, which makes the expression an integral sum. Finally, considering the limit $N \to \infty$, we obtain an integral equation for some function $u(x)$ acting in Ω.

$$\psi(x) = -\int_\Gamma \psi(y) G(x, y, k)[\hat{g}(k, k_0)dy]^{-1}dy =$$
$$= -\int_\Gamma \psi(y) G(x, y, k) k \tan[kw] dy, \tag{33}$$

This integral equation is equivalent to the following eigenvalue problem with boundary conditions in the region Ω_0:

$$\begin{cases} \Delta u + k^2 u = 0 \\ \frac{\partial u}{\partial n}|_\Gamma = -k \tan(kw) u|_\Gamma \\ \frac{\partial u}{\partial n}|_{\partial\Omega \setminus \Gamma} = 0 \end{cases}$$

The theorem has been proven.

In conclusion, we note that the area consisting of strips, in fact, approaches the area in which the Laplace operator is replaced by another operator:

$$L^{(1)}u = \frac{\partial^2 u}{\partial x^2},$$

however, in addition to this, the function can now have discontinuities in the direction of the Y axis, and continuity must be preserved at the right boundary of the region. The question of a rigorous description of the operator and function space in the domain of strips remains open.

1.1.7 Border of strips: Numerical results

This section describes the obtained numerical results for a system with a border corrugated by strips. The Mathematica system was used.

Eigenfunctions of systems with exact geometry (i.e. without zero-width slit approximation) were constructed. Examples of three-dimensional graphs of the obtained eigenfunctions are shown in fig. 7. It shows the results for two systems, with the number of bands equal to ten and fifty. The numbers of functions were chosen so as to show the main features of the constructed functions, the energies increase in each column separately (from top to bottom).

The following are two graphs, 8 and 9, which plot the ratio of the eigenfunction derivative to its value as a function of the state's eigenenergy. Each value is obtained as follows: the ratio is calculated at N points $x_i + dx$, and the arithmetic mean is taken (with 10% of extreme values discarded). The value of dx is small compared to the size of the holes, does not change, and is chosen to minimize the difference between the eigenfunction built from Green's functions (see the left side (28)) and the numerical value of the function. All parameters of the system are unchanged, except for the number of resonators and the hole size.

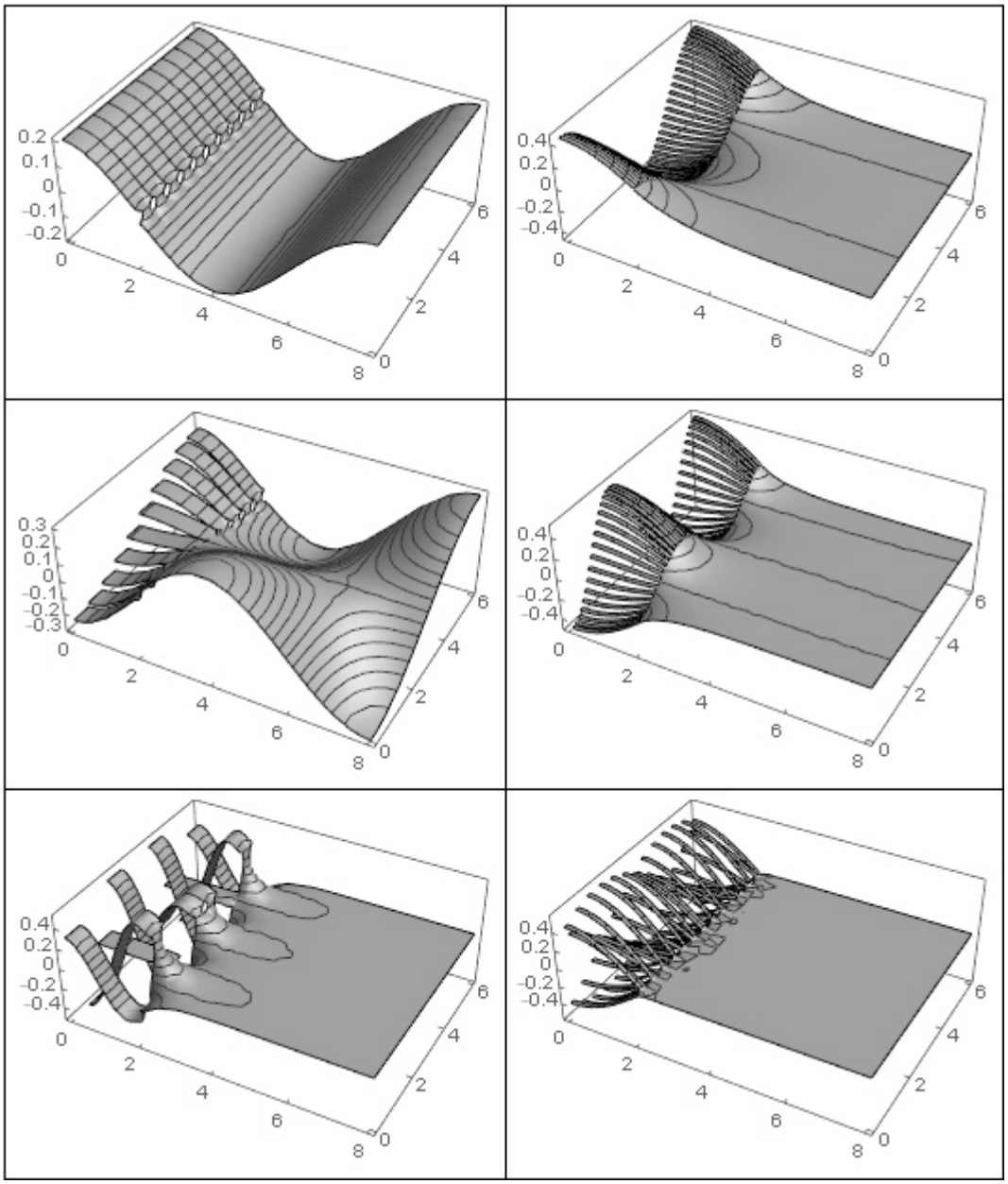

Figure 7 – Examples of numerically constructed eigenfunctions of an operator with a corrugated boundary of strips. Left - $N = 10$, right - $N = 50$. The energy increases from the top line to the bottom, in each column (non-consecutive eigenfunctions are given). Hole size $\delta = 0.5\epsilon$.

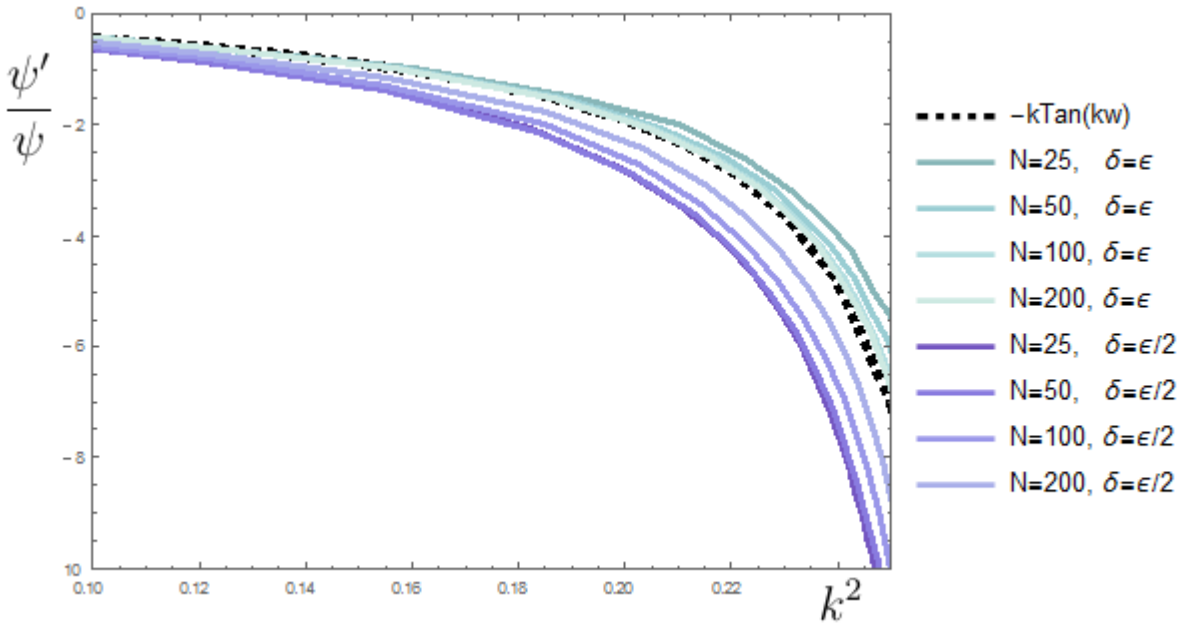

Figure 8 – System with a border corrugated by strips. Graphs of the ratio of the derivative of a function to its value, taken along the perturbed boundary of the Ω domain (average value). Each line corresponds to a fixed geometry of the system, with parameters N and δ (other parameters are unchanged). Two sets of four lines are shown: for holes equal to half the width of the strips and for holes equal to the width of the strips (i.e., with the resonator wall completely absent). Also shown is the dotted line corresponding to the theoretical limit, $-k \tan kw$.

We used the zero-width slit model, so our result applies to the case with a small hole in the resonator wall. In addition to this case, the graph also shows the results for the case with a completely absent Ω wall that is perturbed, i.e. the strips are directly attached to the main resonator. As seen on the scale of Fig. 8, in the case of a missing wall, the convergence to the limit value $-k \tan kw$ is noticeably better. Moreover, this pattern applies to all hole sizes, i.e. convergence is better the closer δ/ϵ is to unity.

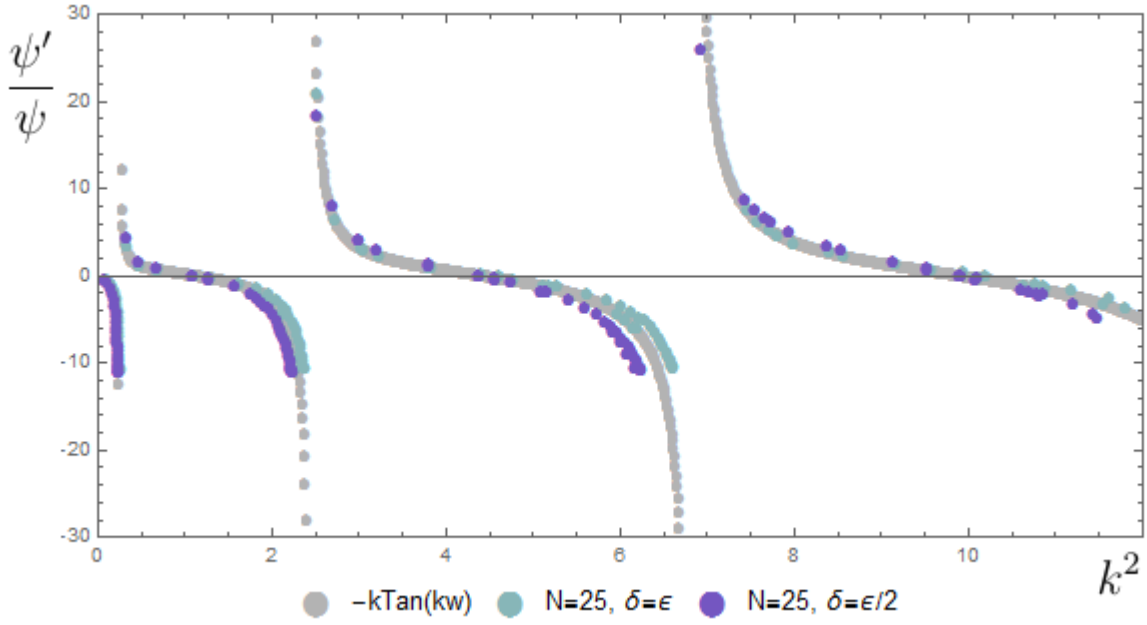

Figure 9 – System with a border corrugated by strips. Graphs of the ratio of the derivative of a function to its value, taken along the perturbed boundary of the Ω domain (average value). The result partially repeats Fig. 8 but on a different scale. Each point corresponds to a specific eigenfunction, points of the same color - the same geometry of the system, with the indicated parameters N and δ (other parameters are unchanged). Three sets of points are shown: the gray points are the theoretical limit, $-k \tan kw$, the other two are for holes equal to half the width of the strips and for holes equal to the width of the strips.

The second graph, fig.9, shows the behavior of the ratio at high energy values, only for the case of $N = 25$. The last limitation is related to the difficulty of obtaining values, with a sufficiently large ratio at the boundary, with a larger number of bands, since this ratio is slowing down. For example, for systems with $N = 200$ shown in Fig.8, the ratio ψ'/ψ of the first 120 eigenfunctions does not exceed 0.3.

1.1.8 Asymptotics for the boundary of square resonators and numerical calculations

This section presents the results obtained by E.S. Trifanova in the yet unpublished article "Energy-dependent boundary condition as a limit of very corrugated

boundary: asymptotic approach", in which the method of matching asymptotics near holes is used to study the corrugated boundary. The results of the author are also presented, where the method of zero-width slits was applied for this system and graphs corresponding to the analytical results were constructed using numerical methods.

The main goal is to get the principal terms of the $\lambda_0 - \lambda_\epsilon$ asymptotics, where $\lambda_0 = \frac{2\pi^2}{d^2}$ is the first eigenvalue of the main domain.

Let us describe the system studied in the work.

- H_0 - Neumann's Laplacian.
- Ω_0 is a square with side d. The upper side is perturbed, i.e. $\Gamma = \{(x, y) : x \in [0, d], y = d\}$. Functions belonging to Ω_0 are marked with '-'.
- Ω_i - square resonators with side ϵ arranged ϵ-periodically. There are no tunnels. Functions belonging to resonators are marked with a '+' sign.
- Hole size is obtained from the ratio:

$$\epsilon = |x_i - x_{i-1}| = m\delta^\theta = \frac{d}{N}, \quad \theta \in (0, 1). \tag{34}$$

Let us briefly present the calculations and the main result. The Green's functions of the Helmholtz equation with the Neumann boundary conditions in the $G(X, X_i, k)$ rectangles are used in the calculations, the exact values of which were given in the section 1.1.6.

Here, in addition to the small parameter ϵ, which characterizes the dimensions of resonators and holes, we consider energies close to the first eigenvalue of the resonator Ω_0, i.e. the difference $\left(k^2 - \frac{2\pi^2}{d^2}\right)$ is small, which will be used in the asymptotics.

Similarly to [23], one can represent the principal terms of the asymptotics with respect to δ of the eigenfunctions of the perturbed problem in the following form:

$$\psi(X) = \begin{cases} \left(k^2 - \frac{2\pi^2}{d^2}\right) \alpha_i G_i^+(X, (x_i, 0), k), & X \in \Omega^+ \setminus S((x_i, 0), r(\delta)); \\ v_0^i(x/\delta) + v_1^i(x/\delta) \ln^{-1} \delta + o(\ln^{-1} \delta), & X \in S((x_1, 0), 2r(\delta)); \\ -\left(k^2 - \frac{2\pi^2}{d^2}\right) \sum_{j=1}^N \alpha_j G^-(X, (x_j, 0), k), & X \in \Omega^- \setminus S((x_i, 0), r(\delta)), \end{cases} \tag{35}$$

where $S(X,r)$ is a sphere with center X and radius r. The radius $r(\delta)$ is chosen so that

$$\delta d < r(\delta) < 2r(\delta) < \epsilon/2.$$

The asymptotic expansion of the energy deviation from the resonator eigenvalue is chosen according to the following formula:

$$k^2 - \frac{2\pi^2}{d^2} = \tau_1 \ln^{-1}\delta + o\left(\ln^{-2}\delta\right). \tag{36}$$

The coefficient τ will be determined below.

Using the asymptotics of the Green's functions for small resonators

$$\begin{aligned} G_N^+((x,0),(x_i,0),k) = \\ -\frac{1}{\pi}\ln\delta + \frac{4N^2\cos(N\pi x_i/d)\cos(N\pi x/d)}{d^2\left(k^2 - 2N^2\pi^2/d^2\right)} + g_1^+(X) - \frac{1}{\pi}\ln|\xi| = \\ = -\frac{1}{\pi}\ln\delta + \frac{4\cos(\pi x_i/\epsilon)\cos(\pi x/\epsilon)}{k^2\epsilon^2 - 2\pi^2} + g_1^+(X) - \frac{1}{\pi}\ln|\xi|, \end{aligned} \tag{37}$$

where $X = (x,y)$, $\xi = \frac{x}{\delta}$, $g_1^+(X)$ is a bounded function. The second term is a bounded function for small ϵ, so we add it to $g_1^+(X)$ and call the resulting bounded function g^+. Next, we obtain the following asymptotic expansion for (35), inside the resonators:

Lemma 1.1.1. *The first terms of the expansion of the* (35) *solution in the resonator i are:*

$$\begin{aligned} \psi^+(x,0) = \alpha_i\left(k^2 - \frac{2\pi^2}{d^2}\right)\left[-\frac{1}{\pi}\ ln\delta + g^+(X) - \frac{1}{\pi}\ln\xi\right] \\ = -\frac{1}{\pi}\alpha_i\tau_1 + o(1), \end{aligned} \tag{38}$$

where $x \to x_i$, $\delta \to 0$.

Similarly, we obtain the asymptotics of the solution in the main resonator:

Lemma 1.1.2. *The asymptotics of the* (35) *solution in the main resonator, near*

the hole i, has the following form:

$$\psi^-(X) = \\ -\alpha_i\left[-\frac{\tau_1}{\pi}+\frac{4}{d^2}\cos^2(\pi x_i/d)\right]- \\ \sum_{j=1,j\neq i}^{N}\alpha_j\left[\frac{4}{d^2}\cos(\pi x_i/d)\cos(\pi x_j/d)-\frac{\theta\tau_1}{\pi}+\right]+o(1). \quad (39)$$

We are now ready to compare the obtained asymptotics near the holes. We omit this procedure, which involves solving a system of N equations, to obtain the coefficients α_i of the (35) solution. As a result of the procedure, we obtain the following expression for the solution inside the main resonator:

$$\psi^-(x)=\frac{d}{2}(2-\theta)\left(k^2-\frac{2\pi^2}{d^2}\right)\sum_{i=1}^{N}G^-((x,0),(x_i,0),k)\big(\psi^-(x_i)+o(1)\big)\cdot\frac{d}{N} \quad (40)$$

This expression is an integral sum. Passing to the limit $N\to\infty$, we get:

Lemma 1.1.3. *The eigenfunctions of the limit problem satisfy the following integral equation:*

$$\psi^-(X)=\frac{d}{2}(2-\theta)\left(k^2-\frac{2\pi^2}{d^2}\right)\int\limits_{\Gamma}G^-(X,X',k)\psi^-(X')dX'. \quad (41)$$

This is equivalent to some boundary value problem, which is formulated in the main theorem:

Theorem 1.1.8. *The Laplacian eigenfunctions corresponding to an eigenvalue close to $\frac{2\pi^2}{d^2}$ for the systems described above with a corrugated boundary converge for $N\to\infty$ to the eigenfunctions of the problem with the following condition on the upper boundary:*

$$\frac{\partial\psi}{\partial n}\Big|_{\partial\Omega}=\frac{d}{2}(2-\theta)\left(k^2-\frac{2\pi^2}{d^2}\right)\psi\Big|_{\partial\Omega}. \quad (42)$$

In this result, the first eigenvalue of the main resonator has been considered only for simplicity. The result generalizes directly to the case of any eigenvalue.

In conclusion, we present the numerical results corresponding to these analytical calculations. Numerical solutions were obtained for model problems with

fixed N. Using the zero-width slit model, we analytically obtain results similar to sec.1.1.5. Let us present the condition on the coefficients α_i in front of the Green's functions for the model problem:

$$\alpha_i g_i(k, k_0) + \sum_{j \neq i}^{N} \alpha_j G(x_i, x_j, k) = -\alpha_i \hat{g}(k, k_0)$$

In this equation, for comparison with numerical calculations for finite holes, we assume

$$\alpha_i g_i(k, k_0) + \sum_{j \neq i}^{N} \alpha_j G(x_i, x_j, k) \approx \psi_{k^2}(x_i),$$

for the values of functions at points, and for the derivatives of these functions, we assume:

$$\alpha_i \approx \frac{\partial \psi_{k^2}}{\partial n}(x_i)$$

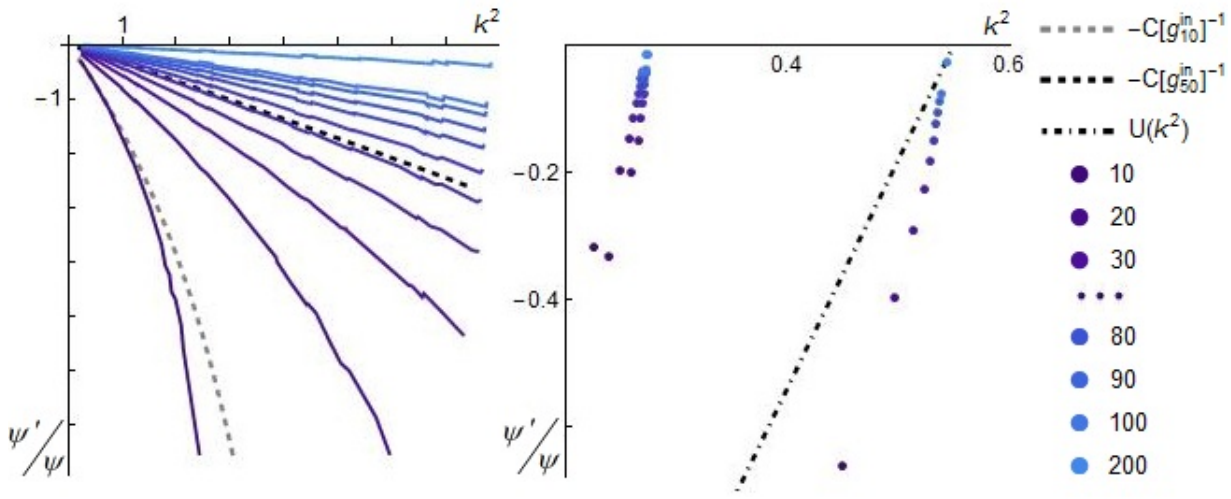

Figure 10 – On the left - the ratio of the derivative of the function to the value, depending on the energy of the state. Different graphs correspond to systems with different N. On the right is the same plot at a different scale, but the points are not connected by (horizontal) lines. The dotted line indicates the analytically obtained functions.

Given these approximations, we can compare the numerically obtained value of $\frac{\partial \psi_{k^2}}{\partial n} / \psi_{k^2}(x_i)$, with its analytical counterpart $g_i(k, k_0) + \sum_{j \neq i}^{N} \frac{\alpha_j}{\alpha_i} G(x_i, x_j, k)$.

Figure 10 shows plots of $\frac{\partial \psi_{k^2}}{\partial n} / \psi_{k^2}(x_i)$ on average over the entire boundary with resonators, for model problems with fixed $N = 10, 20, ...90, 100, 200$ (in

all cases, the standard deviation is $\sigma \ll 1$), i.e. each point is one of the numerically found bound states with fixed N and k^2. The parameter $\theta = 0.8$ is used. The dotted line on the left graph shows the theoretically obtained function $-C[\hat{g}(k, k_0)]^{-1}$, multiplied by the constant C, the value of which is determined by taking the derivative at the boundary: for the presented graphs, the derivative is taken at a small distance from the wall, at a point opposite each hole. Thus, it is shown that for model eigenfunctions, $\frac{\partial \psi_{k^2}}{\partial n}(x_i + \vec{n}\xi)/\alpha_i$, for small ξ does not depend on i and energy k^2. To improve the convergence of $G(x, x_i, k)$ in numerical calculations, you can use the formula from [31]. The dotted line on the right graph shows the function $\frac{\epsilon}{2}(2 - \theta)[k^2 - \lambda]$, the points to which the sequences converge are the eigenvalues of the large resonator. The obtained values, as N increases, converge to the theoretically obtained function $U(k^2)$, see (42). It can also be seen that the paired values converging to $\lambda < 0.4$ turn parallel to $U(k^2)$ as N increases.

1.2 Translucent corrugated barrier

Let's move on to the next problem - systems with translucent barriers. These systems are discussed in this section, and further in the next chapter, where the barrier is modeled using a singular δ potential.

First, consider applying the asymptotic expansion methods of the 1.1.8 section to a system with a small hole in a semitransparent barrier, and then apply the developed methods for working with a corrugated boundary to construct a corrugated barrier.

1.2.1 Asymptotics for a semitransparent barrier with a small hole

This section presents the results of our article [1]. We consider a quantum waveguide with a semitransparent barrier located across it (see Fig.11). It is assumed that the barrier has a small window. This local perturbation of the waveguide leads to the appearance of resonant states. localized near the barrier with a window. The asymptotic behavior (with respect to a small parameter,

the window width) of resonances (quasi-bound states) is obtained. A procedure for constructing a complete formal asymptotic expansion is described; the first two terms are obtained explicitly. These terms describe the displacement of the resonance from the threshold and the lifetime of the corresponding resonance state.

A system of two waveguides with a common semitransparent wall was studied in [34]. We will consider a similar system, but with a semitransparent barrier located across the waveguide.

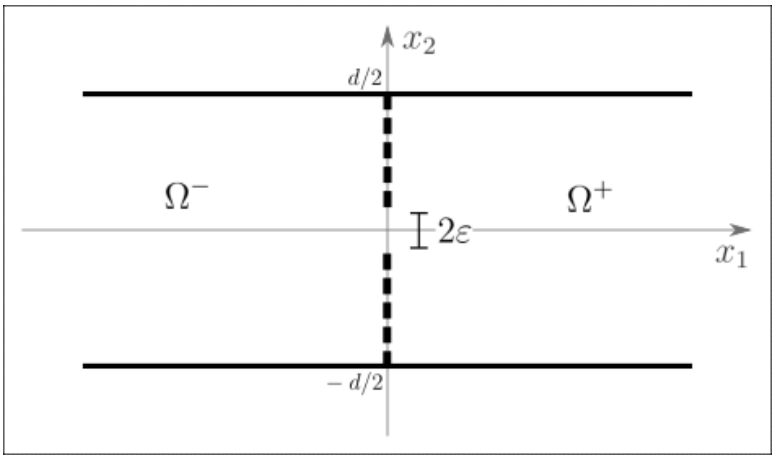

Figure 11 – A waveguide with a translucent border with a small hole in the middle.

Let's set the introductory formulas. α - transparency parameter. $\alpha = 0$ means no barrier, $\alpha = \infty$ - opaque barrier. The boundary conditions on both walls of the waveguide are the Dirichlet conditions. But there are special conditions for the barrier:

$$\begin{cases} u_+ = u_- \\ u'_+ - u'_- = \alpha u \end{cases} . \tag{43}$$

The second condition characterizes the "jump" of the derivative on the barrier, α is a real constant. Conditions of this type appear if we consider a singular potential supported on a hypersurface. Such potentials have been intensively studied over the past two decades (see, for example, [35, 36, 37, 38, 39]).

The window size is 2ε, the window is located in the center barrier. For the corresponding unperturbed system (i.e., without a window), a separation of variables can be carried out. The eigenvalues and orthonormal eigenfunctions for the Laplacian (i.e. the second derivative), in a waveguide cross section, are as

follows:

$$\psi_n(x_2) = \sqrt{\frac{2}{d}} \sin \frac{\pi n x_2}{d}, \quad \lambda_n = \left(\frac{\pi n}{d}\right)^2.$$

These eigenvalues play the role of thresholds for the corresponding branches of the continuous spectrum of the waveguide Hamiltonian. Lower the boundary of the continuous spectrum of the Dirichlet Laplacian is greater zero. We are looking for the principal terms of the asymptotic expansion of the quasi-eigenvalues near the first threshold:

$$\sqrt{\left(\frac{\pi}{d}\right)^2 - \tau_\varepsilon^2} = \sum_{j=2}^{\infty} \sum_{i=0}^{[j/2]-1} \tau_{ji} \varepsilon^j \left(\ln \frac{\varepsilon}{\varepsilon_0}\right)^i. \tag{44}$$

This is not the only possible extension, but it is handy in this case. The asymptotic series for the corresponding eigenfunctions have the following form:

$$\psi_\varepsilon(x) = \sqrt{\left(\frac{\pi}{d}\right)^2 - \tau_\varepsilon^2} \cdot \sum_{j=0}^{\infty} \varepsilon^j \; P_{j+1}\left(D_y, \ln \frac{\varepsilon}{\varepsilon_0}\right) G^-(x, y, k)\Big|_{y=0}, \quad x \in \Omega^- \backslash S_{\varepsilon_0(\varepsilon/\varepsilon_0)^{1/2}}, \tag{45}$$

$$\psi_\varepsilon(x) = \sum_{j=1}^{\infty} \sum_{i=0}^{[(j-1)/2]} v_{ji}\left(\frac{x}{\varepsilon}\right) \varepsilon^j \ln^i \frac{\varepsilon}{\varepsilon_0}, \quad x \in S_{2\varepsilon_0(\varepsilon/\varepsilon_0)^{1/2}}, \tag{46}$$

$$\psi_\varepsilon(x) = -\sqrt{\left(\frac{\pi}{d}\right)^2 - \tau_\varepsilon^2} \cdot \sum_{j=0}^{\infty} \varepsilon^j \; P_{j+1}\left(D_y, \ln \frac{\varepsilon}{\varepsilon_0}\right) G^+(x, y, k)\Big|_{y=0}, \quad x \in \Omega^+ \backslash S_{\varepsilon_0(\varepsilon/\varepsilon_0)^{1/2}}. \tag{47}$$

Here ε_0 is the natural unit of length, e.g. d, S_t is a circle of radius t centered in the middle of the window,

$$v_{ji} \in W^1_{2,loc}(\Omega^- \cup \Omega^+),$$

$$P_1\left(D_y, \ln \frac{\varepsilon}{\varepsilon_0}\right) = c_{10}^{(1)} \frac{\partial}{\partial n_y},$$

n_y - normal to the barrier at y,

$$P_m\left(D_y, \ln \frac{\varepsilon}{\varepsilon_0}\right) = \sum_{q=1}^{m-1} \sum_{i=0}^{[(q-1)/2]} c_{qi}^{(m)} \left(\ln \frac{\varepsilon}{\varepsilon_0}\right) D_y^{m-q+1}, \quad m \geq 2,$$

$$D_y^{2j+1} = \frac{\partial^{2j+1}}{\partial n_y^{2j+1}}, \quad D_y^{2j} = \frac{\partial^{2j}}{\partial n_y^{2j-1} \partial l_y}.$$

The first thing we are going to calculate is the Green's function for such systems. The Green's function for a standard planar quantum waveguide is well known [40], and is written as:

$$G(x,y,k) = \sum_{n=1}^{\infty} \frac{\psi_n(x_2)\cdot\psi_n(y_2)}{2p_n}\cdot e^{-p_n\cdot|x_1-y_1|}$$

Here x_1 and y_1 are the coordinates on the waveguide axis, ψ is orthonormal eigenfunctions for the unperturbed case, $p_n = \sqrt{\lambda_n - k^2}$. For $n = 1$ this is exactly the left hand side of the asymptotic extension given earlier.

Consider our case, when the waveguide is located as in the figure, x_0 is the abscissa of the barrier, and the two arguments of the Green's function are x and y. One can write the Green's function with some coefficients, considering three subdomains:

$$G(x,y,k) = \sum_{n=1}^{\infty} \frac{\psi_n(x_2)\cdot\psi_n(y_2)}{2p_n}\cdot\phi(x_1,y_1,k),,$$

where

$$\phi(x_1,y_1,k) = \begin{cases} a_n\cdot e^{-p_n\cdot(x_1-y_1)}, & y_1 < x_1, \\ b_n\cdot e^{-p_n\cdot(x_1-y_1)} + c_n\cdot e^{p_n\cdot(x_1-y_1)}, & x_0 < x_1 < y_1, \\ d_n\cdot e^{p_n\cdot(x_1-y_1)}, & x_1 < x_0. \end{cases}$$

The coefficients are calculated using the conditions (43):

$$\begin{cases} a_n\cdot e^{-p_n\cdot(x_1-y_1)}\Big|_{x_1=y_1} = b_n\cdot e^{-p_n\cdot(x_1-y_1)}\Big|_{x_1=y_1} + c_n\cdot e^{p_n\cdot(x_1-y_1)}\Big|_{x_1=y_1} \\ -p_n a_n\cdot e^{-p_n\cdot(x_1-y_1)}\Big|_{x_1=y_1} + p_n b_n\cdot e^{-p_n\cdot(x_1-y_1)}\Big|_{x_1=y_1} - p_n c_n\cdot e^{p_n\cdot(x_1-y_1)}\Big|_{x_1=y_1} = 1 \\ b_n\cdot e^{-p_n\cdot(x_1-y_1)}\Big|_{x_1=y_1} + c_n\cdot e^{p_n\cdot(x_1-y_1)}\Big|_{x_1=y_1} = d_n\cdot e^{p_n\cdot(x_1-y_1)}\Big|_{x_1=y_1} \\ -p_n b_n\cdot e^{-p_n\cdot(x_1-y_1)}\Big|_{x_1=y_1} + p_n c_n\cdot e^{p_n\cdot(x_1-y_1)}\Big|_{x_1=y_1} - p_n\, d_n\cdot e^{p_n\cdot(x_1-y_1)}\Big|_{x_1=y_1} = \\ \qquad = \alpha\cdot d_n\cdot e^{p_n\cdot(x_1-y_1)}\Big|_{x_1=y_1} \end{cases} \Leftrightarrow$$

$$\begin{cases} a_n = b_n + c_n \\ p_n(b_n - a_n - c_n) = 1 \\ b_n\frac{1}{\gamma} + c_n\gamma = d_n\gamma \\ 2c_n p_n = d_n(\alpha + 2p_n) \end{cases} \Leftrightarrow \begin{cases} a_n = \frac{\alpha\gamma^2-\alpha-2p_n}{2p_n(\alpha+2p_n)} \\ b_n = \frac{\alpha\gamma^2}{2p_n(\alpha+2p_n)} \\ c_n = -\frac{1}{2p_n} \\ d_n = -\frac{1}{\alpha+2p_n} \end{cases},$$

where $\gamma = e^{p_n \cdot (x_0 - y_1)}$. notice, that for the case without a barrier, ($\alpha = 0$), we obtain coefficients satisfying the usual formulas:

$$a_n = c_n = d_n = -\frac{1}{2p_n}, \quad b_n = 0.$$

The derivative of the Green's function is used in (45) and (47), so we need the following representation:

$$D_y^j G^{\pm}(x, 0, k) =$$
$$= \frac{1}{d} \sin \frac{\pi x_2}{d} \sin \frac{\pi y_2}{d} D_y^j \left(\phi(x_1, y_1, k)\right)\Big|_{y_1 = y_0} \left(\left(\frac{\pi}{d}\right)^2 - k^2\right)^{-1/2} +$$
$$+ \Phi_j(x, k) \ln \frac{r}{\varepsilon_0} + g_j^{\pm}(x, k),$$

where $g_j^{\pm}(x, k)$ has no singularity at $x = 0$.

Boundary value problems for the coefficients v_{ji} can be obtained as follows. Consider the asymptotic series τ_ε^2 based on (44):

$$\tau_\varepsilon^2 = \sum_p \sum_q \Lambda_{pq} \varepsilon^p \ln^q \frac{\varepsilon}{\varepsilon_0}, \tag{48}$$

where the coefficients Λ_{pq} are polynomials in τ_{ji}, which can be easily calculated. Then, you can substitute (46) and (48) into the Helmholtz equation, change the variables $\xi = \dfrac{x}{\varepsilon}$ and match the terms of the corresponding orders in both series. Thus, the following equation is obtained:

$$\begin{aligned} &\Delta_\xi v_{ji} = -\sum_{p=0}^{j-3} \sum_{q=0}^{[p/2]-1} \Lambda_{pq} v_{j-p-2,i-q}, \quad \xi \in R^2 \backslash \Gamma_1, \\ &v_{ji} = 0, \ \ \xi \in \Gamma_1, \end{aligned} \tag{49}$$

Where

$$\Gamma_1 = \{\xi | \xi_1 = 0 \wedge \xi_2 \in (-\infty; -1] \cup [1; +\infty)\}.$$

We define the operator K_{pq} for sums $S(x, \varepsilon)$ of type (45) and (47) in the following way: if $S(x, \varepsilon)$ has coefficient $\mu(\xi)$ for $\varepsilon^p \ln^q \dfrac{\varepsilon}{\varepsilon_0}$ in asymptotic expansion, then $\mathrm{K}_{pq}(S) = \mu$. We also define $\mathrm{K}_p = \sum\limits_q \mathrm{K}_{pq}$.

Taking into account the representation of the derivative of the Green's function, we can use a procedure similar to that described in [41], [42] and get:

$$\lim_{k \to \frac{\pi}{d}} \left(\sqrt{\left(\frac{\pi}{d}\right)^2 - k^2} P_1 G^-(x, 0, k) \right) = -\frac{\pi}{d^2} c_{10}^{(1)} \sin \frac{\pi x_2}{d},$$

$$\lim_{k\to\frac{\pi}{d}}\left(\sqrt{\left(\frac{\pi}{d}\right)^2-k^2}P_1G^+(x,0,k)\right)=0,$$

$$\varepsilon^{-1}\mathrm{K}_1\left(\sqrt{\left(\tfrac{\pi}{d}\right)^2-\tau_\varepsilon^2}\cdot P_1G^+(x,0,\tau_\varepsilon)\right)=$$
$$=\varepsilon^{-1}c_{10}^{(1)}\mathrm{K}_1\left(\left(\tau_{20}\varepsilon^2+\tau_{30}\varepsilon^3+\tau_{40}\varepsilon^4+\tau_{41}\varepsilon^4\ln\tfrac{\varepsilon}{\varepsilon_0}+\ldots\right)\cdot\tfrac{\partial}{\partial x_1}\left(\tfrac{1}{\pi}\ln\rho+g(x,0,\tau_\varepsilon)\right)\right)=$$
$$=\varepsilon^{-1}c_{10}^{(1)}\cdot\tau_{20}\cdot\tfrac{x_1}{\pi\rho^2}=\xi_1\cdot c_{10}^{(1)}\cdot\tau_{20}\cdot\pi^{-1}\rho^{-2}$$

Lemma 1.2.1. *There are harmonic functions $Y_q(\xi)$ that have the following differentiable asymptotics in $\rho\to\infty$:*

$$Y_q=\begin{cases}-\sum\limits_{j=1}^{\infty}\rho^{-j}(a_{qj}^+\cos j\theta+b_{qj}^+\sin j\theta), & \xi_1>0\\ \rho^q(a_q^0\cos q\theta+b_q^0\sin q\theta)+\sum\limits_{j=1}^{\infty}\rho^{-j}(a_{qj}^-\cos j\theta+b_{qj}^-\sin j\theta), & \xi_1<0\end{cases}$$

To match members from (49) we can select v_{10} like this:

$$v_{10}(\xi)=c_{10}^{(1)}\sum_{j=1}^{\infty}\rho^{-j}(a_{qj}^+\cos j\theta+b_{qj}^+\sin j\theta). \tag{50}$$

Now, we can equate the $\rho^{-1}\cos\theta$ coefficients in (49) and (50) to get τ_{20}:

$$\xi_1\cdot c_{10}^{(1)}\cdot\tau_{20}\cdot\pi^{-1}\rho^{-2}=\rho\cos\theta\cdot c_{10}^{(1)}\cdot\tau_{20}\cdot\pi^{-1}\rho^{-2}=\rho^{-1}\cos\theta\cdot c_{10}^{(1)}\cdot\tau_{20}\cdot\pi^{-1}\Rightarrow$$

$$\tau_{20}\cdot\pi^{-1}=a_{q1}^+\Rightarrow\tau_{20}=\pi\cdot a_{q1}^+.$$

Conclusion The proposed procedure can be extended to obtain terms of the asymptotic expansion of any order. The results concerning the real part of the resonance make it possible to estimate the shift of the resonance relative to the threshold. As for the last formula for τ_{20}, it shows the imaginary part of the resonance, which corresponds to the decay rate for the resonance state, i.e. the lifetime of the quasi-bound state.

1.2.2 Barrier made of strips

All the existing results concerned the perturbation of the boundaries of regions. Our next goal is to extend the developed methods to a wider range of

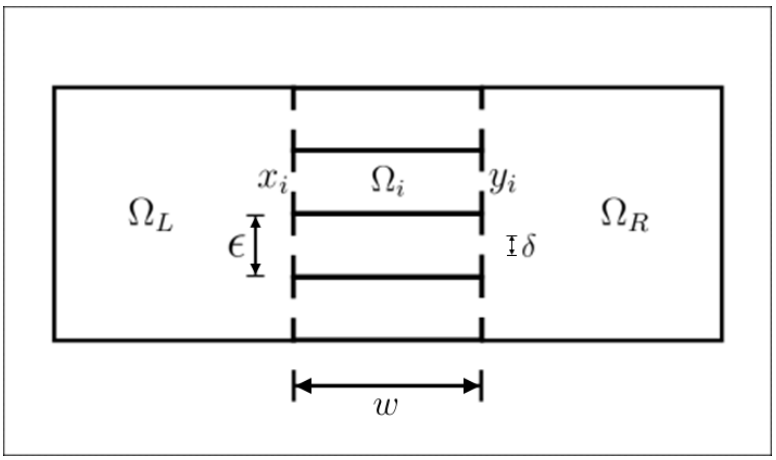

Figure 12 – Two square resonators connected through a corrugated boundary of N (here $N = 4$) rectangular resonators, each of which has two holes at the points x_i and y_i.

system geometries. Consider a perturbation in the form of a barrier of resonators.

The general view of the corrugated barrier system is shown in Fig.12. We expand the notation used earlier:

- Let Ω_L, Ω_R be two disjoint domains in $\mathbb{R}^2$ with common boundary Γ.
- N resonators $\Omega_i, i = 1, 2, ...N$ are inserted along the boundary between the main regions (without changing the shape of the regions, but shifting one of them by the required distance).
- Each resonator is connected to both regions through two δ holes. The midpoints of the holes are denoted by x_i, for holes from the left region Ω_L, and y_i from the right Ω_R (each of the points is a 2-vector). (Tunnels for barriers are not considered in this paper)
- The resonators are rectangular, with sides w, h.
- Operators acting in the areas Ω_L, Ω_R will be marked with letters: Δ_L, Δ_R. The boundary corresponding to Γ lying in Ω_L after splitting - Γ_L is similarly defined by Γ_R.
- The small parameter $\epsilon = \frac{|\Gamma|}{N}$, corresponds to the distance between adjacent hole centers along the Γ boundary in each of the main regions.

- The Laplace operator, with Neumann boundary conditions, acting on two isolated domains Ω_L, Ω_R is denoted by H_0, and the operators on perturbed domains with applied zero-width slit approximation are H_ϵ or H^N.

In this section, similarly to the previous sections, we apply the zero-width slit model to derive exact expressions for H^N eigenfunctions and consider the $N \to \infty$ limit. The next section presents the numerical results corresponding to the analytical ones. The form of resonators in the form of strips with a fixed length is considered:

$$w = const, h = \epsilon$$

So, after applying the zero-width slit approximation, we get the following expression for functions from the domain of the operator H^N:

$$\begin{pmatrix} u_L \\ u_1 \\ \vdots \\ u_n \\ u_R \end{pmatrix} = \begin{pmatrix} \tilde{u}_L \\ \tilde{u}_1 \\ \vdots \\ \tilde{u}_n \\ \tilde{u}_R \end{pmatrix} + \begin{pmatrix} \sum_{i=0}^{n} a_i^{ex} G^L(x, x_i, k_0) \\ a_1^{in} G_i(x, x_1, k_0) + b_1^{in} G_i(x, y_1, k_0) \\ \vdots \\ a_n^{in} G_i(x, x_n, k_0) + b_n^{in} G_i(x, y_n, k_0) \\ \sum_{i=0}^{n} b_i^{ex} G^R(x, y_i, k_0) \end{pmatrix} \tag{51}$$

The parameter k_0 is chosen according to (16): $k_0 = \frac{2i}{\delta} \exp -\gamma$, where $\gamma \approx 0.577$.

Lemma 1.2.2. *The boundary form for $u, v \in D(H^{N*})$ is:*

$$\begin{aligned}(H^* u, v) - (u, H^* v) = \\ \sum_i a_i^{u,in} \overline{C_i^{v,in}} - \overline{a_i^{v,in}} C_i^{u,in} + a_i^{u,ex} \overline{C_i^{v,ex}} - \overline{a_i^{v,ex}} C_i^{u,ex} + \\ \sum_i b_i^{u,in} \overline{\tilde{C}_i^{v,in}} - \overline{b_i^{v,in}} \tilde{C}_i^{u,in} + b_i^{u,ex} \overline{\tilde{C}_i^{v,ex}} - \overline{b_i^{v,ex}} \tilde{C}_i^{u,ex}\end{aligned}$$

Here $C_i^{u,in/ex} = \tilde{u}_L^{in/ex}(x_i)$, and $\tilde{C}_i^{u,in/ex} = \tilde{u}_R^{in/ex}(y_i)$.

We reset the boundary form by choosing an extension that corresponds to

the physical meaning, i.e. maintains flow through the orifice:

$$\begin{aligned} a_i &:= -a_i^{in} = a_i^{ex}, \\ b_i &:= -b_i^{in} = b_i^{ex}, \\ C_i^{in} &= C_i^{ex}, \\ \tilde{C}_i^{in} &= \tilde{C}_i^{ex}, \\ i &= 1, 2, ...N \end{aligned} \tag{52}$$

Let us write the conditions as a system of $2N$ equations for $i = 1, 2, ...N$:

$$\begin{cases} \sum_{j\neq i} a_j G^L(x_i, x_j, k) + a_i g_i^L(k, k_0) = \\ \qquad\qquad -a_i g_i^{in}(k, k_0) - b_i G^{in}(x_i, y_i, k) \\ \sum_{j\neq i} b_j G^R(y_i, y_j, k) + b_i g_i^R(k, k_0) = \\ \qquad\qquad -b_i g_i^{in}(k, k_0) - a_i G^{in}(y_i, x_i, k) \end{cases}, \tag{53}$$

where $g_i^\bullet(k, k_0) = \left[G^\bullet(x, z_i, k) - G^\bullet(x, z_i, k_0)\right]_{x\to z_i}$, z_i is either x_i or y_i, depending on the side. Note that $g_i^{in}(k, k_0)$ does not depend on the side due to the symmetry of small resonators, and $G^{in}(y_i, x_i, k) = G^{in}(x_i, y_i, k)$ due to the general symmetry property of the Green's functions. The first part of the theorem is proved.

Next, we consider the limit $N \to \infty$.

Setting $h = \epsilon$ and passing to the limit $\epsilon \to \infty$, we use the expressions for the Green's functions (29) and obtain the coefficients for the limit conditions $\left(\lambda_{i,j}^\epsilon = \frac{i^2\pi^2}{w^2} + \frac{j^2\pi^2}{\epsilon^2}\right)$:

$$\hat{G}_\epsilon(k) = \frac{1}{\epsilon}\sum_{i=0}^{\infty}\sum_{j=0}^{\infty}\frac{c_{i,j}}{w}(-1)^i \cos^2\frac{\pi j}{2}\frac{1}{k^2 - \lambda_{i,j}^\epsilon}$$

$$\hat{g}_\epsilon(k, k_0) = \frac{1}{\epsilon}\sum_{i=0}^{\infty}\sum_{j=0}^{\infty}\frac{c_{i,j}}{w}\cos^2\frac{\pi j}{2}\frac{k_0^2 - k^2}{(k^2 - \lambda_{i,j}^\epsilon)(k_0^2 - \lambda_{i,j}^\epsilon)}$$

$$c_{i,j} = 2^{2-\delta_i-\delta_j}, \quad \delta_i = \begin{cases} 0, & i \neq 0 \\ 1, & i = 0 \end{cases} \quad \text{- Kronecker delta function}$$

Let us express the limits $\hat{G}(k) = \lim_{\epsilon\to 0}\hat{G}_\epsilon(k)$, $\hat{g}(k, k_0) = \lim_{\epsilon\to 0}\hat{g}_\epsilon(k, k_0)$, for convenience further multiplying them by an infinitesimal value $dy = \epsilon$:

$$\hat{G}(k)dy = \frac{1}{wk^2} + \frac{2}{w}\sum_{i=1}^{\infty}\frac{(-1)^i}{k^2 - \frac{i^2\pi^2}{w^2}}$$

$$\hat{g}(k,k_0)dy = \frac{k_0^2-k^2}{wk_0^2k^2} + \frac{2}{w}\sum_{i=1}^{\infty}\frac{k_0^2-k^2}{(k^2-\frac{i^2\pi^2}{w^2})(k_0^2-\frac{i^2\pi^2}{w^2})}$$

We give the following formulas for the series:

$$\sum_{i=1}^{\infty}\frac{1}{(i^2-a^2)(i^2+b^2)} = \frac{a^2+b^2-a^2b\pi\coth(b\pi)-ab^2\pi\cot(a\pi)}{2a^2b^2(a^2+b^2)}$$

$$\sum_{i=1}^{\infty}\frac{(-1)^i}{i^2-a^2} = \frac{1-a\pi\csc(a\pi)}{2a^2},$$

We use them to get explicit expressions for the limits:

$$\hat{G}(k)dy = \frac{1}{k\sin kw}$$

$$\hat{g}(k,k_0)dy = \frac{\coth pw}{p} + \frac{\cot kw}{k}$$

$$p := \sqrt{-k_0^2}$$

Consider the general form for the eigenfunctions of the model operator H^N corresponding to the eigenvalue k^2:

$$u_n(x) = \begin{cases} \sum_{j=1}^n \alpha_j^{ex} G(x,x_j,k) & x\in\Omega_L \\ \alpha_i^{in}G_i(x,x_i,k) + \beta_i^{in}G_i(x,y_i,k) & x\in\Omega_i \\ \sum_{j=1}^n \beta_j^{ex} G(x,y_j,k) & x\in\Omega_R \end{cases}.$$

In order to correlate $a_\bullet, b_\bullet$ and $\alpha_\bullet, \beta_\bullet$, and express the conditions (53) in terms of $\alpha_i^{in,ex}$, we have to isolate singularities of $G_i(x,x_i,k_0)$. For each hole l, do the following:

$$u_n(x) = \begin{cases} \alpha_l^{ex}G^L(x,x_i,k_0) + \alpha_l^{ex}g^L(x,x_i,k,k_0) + \sum_{j\neq l}^n \alpha_j^{ex}G^L(x,x_j,k) & x\in\Omega^L \\ \alpha_l^{in}G_l(x,x_l,k_0) + \alpha_l^{in}g_l(x,x_l,k,k_0) + \beta_l^{in}G_l(x,x_l',k) & x\in\Omega_l \\ \alpha_j^{in}G_j(x,x_j,k) + \beta_j^{ln}G_j(x,x_j',k) & x\in\Omega_{j\neq l} \\ \sum_{j=1}^n \beta_j^{ex}G^R(x,x_j',k) & x\in\Omega_R \end{cases} \tag{54}$$

$$g^\bullet(x,z,k,k_0) = G^\bullet(x,z,k) - G^\bullet(x,z,k_0)$$

Comparing this with (51) and using (52) we get

$$\begin{cases} \alpha_i := \alpha_i^{ex} = -\alpha_i^{in} \\ \beta_i := \beta_i^{ex} = -\beta_i^{in} \end{cases}$$

and the (53) conditions take the following form:

$$\begin{cases} \alpha_i g_i^L(k,k_0) + \sum_{j\neq i}^N \alpha_j G^L(x_i,x_j,k) = -\alpha_i \hat{g}(k,k_0) - \beta_i \hat{G}(k) \\ \beta_i g_i^R(k,k_0) + \sum_{j\neq i}^N \beta_i G^R(x'_i,x'_j,k) = -\beta_i \hat{g}(k,k_0) - \alpha_i \hat{G}(k) \end{cases} \tag{55}$$

Let also

$$u_i^L = u(x_i) = \alpha_i g_i^L(k,k_0) + \sum_{j\neq i}^N \alpha_j G^L(x_i,x_j,k)$$

$$u_i^R = u(y_i) = \beta_i g_i^R(k,k_0) + \sum_{j\neq i}^N \beta_i G^R(y_i,y_j,k)$$

The (55) condition can be represented as

$$\begin{cases} u^R + u^L = -(\beta_i + \alpha_i)(\hat{G}(k) + \hat{g}(k,k_0)) \\ u^R - u^L = (\beta_i - \alpha_i)(\hat{G}(k) - \hat{g}(k,k_0)) \end{cases}$$

Denote $r_+^\delta(k) := \left[\epsilon\hat{g}(k,k_0) + \epsilon\hat{G}(k)\right]^{-1}$, $r_-^\delta(k) := \left[\epsilon\hat{g}(k,k_0) - \epsilon\hat{G}(k)\right]^{-1}$, and express the coefficients

$$\begin{cases} \alpha_i = \left[r_-^\delta(k)(u^R - u^L)/2 - r_+^\delta(k)(u^R + u^L)/2\right]\epsilon \\ \beta_i = -\left[r_-^\delta(k)(u^R - u^L)/2 + r_+^\delta(k)(u^R + u^L)/2\right]\epsilon \end{cases}$$

Let $\breve{u} = (u^R - u^L)/2, \overline{u} = (u^R + u^L)/2$. Multiplying each of these $2N$ equations by $G^L(x,x_i,k)$ or $G^R(x,x'_i,k)$ and summing, we get

$$\begin{cases} \sum_{i=1}^N \alpha_i G^L(x,x_i,k) = \sum_{i=1}^N G^L(x,x_i,k)\left[r_-^\delta(k)\breve{u} - r_+^\delta(k)\overline{u}\right]\epsilon \\ \sum_{i=1}^N \beta_i G^R(x,x'_i,k) = \sum_{i=1}^N G^R(x,x'_i,k)\left[-r_-^\delta(k)\breve{u} - r_+^\delta(k)\overline{u}\right]\epsilon \end{cases}$$

The left side of this expression is the original eigenfunction, and the right side contains the values of this function at the hole points, multiplied by the

distance between them $dx = \epsilon$, which makes the expression an integral sum. Finally, considering the limit $N \to \infty$, we obtain an integral equation for some functions $u^L(x), u^R(x)$ acting in the domains Ω^L, Ω^R respectively .

$$\begin{cases} u^L(x) = \int_\Gamma G^L(x,y,k)\left[r_-(k)\check{u} - r_+(k)\overline{u}\right] dy \\ u^R(x) = \int_\Gamma G^R(x,y,k)\left[-r_-(k)\check{u} - r_+(k)\overline{u}\right] dy \end{cases}$$

$$\begin{aligned} r_-(k) &= \lim_{\delta\to 0} r_-^\delta = \frac{k\sin kw}{\cos kw - 1} \\ r_+(k) &= \lim_{\delta\to 0} r_+^\delta = \frac{k\sin kw}{\cos kw + 1} \end{aligned} \tag{56}$$

These integral equations are equivalent to the following eigenvalue problem with boundary conditions:

$$\begin{cases} \Delta u + k^2 u = 0 \\ \frac{\partial u}{\partial n^L}|_{\Gamma^L} = r_-(k)\check{u} - r_+(k)\overline{u}|_{\Gamma^L} \\ \frac{\partial u}{\partial n^R}|_{\Gamma^R} = -r_-(k)\check{u} - r_+(k)\overline{u}|_{\Gamma^R} \\ \frac{\partial u}{\partial n}|_{\partial\Omega_0\setminus\Gamma} = 0 \end{cases}$$

or

$$\begin{cases} \Delta u + k^2 u = 0 \\ \frac{\partial u}{\partial n^R}|_{\Gamma^R} + \frac{\partial u}{\partial n^L}|_{\Gamma^L} = -r_+(k)(u_R + u_L)|_\Gamma \\ \frac{\partial u}{\partial n^R}|_{\Gamma^R} - \frac{\partial u}{\partial n^L}|_{\Gamma^L} = -r_-(k)(u_R - u_L)|_\Gamma \\ \frac{\partial u}{\partial n}|_{\partial\Omega_0\setminus\Gamma} = 0 \end{cases}$$

Let us formulate the results of this section in the form of a theorem.

Theorem 1.2.1. *Let $\psi_n^N(x), n = 1, 2...$ be the eigenfunctions of the perturbed model operator H^N from the family described above.*

1. *The functions $\psi_n^N(x)$ have the following form:*

$$u_n(x) = \begin{cases} \sum_{j=1}^n \alpha_j G(x, x_j, k) & x \in \Omega_L \\ -\alpha_i G_i(x, x_i, k) - \beta_i G_i(x, y_i, k) & x \in \Omega_i \\ \sum_{j=1}^n \beta_j G(x, y_j, k) & x \in \Omega_R \end{cases} .$$

where the coefficients satisfy the following system of $2N$ *conditions* ($i = 1, 2, ...N$*):*

$$\begin{cases} \alpha_i g_i^L(k,k_0) + \sum_{j\neq i}^N \alpha_j G^L(x_i,x_j,k) = -\alpha_i \hat{g}(k,k_0) - \beta_i \hat{G}(k) \\ \beta_i g_i^R(k,k_0) + \sum_{j\neq i}^N \beta_i G^R(x'_i,x'_j,k) = -\beta_i \hat{g}(k,k_0) - \alpha_i \hat{G}(k) \end{cases} \tag{57}$$

2. *In the* $N \to \infty$ *limit, the* $\psi_n^N(x)$ *functions converge to* $\psi(x) = \begin{cases} u^L(x), x \in \Omega_L \\ u^R(x), x \in \Omega_R \end{cases}$ *- solutions of the following pair of integral equations (functions* r^+, r^- *are defined in* (56)*):*

$$\begin{cases} u^L(x) = \int_\Gamma G^L(x,y,k)\left[r_-(k)\check{u} - r_+(k)\overline{u}\right] dy \\ u^R(x) = \int_\Gamma G^R(x,y,k)\left[-r_-(k)\check{u} - r_+(k)\overline{u}\right] dy \end{cases}$$

which correspond to the following eigenvalue problem for the differential operator:

$$\begin{cases} \Delta u + k^2 u = 0 \\ \frac{\partial u}{\partial n^R}|_{\Gamma^R} + \frac{\partial u}{\partial n^L}|_{\Gamma^L} = -r_+(k)(u_R + u_L)|_\Gamma \\ \frac{\partial u}{\partial n^R}|_{\Gamma^R} - \frac{\partial u}{\partial n^L}|_{\Gamma^L} = -r_-(k)(u_R - u_L)|_\Gamma \\ \frac{\partial u}{\partial n}|_{\partial\Omega_0\setminus\Gamma} = 0 \end{cases}$$

1.2.3 Barrier of strips: Numerical calculations

In this section, numerical results are presented for a system with a corrugated narrow strip barrier. The Mathematica system was used.

Examples of numerically obtained eigenfunctions are shown in Fig.13. Graphs are organized similarly to Fig.7 (see the description in the 1.1.7 section).

The graphs in Fig.14 show numerically obtained data for systems with a barrier of 25 resonators (bands). The marginal function is also shown in gray on the graph. As can be seen from the figure, the theoretically predicted asymptotes and zeros are present on the numerical graphs, and also, on each graph, there are areas where the values strongly deviate from the theoretical ones. At the moment we do not have a good explanation for this deviation.

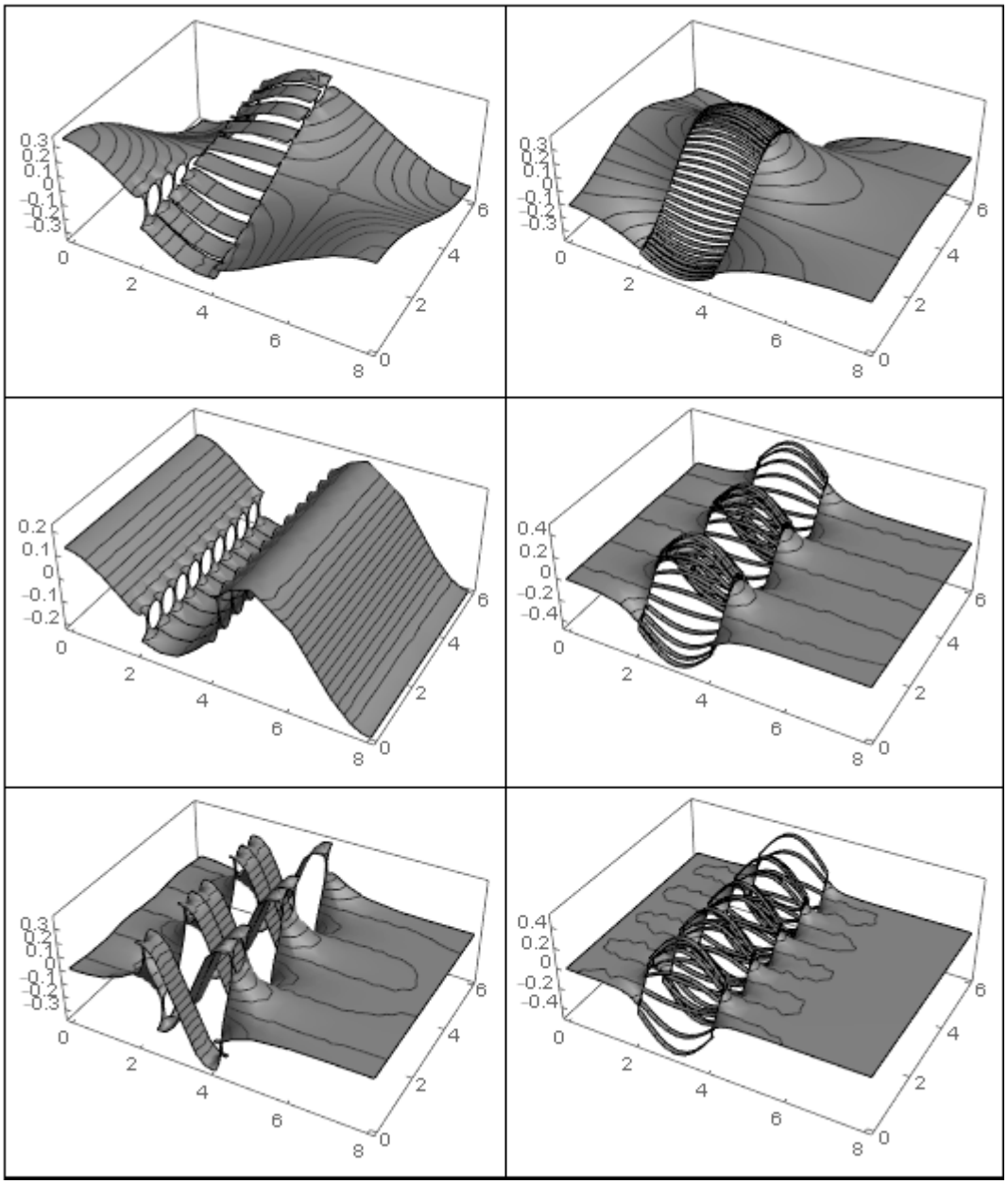

Figure 13 – Examples of numerically constructed eigenfunctions of an operator with a corrugated barrier of strips. Left - $N = 10$, right - $N = 50$. The energy increases from the top line to the bottom, in each column. (nonconsecutive eigenfunctions are given). Hole size $\delta = 0.1\epsilon$.

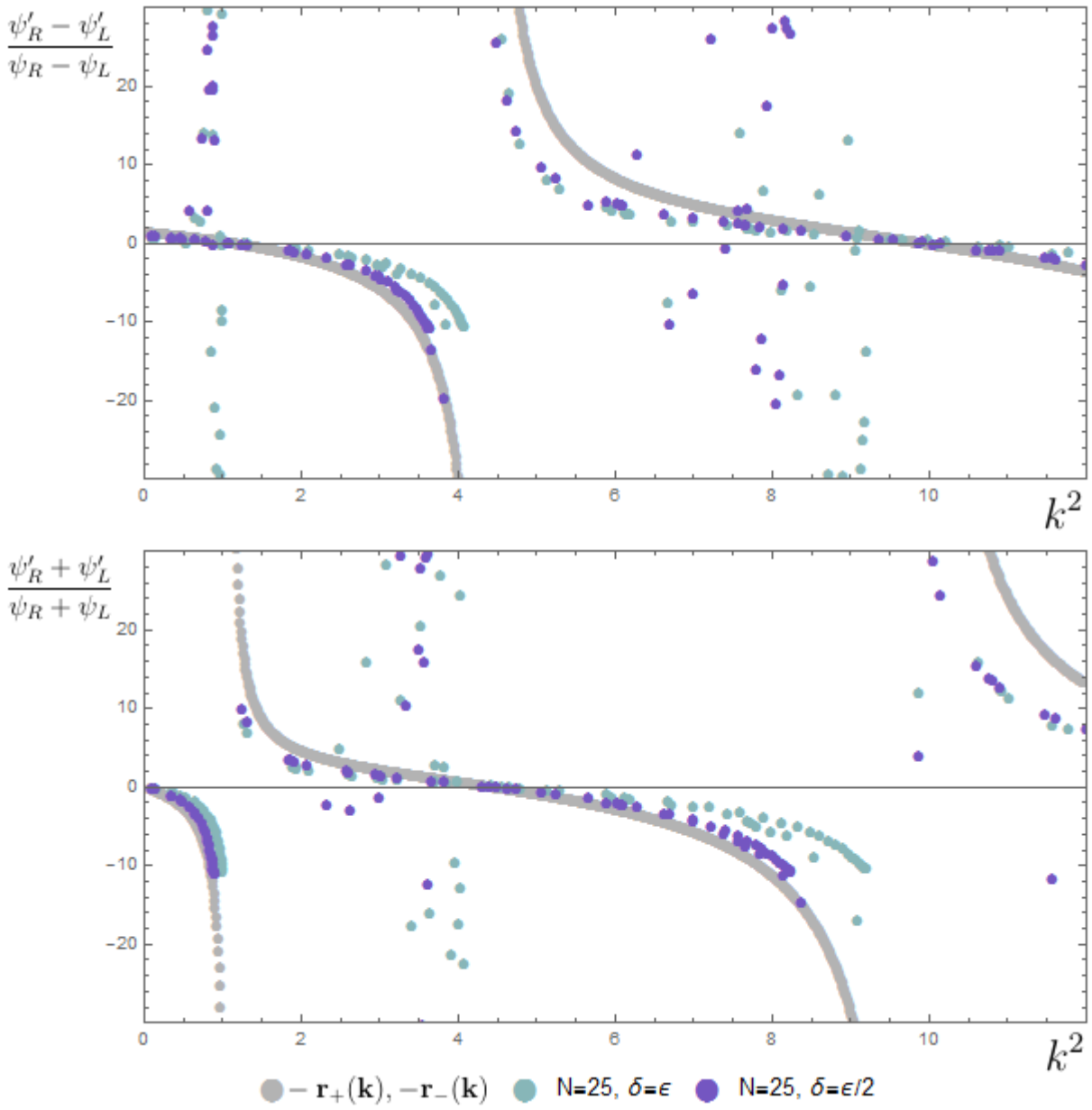

Figure 14 – System with translucent barrier, corrugated strips. Graphs of the ratio of the sums and differences of the derivatives of the function on different sides of the barrier to its values. Each point corresponds to a specific eigenfunction, points of the same color - the same geometry of the system, with the indicated parameters N and δ (other parameters are unchanged). Three sets of points are shown: gray points - the theoretical limit, $-r_-(k)$ - above and $-r_+(k)$ - below, the remaining two sets are for holes equal to the width of the strips and for holes equal to half the width of the strips.

1.2.4 Conclusions

In this chapter, we have considered boundary perturbation with multiple Helmholtz resonators connected through small holes. In particular, we were interested in the limit as the number of resonators tends to infinity.

In the first part, the theoretical base is given and some existing results are presented, which show the general direction of development of thought within the framework of this topic. In the second half of the first part, the results for the system we developed with a strip boundary are presented, which include an analytical part with the proof of the theorem on the limit problem and a numerical part that supports the theory.

In the second part, we propose a new application of the concept of perturbation by means of a corrugated boundary to the case of a barrier between two resonators. For this case, we present a study of a strip barrier, with results similar to the first part.

In the future, we plan to continue research on this topic, with the inclusion of the mass density coefficient in the system under consideration, which will make it possible to make the barrier infinitely thin.

In the next chapter, we continue the study of systems with semitransparent barriers on a plane, considering a singular delta potential concentrated on a straight line.

Chapter 2. Potentials concentrated on one-dimensional sets

In this chapter, we consider problems about quantum systems in which the potential is concentrated on a set of measure zero with respect to the dimension of the underlying space. In particular, the main results concern a system with a potential concentrated on a line in the space $\mathbb{R}^3$ and a system with a potential on two parallel lines in the space $\mathbb{R}^2$. The spectrum of operators is investigated, namely, theorems on the boundary of the continuous spectrum are proved and the number of points of the discrete spectrum, as well as the gap between the continuous spectrum and the first point of the discrete spectrum are estimated.

A large number of studies in recent years have focused on systems with potentials concentrated on a one-dimensional set in $\mathbb{R}^2$ or $\mathbb{R}^3$. In addition to being interesting from a mathematical point of view, the systems have important physical interpretations, such as modeling the interactions of long molecules.

There are many works that explore this topic [47, 50, 49, 51, 52, 53, 54, 55, 56, 58, 59, 60, 64, 65]. A common approach to describing such potentials is based on the theory of self-adjoint extensions of symmetric operators. A similar model has also been developed for narrow holes in surfaces [63, 62], and for potentials concentrated on hypersurfaces [48, 46, 57] (surfaces of dimension 1 less than the main space are called hypersurfaces).

In the **first section** we provide a brief overview of the existing results needed for what follows, including:

- A method for describing operators with singular interactions based on the use of a formula for the resolvent similar to Krein's formula,
- The Birman-Schwinger method, given, for example, in [78], allows, by constructing an operator in a certain way, to find an upper bound for the number of points in the discrete spectrum,

as well as some of the systems considered in existing works and the corresponding results.

Our first main result for this chapter is given in **the second section**. The system considered in it consists of two parallel straight lines in a plane, with a potential of variable intensity concentrated on them. This system is proposed as a model for the interaction of long molecules, such as DNA, in situations where the structure of these molecules creates different types of interaction. The particle whose bound states we are studying is in this case a possible factor participating in the process of fixing the molecules relative to each other.

The third section is devoted to a system with a simple geometry: a straight line is located in three-dimensional space, a delta potential with a variable intensity is concentrated on it. Systems of this type are a representative of a well-studied class of models. They can be generalized as the Schrödinger operator in 3D, with a singular delta interaction centered on a subset of measure zero, with a codimension of two (i.e. a one-dimensional subset), and such systems are often referred to as leaky quantum wires (leaky quantum wires). These models, containing a delta potential focused on one-dimensional subsets, are designed to approximate the behavior of quantum systems such as quantum wires. The operator can be formally written as

$$-\Delta - \alpha\delta(x - \gamma),$$

where γ corresponds to the wire line. An important property of such models is the possibility of tunneling between different parts of the wire, which reflects the property of the systems being modeled. The region outside the wire is classically a band gap, therefore, for bound states, the probability of finding a particle in this region tends exponentially to zero and all energies of the bound states are negative. In the source [72] you can find a complete overview of different types of model graphs, their comparison and results.

One of the most important characteristics of quantum wires is the existence and number of bound states, which corresponds to the localized states of particles. To investigate the spectrum of an operator, we use a well developed method, using a formula similar to Krein's formula for the resolvent of a perturbed operator, described in the first section. This approach allows using theorems from perturbation theory.

2.1 Overview of existing results

2.1.1 Resolvent of an operator with singular interactions

First, we present a generalized method for describing operators with singular interactions. This method is used in most of the examples of systems discussed below. The method has been developed over a number of papers, one of the first appearances of the method was in Russian papers in 1977 and 1983, [77, 76], where one-dimensional lines in three-dimensional space were considered and a formula similar to Krein's resolvent was used. Later, in the 1994 article [49], this issue was considered in the most general sense, without limiting the number of dimensions of the main space. Subsequent articles dealing with such systems rely heavily on the variant of the method from [49]. Also, a more specific form of the method can be found in the new 2017 paper [47], which deals with three-dimensional space. The formula for the resolvent was fully presented in [64]. Here we present the method in a form similar to these works.

There are many studies using this procedure for various types of lines, [53, 56, 74, 55, 75]. We also consider cases of the two-dimensional space $\mathbb{R}^2$, with subspaces of co-dimension 1 [68, 69, 70], on bending lines and cycles [51, 60], as well as for lines of finite length and different types of singular interactions on lines [52, 73, 71]. The model of windows in the form of narrow slots in the boundary, which can be considered as a generalization of the singular potential, was proposed in [79, 16, 63, 62].

So, first we present the derivation of the formula for the Kerin-type resolvent (see [64]). We restrict ourselves to the case of a three-dimensional space, i.e. basic Hilbert space:

$$\mathbb{H} := L^2(\mathbb{R}^3)$$

Consider the Laplace operator in $\mathbb{H}$:

$$-\Delta : D(\Delta) \to L^2,$$

defined on functions from Sobolev space (i.e. functions with derivatives up to order k belonging to L^2)

$$D(-\Delta) = H^2(\mathbb{R}^3).$$

It is known that $-\Delta$ is self-adjoint on this space.

For any parameter z belonging to the Laplacian resolvent set $\rho(-\Delta) = \mathbb{C} \setminus [0, \infty)$, we define the resolvent as a bounded operator:

$$R^z := (-\Delta - z)^{-1} : L^2 \to H^2.$$

Consider the bounded operator

$$\tau : H^2 \to X,$$

acting on the complex Banach space X and its dual on the dual space X'. (For a closed linear operator $A : X \to Y$, the adjoint operator is defined through the expression: $(A^* l)x = l(Ax),\ \forall x \in D(A), l \in D(A^*) \subseteq Y')$.

Let's introduce operators:

$$R^z_\tau = \tau R^z : L^2 \to X,$$

$$\check{R}^z_\tau = R^z_\tau : X' \to L^2,$$

which are bounded.

Let Z be an open subset of $\rho(-\Delta)$ symmetric about the Real axis, i.e.

$$Z = \{z : z \in \rho(-\Delta)\}, z \in Z \Rightarrow \bar{z} \in Z$$

Assume that, for any $z \in Z$, there exists a closed operator $Q^z : D \subseteq X' \to X$ satisfying the following conditions:

$$Q^z Q^w = (zw) R^w_\tau \check{R}^w_\tau, \tag{58}$$

$$\forall l_1, l_2 \in D,\ l_1(Q^{\bar{z}} l_2) = \overline{l_2(Q^z l_1)}. \tag{59}$$

These operators will be used to construct a family of self-adjoint operators that are the same as $-\Delta$ when restricted to the kernel τ. The family can be parametrized by the symmetric operators $\Theta : D(\Theta) \subseteq X' \to X$. We define this family:

$$Q^z_\Theta = \Theta + Q^z : D(\Theta) \cap D \subseteq X' \to X, \tag{60}$$

$$Z_\Theta := \{z \in \rho(-\Delta) : (Q^z_\Theta)^{-1}, (Q^z_\Theta)^{-1} \text{ exists and bounded}\}. \tag{61}$$

Using these definitions, we can formulate without proof a theorem on the resolvents of operators with singular interactions:

Theorem 2.1.1. *Let's assume that the conditions*

$$Z_\Theta \neq \emptyset$$

and

$$Ran\ \tau^* \cap L^2 = \{0\}$$

are fulfilled. Then bounded operator

$$R^z_{\tau,\Theta} := R^z - \check{R}^z_\tau (Q^z_\Theta)^{-1} R^z_\tau,\ z \in Z_\Theta,$$

is the resolvent of the self-adjoint operator $-\Delta_{\tau,\Theta}$ *defined as follows:*

$$D(\Delta_{\tau,\Theta}) = \{f \in L^2 : f = f_z - \check{R}^z_\tau (Q^z_\Theta)^{-1} \tau f_z, f_z \in D(\Delta)\}, \tag{62}$$

$$(-\Delta_{\tau,\Theta} - z) f := (-\Delta - z) f_z, \tag{63}$$

which coincides with the Laplacian $-\Delta$ *on the set* $\ker \tau$.

2.1.2 Singular interactions as generalized boundary conditions

This section presents a method for describing operators with singular interactions in terms of generalized boundary conditions. This method is extremely useful in the study of the spectrum and is used when working with the model of loose quantum wires [53, 54]. We use this method in the last section to describe the δ interaction on a line in 3D space.

The method of generalized boundary conditions allows one to work with singular interactions on a line in $\mathbb{R}^3$. The line can be either finite or infinite. Let a smooth continuous function of one variable describe this line:

$$\gamma(s) : \mathbb{R} \to \mathbb{R}^3,$$

moreover, it belongs to C^2 almost everywhere. Let Γ denote the set of values of γ, that is, be a one-dimensional line in $\mathbb{R}^3$, with the necessary smoothness restrictions. The s parameter corresponds to the length of the line (signed), from some origin.

Next, we impose the following condition, which excludes the possibility of self-intersection:

$$\begin{aligned} &\exists c = const > 0 : \\ &\qquad \forall s_1, s_2 \in \mathbb{R}, \\ &\qquad |\gamma(s_1) - \gamma(s_2)| \geq c|s_1 - s_2| \end{aligned} \tag{64}$$

Now we introduce the Frenet frame for Γ, i.e. triplet $(t(s), b(s), n(s))$, which corresponds to each point on the curve: $t(s)$ - tangent unit vector co-directed with the curve, $b(s)$ - unit the binormal vector perpendicular to the normal and the tangent vector, and $n(s)$ the unit principal normal, which is orthogonal to $t(s)$ and lies in the point's acceleration plane, if the curve is considered as a time-dependent trajectory. Classically, this triplet exists and is uniquely defined, in those regions where the line has nonzero curvature $k(s) = ||\gamma''|| : \mathbb{R} \to [0, \infty)$. We additionally assume that on any intervals where $k(s) = 0$ (i.e. when the line coincides with the straight line), the triplet takes some fixed value $(t_l(s), b_l(s), n_l(s))$, so that the first vector is a tangent, and the other two are arbitrary orthogonal vectors perpendicular to the tangent.

Thus, the triplet $(t(s), b(s), n(s))$ consists of piecewise continuous functions, with the help of which we can define a shifted piecewise smooth function:

$$\Gamma_r = \{\gamma_r(s) = \gamma(s) + \xi b(s) + \eta n(s)\,,\ \ r = (\xi^2 + \eta^2)^{1/2}\,,\ \xi\,, \eta \in \mathbb{R}\}\,.$$

proceeding from (64), there exists $r_0 > 0$ such that $\Gamma_r \cap \Gamma = \emptyset$ is executed For all $r \leq r_0$.

So How any the function $f \in H^2_{\text{loc}}(\mathbb{R}^3 \setminus \Gamma)$ is continuous to $\mathbb{R}^3 \setminus \Gamma$, her the attachment in Γ_r uniquely $r < r_0$ is defined . Let's denote this embedding $f_{\Gamma_r}(s)$.

Next, we construct a self-adjoint operator corresponding to the Schrödinger operator, with δ-potential centered on Γ. Let's denote it $-\Delta_{\alpha,\Gamma}$.

Theorem 2.1.2. *Let $D(-\Delta_{\alpha,\Gamma}) : D(-\Delta_{\alpha,\Gamma}) \to L^2(\mathbb{R}^3)$ act on the functions as*

$$-\Delta_{\alpha,\Gamma} f(x) = -\Delta f(x)\,,\ \ x \in \mathbb{R}^3 \setminus \Gamma\,,$$

and contains functions that satisfy the following conditions:

1. *Limits*

$$\Xi(f)(s) = -\lim_{r\to 0}\frac{1}{\ln r}f_{\Gamma_r}(s),$$
$$\Upsilon(f)(s) = -\lim_{r\to 0}(f_{\Gamma_r}(s) + \Xi(f)(s)\ln r),$$

exist, i.e. belong to $\mathbb{R}$*, do not depend on the direction of* $\frac{1}{r}(\xi,\eta)$*, and define functions from* $L^2(\mathbb{R})$*,*

2. *The following condition is met:*

$$2\pi\alpha\Xi(f)(s) = \Upsilon(f)(s). \tag{65}$$

Then this operator describes a system with a singular δ*-interaction on* Γ*.*

2.1.3 Birman-Schwinger method

This section describes a method for "counting" the eigenvalues of an operator, which is often used to obtain estimates for the size of a discrete spectrum. We will follow the theorem presented in [78] (Chapter XIII, Section 3-C). In this paper, the method is applied in the last section of the chapter to find an upper bound on the number of bound states for a system with an inhomogeneous singular interaction on a straight line in three-dimensional space.

Below we briefly present the essence of the proof of Theorem XIII.10 in [78].

Theorem 2.1.3. *Let the Schrödinger operator* $H_\lambda : H^2(\mathbb{R}^3) \to L^2(\mathbb{R}^3)$ *be a perturbation of the operator* $H_0 = -\Delta$*, another operator* $V \in R$ *(R - Rolnik class see [78], Volume 2)*

$$H = H_0 + \lambda V.$$

Then the following constraint on $N(V)$*, the number of bound states of the system, takes place:*

$$N(V) \le \frac{1}{16\pi^2}\int\frac{\big|V(X)\big|\big|V(y)\big|}{|xy|^2}d^3xd^3y$$

In particular, $N(V) < \infty$*.*

Proof. Let $E < 0$. Let us introduce the notation for the eigenvalues:

$$\mu_n(\lambda) = \mu_n(-\Delta + \lambda V).$$

Let

$$N_E(V) = \#\{n|\mu_n(1) < E\},$$

where $\#\{\bullet\}$ is the cardinal number of the set.

According to Lemma 1 XIII.2.C, [78], $\mu_n(\lambda)$ is a monotonic and continuous function of the parameter. Using the well-known fact about the Laplacian spectrum, $\mu_n(0) = 0$, we obtain

$$\mu_n(1) < E \iff \exists!\lambda \in (0,1) : \mu_n(\lambda) = E.$$

So way ,

$$\begin{aligned} N_E(V) = \#\{n|\exists\lambda \in (0,1) : \mu_n(\lambda) = E\} \leq \\ \leq \sum_{\{\lambda|\mu_k(\lambda)=E;k=1,\dots N_E(V)\}} \lambda^{-2} \leq \\ \leq \sum_{\{\lambda|\mu_k(\lambda)=E;k=1,2,\dots\}} \lambda^{-2} \end{aligned}$$

Next , we note What

$$\begin{aligned} (H_0 + \lambda V E)\psi = 0 \iff \\ \iff \lambda(|V|^{1/2}\,(H_0 - E)^{-1}|V|^{1/2})(|V|^{1/2}\,\psi) = (|V|^{1/2}\,\psi) \end{aligned}$$

which, in turn, is equivalent to

$$\lambda \int \frac{\left|V(x)\right|^{1/2} e^{-\sqrt{-E}|xy|} \left|V(y)\right|^{1/2}}{4\pi|xy|}\phi(y)dy = \phi(x) \tag{66}$$

has a non-trivial solution $\phi \in L^2$.

We construct the operator K as follows:

$$K\phi = \int \frac{\left|V(x)\right|^{1/2} e^{-\sqrt{-E}|xy|} \left|V(y)\right|^{1/2}}{4\pi|xy|}\phi(y)dy$$

Due to the fact that $V \in R$, K is a Hilbert-Schmidt operator and self-adjoint, as a consequence of the fact that the kernel is real and symmetric.

As a result,

$$\begin{aligned} \sum_{\{\mu|\mu \text{ - eigenvalue } K\}} \mu^2 = & Tr(K^*K) = \\ = & \frac{1}{16\pi^2} \int e^{-2\sqrt{-E}|xy|} \frac{\left|V(X)\right|\left|V(y)\right|}{|xy|^2} dxdy \end{aligned}$$

Further, from the expression (66) it follows:

$$\sum_{\{\lambda|\mu_k(\lambda)=E\}} \lambda^{-2} = \sum_{\{\mu|\mu \text{ - eigenvalue } K\}} \mu^2,$$

where

$$N_E(V) \leq \frac{1}{16\pi^2} \int \frac{\big|V(X)\big|\big|V(y)\big|}{|xy|^2} d^3x d^3y$$

And it remains to direct $E \nearrow 0$ to cover all bound states. □

The essence of the method used in the proof is as follows:

- We use the continuity and monotonicity of the eigenvalues as the perturbation increases to obtain

$$N_E(V) = \#\{n|\exists\lambda \in (0,1) : \mu_n(\lambda) = E\}$$

- We construct a context-specific helper operator that is linked to the original one via the λ parameter, which should have feedback to the new operator's own values. Moreover, the new operator must be a Hilbert-Schmidt operator.

- Now, using the norm of the Hilbert-Schmidt operators, we find a trace that, thanks to the feedback with the λ parameter and the property of the $0 < \lambda < 1$ parameter, gives an upper bound on the size of the discrete spectrum of the original operator.

This method will be used in the third section, where the constructed operator has a very different character, but is still associated with the feedback perturbation parameter.

The rest of the section is devoted to the results for systems with different geometries obtained using the methods described.

2.1.4 Bound states of a twisted wire in $\mathbb{R}^2$

This section contains the results of the article [51]. It considers a system in $\mathbb{R}^2$, with a perturbation in the form of a δ-interaction concentrated on a one-dimensional line Γ. The smooth line Γ in this case approaches the straight line at

infinity, but locally it deviates from the straight line. Throughout the entire line δ-interaction has a constant intensity.

First, the resolvent of the main operator is described, according to a formula similar to the one given in this section (theorem 2.1.1).

$$R^k := R_0^k + \alpha R_{dx,m}^k [I - \alpha R_{m,m}^k]^{-1} R_{m,dx}^k$$

Here $L^2(\mathbb{R})$ acts as the space X - functions on the one-dimensional line space, operators $R_{m,dx}^k, R_{dx,m}^k$ - translate and return from this space.

Turning to a more rigorous description of the system, we present the condition imposed on the line. Let Γ be a line in $\mathbb{R}^2$, the corresponding function $\gamma : \mathbb{R} \to \mathbb{R}^2$ be continuous, piecewise-C^1 smooth, with an argument, counting the length of the line.

There are the following line restrictions:

-1-

$$\left|\gamma(s) - \gamma(s')\right| \leq \left|s - s'\right|,$$

expression equivalent to continuity.

-2-

$$\exists c \in (0,1) :$$
$$\left|\gamma(s) - \gamma(s')\right| \geq c\left|s - s'\right|$$

In particular, this means that the line does not have self-intersections and too sharp corners, and also that the possible asymptotes of the line cannot be parallel to each other.

-3- Γ asymptotically approximates a straight line, in the following sense:

$$\exists d, \mu, w \in (0,1) :$$
$$1 - \frac{\left|\gamma(s) - \gamma(s')\right|}{\left|s - s'\right|} \leq d[1 + \left|s + s'\right|^{2\mu}]^{-1/2},$$
$$\forall (s, s') \in \{(s, s') : w < \frac{s}{s'} < w^{-1}\}$$

After defining the line, a family of operators is built

$$H_\epsilon(W, \gamma) := -\Delta + V_\epsilon$$

$$V_\epsilon(x) := \begin{cases} 0 & , \ x \notin \Sigma_\epsilon \\ -\frac{1}{\epsilon} W(\frac{u}{\epsilon}) & , \ x \in \Sigma_\epsilon \end{cases},$$

where Σ_ϵ - is a ϵ-neighborhood of a line, $W \in L^\infty((-1,1))$ - some function.

This family distributes the potential along a thickened line, the measure of which becomes nonzero. The first theorem concerns the convergence of operators with a distributed potential to the required operator with a singular potential.

Theorem 2.1.4.

$$H_\epsilon(W,\Gamma) \to H_{\alpha,\gamma}, \ \textit{for } \epsilon \to 0,$$

where $\alpha = \int_{-1}^{1} W(t)dt$, *convergence of operators is meant in the sense of resolvent norms convergence.*

The continuous spectrum of the operator $H_{\alpha,\gamma}$ is equivalent to the operator with a delta potential on the line:

Proposition 2.1.1. *Let* $\alpha > 0$ *and assume that* $\gamma : \mathbb{R} \to \mathbb{R}^2$ *is a continuous piecewise function belonging to* C^1 *satisfying conditions -1,2,3-. Then*

$$\sigma_{ess}(H_{\alpha,\gamma}) = [-\frac{\alpha^2}{4}, \infty).$$

And the basic bound state theorem:

Theorem 2.1.5. *Let the conditions of the previous statement be satisfied. If inequality -1- is strict for some* $s, s' \in \mathbb{R}$ *then* $H_{\alpha,\gamma}$ *has at least one isolated eigenvalue below* $-\frac{\alpha^2}{4}$.

2.1.5 Bound states of a twisted wire in $\mathbb{R}^3$

This section contains the results of the article [53]. Similarly to the previous paragraph, the system contains a line asymptotically approaching a straight line.

First, the resolvent of the main operator $H_{\alpha,\gamma}$ is constructed according to the described method (theorem 2.1.1). Here the space X is also the space of functions on the line $L^2(\mathbb{R})$, now having co-dimension equal to two. The operator $\tau : H^2(\mathbb{R}^3) \to L^2(\mathbb{R})$ acts as

$$\tau\phi(s) := \phi(\gamma(s)).$$

Its adjoint operator $\tau^* : L^2(\mathbb{R}) \to H^{-2}(\mathbb{R}^3)$ is defined via

$$(\tau^* h, w) = (h, \tau w)_l \ , \ h \in L^2(\mathbb{R}) \ , \ w \in H^{-2}(\mathbb{R}^3),$$

and can be formally written as

$$\tau^* h = h\delta_\Gamma,$$

where δ_Γ is the Dirac measure, on the set Γ.

Conditions on γ repeat -1- and -2-, but -3- is replaced with the following:

-3'- $\exists \mu \geq 0, w \in (0,1), \epsilon, d > 0$:

$$1 - \frac{\left|\gamma(s) - \gamma(s')\right|}{|s - s'|} \leq d \frac{|s - s'|}{(|ss'| + 1)(1 + (s^2 + s'^2)^\mu)^{1/2}},$$

$$\forall (s, s') \in \left\{ (s, s') : \begin{cases} w < \frac{s}{s'} < w^{-1}, \ |s + s'| > \xi(w)\epsilon \\ |s - s'| < \epsilon, \ |s + s'| < \xi(w)\epsilon \end{cases} \right\}, \xi(w) = \frac{1 + w}{1 - w}$$

The main theorem again points to the existence of one or more bound states, in the case of sufficient bending.

Theorem 2.1.6. *Let Γ and γ satisfy the described conditions, and let μ from condition -3'- : $\mu > \frac{1}{2}$. Then the operator $-\Delta_{\gamma,\alpha}$ has at least one isolated eigenvalue below the continuous spectrum.*

2.2 Potential on parallel lines in 2D

This section includes the results we published in [44]. In this section, we analyze a two-dimensional strip with boundaries formed by potentials centered on parallel lines. These potentials resemble semitransparent borders [84, 17, 67]. The potentials are assumed to be negative (ie, attractive), having a local perturbation and the same on each side of the strip, but having a shift in the direction of the straight line relative to each other. We prove the existence of an eigenvalue caused by a local perturbation of the potentials and follow its behavior with changes in the shift of the potentials relative to each other.

The result is of a biophysical nature and is a model of the interaction of long molecules, for example, during the introduction of a virus into a cell or the

connection of two DNA strands. These processes can be superficially described as follows: one molecule identifies some character sequence on the second one, approaches that position and forms a bond. In our simplest model, molecules are represented by straight lines with potentials on them, and a symbolic sequence from DNA is represented by local perturbations of potentials. A natural question arises: what factors influence the preservation of the close position of molecules during such interactions? If we consider an electron in such a system of two attractive potentials, due to local perturbations, there is a bound state for the particle. This state helps to maintain a small distance between molecules. In a real system, such a state is more stable if there is a sufficient gap between the continuous spectrum and the eigenvalue. In our model, we demonstrate that an increase in the shift between potentials leads to a decrease in the gap, that is, the most stable position is in the case of no shift. This means that the bound state of the electron is a factor that maintains the molecules in the desired position.

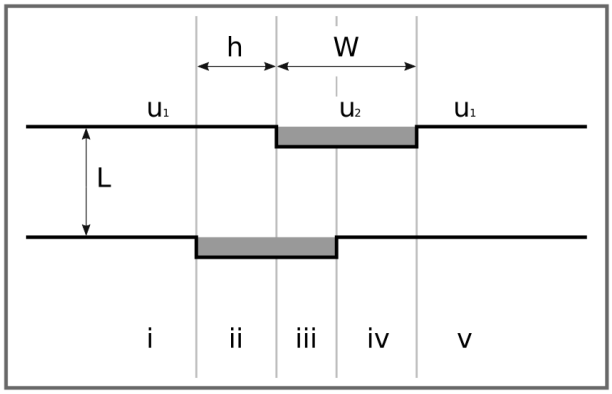

Figure 15 – A system of two parallel lines, on which a constant delta potential is concentrated, with a local variation in intensity.

Consider the system shown in Fig.15. It consists of two infinite parallel lines, at distance L, on $\mathbb{R}^2$. The attracting delta potential of constant intensity $-u_1 < 0$ is concentrated along the straight lines, except for a finite region of length W, on each straight line, on which the intensity changes to another constant $-u_2 < 0$, such that $-u_2 < -u_1$. Denote by $h < W$ the shift distance of one region W relative to another. We use the atomic system of units, where $m = 0.5, \hbar = 1$. Hence the Hamiltonian of the system is the Laplacian

$$\hat{H}\psi = -\Delta\psi,$$

defined on continuous functions $\psi \in \mathbb{L}^2(\mathbb{R})$ that satisfy the following condition on lines imposed by the delta potential:

$$\frac{\partial\psi}{\partial y}(x, y_l + 0) - \frac{\partial\psi}{\partial y}(x, y_l - 0) = -\alpha_x \psi(x, y_l) \tag{67}$$

where $y_l = 0$ or L, and $\alpha_x = u_2$ inside the perturbed region W on the line, and $\alpha_x = u_1$ outside it.

2.2.1 Continuous spectrum

Consider the continuous spectrum of the operator $\hat{H}$. Since the entire described system can be considered as a local perturbation of another system $\hat{H}_0$, for which the intensity of the potential does not change along both straight lines, the continuous spectrum coincides with the continuous spectrum of $\hat{H}_0$.

$$\sigma_c(\hat{H}) = \sigma_c(\hat{H}_0)$$

Consider the system $\hat{H}_0$. In this case, you can apply the method of separation of variables. We assume that the wave function has the form

$$\psi(x, y) = \chi(x)\xi(y).$$

Therefore, the lower bound of the continuous spectrum of the operator $\hat{H}_0$ is given by the smallest eigenvalue of the transverse problem, i.e. one-dimensional equation for the function $\xi(y)$. To find it, consider the operator $-\frac{d^2}{dy^2}$ on $\mathbb{R}$ with the following conditions at two points:

$$\begin{aligned} \xi(+0) =& \xi(-0), \\ \xi(L+0) =& \xi(L-0), \\ \frac{\partial\xi}{\partial y}(+0) - \frac{\partial\xi}{\partial y}(-0) =& -\alpha\xi(-0), \\ \frac{\partial\xi}{\partial y}(L+0) - \frac{\partial\xi}{\partial y}(L-0) =& -\alpha\xi(L-0), \end{aligned} \tag{68}$$

Theorem 2.2.1. *Continuous range operator $\hat{H}$ has kind :*

$$\sigma_c(\hat{H}) = [-max_j \kappa_j^2, \infty),$$

where κ_j are the real roots of the transcendental equation

$$\frac{4}{\alpha^2}\kappa(\kappa + L) = e^{2\kappa L} - 1 \tag{69}$$

Proof. The differential equation for the transverse part $\hat{H}$, for the eigenfunction $\xi(y)$ corresponding to the eigenvalue k^2 has the form:

$$-\frac{d^2\xi}{dy^2} = k^2\xi,$$

with additional conditions (68).

Let's take the general solutions $e^{\pm iky}$, and satisfying the conditions (68), we get (69), where $\kappa = ik \in \mathbb{R}_-,\ k \in Im(\mathbb{C})$. □

The eigenfunction must be normalized, hence decreasing at infinity is necessary, i.e. $\kappa < 0$. Considering that the function on the left side (69) takes the minimum value -1 at the point $\kappa = -\frac{\alpha}{2}$, we can conclude that there is a root κ_1 of the equation (69) such that:

$$-\alpha < \kappa_1 < -\frac{\alpha}{2}.$$

Remark. It is known that in the case of a single line, the lower limit of the continuous spectrum is equal to $-\frac{\alpha}{2}$. In the case of two lines with the conditions (68), the limit of the boundary defined by the equation (69) tends to $-\alpha^2$, as $L \to 0$. This case corresponds to a single line with potential -2α. Therefore, for the conditions (68), one obtains an eigenvalue between the value for two distant single lines and the value for one line with twice the intensity.

2.2.2 Test functions

To find the discrete spectrum, we use the variational method. consider the relation

$$E = \frac{(\hat{H}\psi, \psi)}{(\psi, \psi)},$$

whose minimum is the smallest eigenvalue of the operator $\hat{H}$.

If the test function ψ is such that this ratio is less than the lower bound of the continuous spectrum, then there is at least one eigenvalue of the operator below the continuous spectrum, and this ratio is its upper bound.

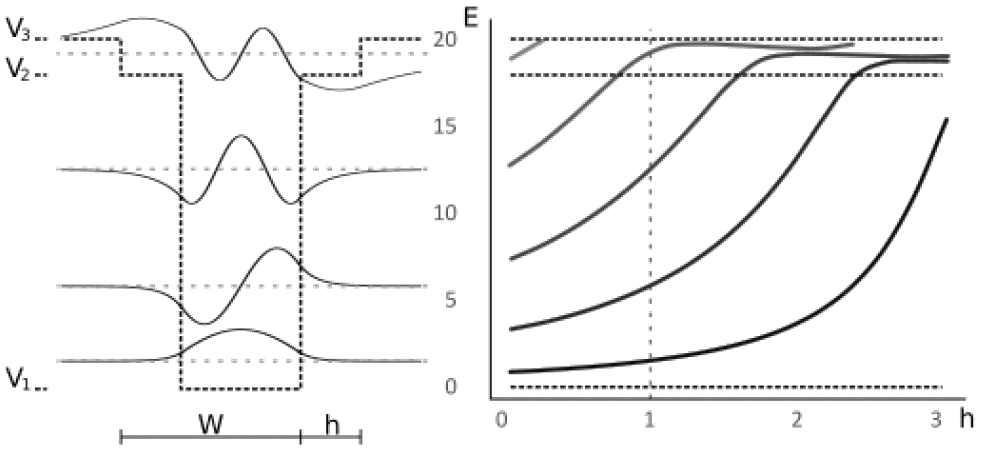

Figure 16 – Longitudinal component of the test function for $\xi_x(y)$ of symmetric type. Parameter values: $W = 3, V_1 = 0, V_2 = 18, V_3 = 20$. The left part contains the image of the stepped well potential at $h = 1$, with the designation of the energy levels and the corresponding eigenfunctions. The graph on the right shows the dependence of the energy levels on the shift h.

We will construct a test function that satisfies the (67) condition on the lines, but is not a continuous function along the X axis. However, it can be approximated with arbitrary accuracy by functions from the domain of the operator.

Specifically, we assume that

$$\psi(x, y) = \chi(x)\xi_x(y),$$

where $\xi_x(y)$ are five eigenfunctions of the operator $-\frac{d^2\xi}{dy^2}$ satisfying the conditions (68), one for each vertical band (zone) with a unique combination of intensities of delta potentials on straight lines (these zones are indicated in Fig.15 by Roman numerals).

First, consider the transverse part $\xi_x(y)$. There are 5 such functions in total, three of them are unique up to symmetry: $(u_1, u_1), (u_1, u_2), (u_2, u_2)$. Let the parameters α_1 and $\alpha_2, \alpha_1 \leq \alpha_2$, take the values u_1 or u_2. The problem is sometimes referred to as a double delta potential system in 1D. For $L > L_0 = \frac{\alpha_1+\alpha_2}{\alpha_1\alpha_2}$, there are two solutions. If we smoothly change the intensities of the delta potentials so that they become equal, these two solutions are transformed into symmetric and asymmetric with respect to the center of symmetry of the problem. We will call the two solutions functions of symmetric and asymmetric type, depending on which function they pass into. The restrictions on the transverse part of the

energy $\tilde{E} = (0.5p)^2$ take the following form:

$$e^{-pL} = \frac{(p - a_1)(p - a_2)}{a_1 a_2}$$

Let us now analyze the longitudinal component $\chi(x)$ of the test function. The transverse variants create five regions, each with its own energy $\tilde{E}_x$. These energy levels can be coupled into a step potential for the longitudinal component of the function. We will consider two separate cases: in one, all transverse components are functions of symmetric type, in the other, they are of asymmetric type. These two variants produce symmetrical longitudinal step potentials, a variation on the classical square well potential, in which an additional step is added on each side. We will call this potential a stepped well (an example of such a potential is shown in Fig.16). Let V_1, V_2, V_3 denote constant potential levels, from smallest to largest. Solutions for the cases $V_1 < E < V_2$ and $V_2 < E < V_3$, which we will call lower and upper, respectively, satisfy different restrictions on energy levels. Let $k_1 = \sqrt{E - V_1}, k_2 = \sqrt{E - V_2}, k_3 = \sqrt{E - V_3}$ and introduce the abbreviation:

$$T_r(E) = \tan(k_1 r). \tag{70}$$

The restrictions on the energies of symmetric and asymmetric solutions are as follows:

$$\begin{aligned} \text{for sym .: } T_r(E) &= \frac{k_2}{k_1} \tan\left(\arctan\left(\frac{k_3}{k_2}\right) - k_2 h\right), \\ \text{for asym .: } T_r(E) &= -\frac{k_2}{k_1} \cot\left(\arctan\left(\frac{k_3}{k_2}\right) - k_2 h\right) \end{aligned} \tag{71}$$

These equations cover the case $E < V_2$, for complex values of k_2. However, in the future, it will sometimes be more convenient to use another expression for the right side of these equations, which avoids the use of complex numbers (here $\tilde{k}_2 = \sqrt{V_2 - E}$):

$$\begin{aligned} T_r(E) = \frac{\tilde{k}_2}{k_1} \tanh\left(\operatorname{arctanh}\left(\frac{k_3}{\tilde{k}_2}\right) + \tilde{k}_2 h\right) = \\ = \frac{\tilde{k}_2}{k_1} \coth\left(\operatorname{arccoth}\left(\frac{k_3}{\tilde{k}_2}\right) + \tilde{k}_2 h\right) \end{aligned} \tag{72}$$

2.2.3 Existence of bound states

The generated functions can be used to find an upper bound for the discrete spectrum $\hat{H}$.

Theorem 2.2.2. *The stepped well potential (see fig. 16) always has at least one eigenvalue below the continuous spectrum σ_c.*

Proof. We denote the right-hand side of (70) as $T(E)$, and $K(E)$ denote the right-hand side of (71) (or (72), which is equivalent). We will prove that there exists an interval on which $T(E) - K(E)$ is continuous and takes values of different signs on the boundaries. Note that in the boundary cases $V_2 = V_1, V_2 = V_3, h = 0$ or $h = W$, the problem turns into a square potential well, for which the existence of a bound state is proven.

First note that $T(V_1) = 0$ and $K(+0) = +\infty$. The only discontinuity points of the functions are the vertical asymptotes. Let us denote these asymptotes A_T and A_K for T and K, respectively. Then $T(A_T - 0) = +\infty, K(A_K - 0) = -\infty$, and hence if $\min(A_T, A_K) \leq V_3$ then the interval $\big(0,\ min(A_T, A_K)\big)$ is the desired one.

Now consider the case $\min(A_T, A_K) > V_3$. We fix some values of the parameter W and V_2. Here $T(V_3) > 0$. Let us prove that $K(V_3) \leq 0$ for all h that are important to us. The equation for $K(E)$ asymptotes can be represented as

$$\cot(k_2 h) = -\frac{k_3}{k_2},$$

which shows that as h increases, A_K decreases monotonically, thus $K(E)$ is continuous on (V_1, V_3), only for values of h from 0 up to the point where $A_K = V_3$. The function $K(V_3) = -\frac{k_2}{k_1}\tan(k_2 h)$ is a monotonically decreasing function and when $h = 0$, $K(V_3) = 0$. This proves $K(V_3) \leq 0$, for $A_K > V_3$, and hence the interval (V_1, V_3) is the desired interval. □

Corollary 2.2.1. *The main operator $\hat{H}$ has at least one bound state.*

Proof. Continuous spectrum of the operator $\sigma_c(\hat{H}) = (V_3, +\infty)$. The constructed function satisfies the condition $\frac{(\hat{H}\psi,\psi)}{(\psi,\psi)} = E$, and can be approximated to an arbitrary degree by functions from the domain of the operator . Therefore, the value E from the 2.2.2 theorem is an upper bound for the discrete spectrum $\hat{H}$. □

2.2.4 Results

Let us now consider the constructed energy levels as functions of the parameter h. While V_2 is changing, note that the edge cases $V_2 = V_1$ and $V_2 = V_3$, produce square well-shaped potentials of width $W + h$ and $W - h$, which, as h increases, become wider and narrower respectively. If V_2 is fixed, increasing h from 0 to W turns the narrow well (W, V_3) into a wide well $(2W, V_2)$ while the energy levels change continuously.

As described above, the constructed functions, for sufficiently large L, allow us to choose one of two transverse eigenvalues: $\tilde{E}_1 < a_1$ and $\tilde{E}_2 > a_2$ for each region, and although regions with $a_1 = a_2$ generate close values, regions with different intensities (those corresponding to V_2) produce eigenvalues with a large gap between them. The choice between two values in each region corresponds to ψ eigenfunctions of symmetric and asymmetric types. Using the results, we can conclude that their energy levels are converted differently. Considering the symmetric type, from Fig.16 we can see that the smallest eigenvalue increases monotonically until it leaves the band under V_2 and reaches the smallest value of the widest square well $(2W, V_2)$. Speaking of real systems, a larger gap between the first eigenvalue and the boundary of the continuous spectrum provides greater stability of the bound state with respect to external influences. This means that bound states with this behavior are more stable for small h.

As mentioned in the introduction to the section, the considered system can be used as the simplest model for the interaction of long molecules (for example, DNA-like, or protein-like). In particular, it can be useful for better understanding the first steps in the process of attaching viral DNA to an organism molecule (identifier recognition from symbols and fixation), see for example [66].

2.3 Potential on a line in 3D

This section includes the results we published in [43]. The system on which this section is focused consists of a straight line in $\mathbb{R}^3$, with an attractive δ-potential, with varying intensity. The study is mainly guided by the sequence of steps from [53].

2.3.1 Hamiltonian for wire in 3D

Let's describe the system. The attractive potential is concentrated on a straight line in three-dimensional space. The potential intensity is $-(\alpha + \beta(s))$, where $\alpha > 0$ is a constant and $0 \leq \beta(s) \in C(a,b) \setminus \{0\}$ is a localized function of the variable s - the distance along the straight line from the origin, which is equal to zero outside some arbitrary finite interval $[a,b]$. We choose the origin on the line so that $\beta(0) \neq 0$. Note that the interval at which the function does not reset to zero can potentially be extended.

First, following [53], we describe the operator $-\Delta_{\alpha,\beta}$, which is a self-adjoint extension of the symmetric operator $-\Delta : C_0^\infty(\mathbb{R}^3 \setminus \Gamma) \to L^2(\mathbb{R}^3)$, and then we construct its resolvent.

Consider the straight line Γ defined by the function $\gamma(s) = (0,0,s) : \mathbb{R} \to \mathbb{R}^3$. Let us introduce a shifted line Γ_r, which corresponds to $\gamma_r(s) = (\xi, \eta, s)$; $(\xi^2 + \eta^2)^{1/2} = r$. Let $f \in H^2_{\text{loc}}(\mathbb{R}^3 \setminus \Gamma)$, and $f_{\Gamma_r}(s)$ be its embedding in $\Gamma_r; r > 0$.

Definition 2.3.1. *Function $f \in H^2_{\text{loc}}(\mathbb{R}^3 \setminus \Gamma) \cap L^2(\mathbb{R}^3)$ belongs to $D(-\Delta_{\alpha,\beta})$ if the following conditions are met:*
1) The following limits exist

$$\Xi(f)(s) = -\lim_{r \to 0} \frac{1}{\ln r} f_{\Gamma_r}(s),$$

$$\Upsilon(f)(s) = -\lim_{r \to 0} (f_{\Gamma_r}(s) + \Xi(f)(s) \ln r),$$

i.e. they reside in $\mathbb{R}$, do not depend on the direction of $\frac{1}{r}(\xi, \eta)$, and define functions from $L^2(\mathbb{R})$,
2) The following conditions apply:

$$2\pi(\alpha + \beta(s))\Xi(f)(s) = \Upsilon(f)(s).$$

Finally we define operator $-\Delta_{\alpha,\beta} : D(-\Delta_{\alpha,\beta}) \to L^2(\mathbb{R}^3)$ which acts like the following:

$$-\Delta_{\alpha,\beta} f(x) = -\Delta f(x)\,, \quad x \in \mathbb{R}^3 \setminus \Gamma\,.$$

For $\sigma(-\Delta_{\alpha,\beta})$ descriptions are useful will following statement from [68]:

Proposition 2.3.1. *A system with a one-point interaction in* $\mathbb{R}^2$ *has the following spectrum with a single point of the discrete spectrum:*

$$\sigma_{\text{ess}} = [0, \infty)$$

$$\sigma_{\text{disc}} = \{\xi_{1,\alpha}\}$$

$$\xi_{1,\alpha} = -4\mathrm{e}^{2(-2\pi\alpha+\psi(1))},$$

where $\psi(x) = \Gamma'(x)/\Gamma(x)$, $\Gamma(x)$ *is Euler's gamma function,* $\psi(1) \approx 0.5772$ *is the Euler's constant.*

Now we construct the resolvent of the operator $-\Delta_{\alpha,\beta}$. The free resolvent is: $R_z = (-\Delta - z)^{-1} : L^2(\mathbb{R}^3) \to H^2(\mathbb{R}^3)$, z belongs to the resolvent set $z \in \rho(-\Delta)$.

We define a bounded direct mapping operator:

$$(\tau\phi)(s) = \phi(s, 0, 0) : H^2(\mathbb{R}^3) \to L^2(\mathbb{R})$$

His conjugate $\tau^* : L^2(\mathbb{R}) \to H^{-2}(\mathbb{R}^3)$ is defined by the following expression,

$$\langle \tau^* h, \omega \rangle = (h, \tau\omega), h \in L^2(\mathbb{R}), \omega \in H^{-2}(\ mathbbR^3)$$

where $\langle \cdot, \cdot \rangle$ denotes correspondence between $H^{-2}(\mathbb{R}^3)$ and $H^2(\mathbb{R}^3)$.

We introduce the self-adjoint operator

$$T_\kappa f(s) = \int_{\mathbb{R}} (\check{T}_\kappa(s - s') + \frac{1}{2\pi}(ln2 + \psi)) f(s') ds' =$$

$$= F^{-1}\left[\frac{1}{2\pi}\left(-ln\left[(p^2 + \kappa^2)^{0.5}\right] + (ln2 + \psi)\delta(p)\right)\hat{f}(p)\right]$$

$$\check{T}_\kappa(s - s') = -\frac{1}{(2\pi)^2}\int_{\mathbb{R}} ln\left[(p^2 + \kappa^2)^{0.5}\right] e^{ip(s-s')} dp,$$

With region definitions $D(T_\kappa) = f \in L^2(\mathbb{R}) : \int_{\mathbb{R}} \check{T}_\kappa(s - s') f(s') ds' \in L^2(\mathbb{R})$, where $\psi \approx 0.577$ is an Euler's constant, and $Ff = \hat{f}$ - transformation Fourier.

Finally, we define a self-adjoint operator

$$Q^\kappa f(s) = (T_\kappa - \beta(s)) f(s) : D(T_\kappa) \to L^2(\mathbb{R}).$$

Now we can compose the resolvent of the main operator, following the theorems from [53]:

$$R^\kappa_{\beta,\alpha} = R_\kappa - R^*_\kappa \tau^* (Q^\kappa - \alpha) \tau R_\kappa \tag{73}$$

2.3.2 Existence of bound states

Denote $\beta_0 > 0$ and $\beta_w > 0$, any two sufficiently small numbers such that $\beta(x) > \beta_0; \forall |x| < \beta_w/2$, and $sup\, \beta(s) = \beta_s$.

First, note that $\beta(s)$, being a local perturbation, does not change the continuous spectrum of the main operator:

$$\sigma_{ess}\left(-\Delta_{\alpha,\beta}\right) = \sigma_{ess}\left(-\Delta_{\alpha}\right) = [\xi_{1,\alpha}, \infty) = [-4e^{2(-2\pi\alpha+\psi)}, \infty)$$

Using the representation in the "momentum" coordinate system of the operator T_κ and the locality of $\beta(s)$, we can obtain

$$\sigma_{ess}(T_\kappa) = \sigma_{ess}(Q^\kappa) = (-\infty, s_\kappa]$$

$$s_\kappa = \frac{1}{2\pi}\left(\psi(1) - ln\frac{\kappa}{2}\right)$$

Note that $s_\kappa = \alpha$ corresponds to $-\kappa^2 = \xi_{1,\alpha}$ of the main operator.

Lemma 2.3.1. *$sup\, \sigma(Q^\kappa) = sup\, \sigma(T_\kappa - \beta(s)) > s_\kappa$*

Proof. The lemma is equivalent to the following statement:

$$(Q^\kappa \phi, \phi) - s_\kappa(\phi, \phi) > 0,$$

for any $\phi \in D(Q^\kappa)$. Let $\phi \in C_0^\infty(\mathbb{R})$, such that $\exists C > 0, \delta > 0 : \phi(s) > C, |s| < \delta$ and we will use $\phi_\lambda(s) = \lambda^{0.5}\phi(\lambda s); \lambda > 0$, note also $\phi(\lambda s) > C, |s| < \delta$, and $\|\phi_\lambda\| = \|\phi\|$. We get

$$\frac{1}{2\pi}\int_{\mathbb{R}} ln\left[\left(1 + \frac{\lambda^2 u^2}{\kappa}\right)^{0.5}\right]\left|F\phi(u)\right|^2 du + \lambda\int_{\mathbb{R}} \beta(s)\left|\phi(\lambda s)\right|^2 ds > 0,$$

where the first term can be represented as $-\frac{1}{4\pi}\left(\frac{\lambda}{\kappa}\right)^2 \int_{\mathbb{R}} u^2\left|F\phi(u)\right|^2 du + \mathcal{O}(\lambda^4)$, and the second term: $\lambda\int_{\mathbb{R}} \beta(s)\left|\phi(\lambda s)\right|^2 ds > \lambda\int_{-\delta}^{\delta} \beta(s)C^2 ds > 2\delta C\beta_0\beta_w$. Thus, if λ is small enough, the second term skews the sum in the positive direction. □

Lemma 2.3.2. *The function $\kappa \to Q^\kappa$ is continuous in the sense of the norm of operators on (κ_0, ∞), and*

$$\lim_{\kappa\to\infty} sup\, \sigma\left(Q^\kappa\right) = -\infty \tag{74}$$

Proof. The function $\kappa \to T_\kappa$ is continuous in the sense of the operator norm:

$$\|(T_\kappa - T'_\kappa)f\| = \frac{1}{4(2\pi)^3}\int_{\mathbb{R}}\left(ln\frac{p^2+\kappa^2}{p^2+\kappa'^2}\right)^2\left|Ff(p)\right|^2 dp \leq$$

$$\frac{1}{4(2\pi)^3}\left(ln\frac{\kappa}{\kappa'}\right)^2\|f\|^2 \xrightarrow[\kappa'\to\kappa]{} 0$$

and $\beta(s)$ is independent of κ, so $Q^\kappa = T_\kappa - \beta(s)$ is continuous. The (74) limit follows from:

$$(Q^\kappa f, f) =$$

$$\frac{1}{(2\pi)^{3/2}}\int_{\mathbb{R}}\left(-ln\sqrt{p^2+\kappa^2} + ln2 + \psi(1)\right)\left|\hat{f}(p)\right|^2 dp + (\beta(s)f, f) \leq$$

$$\frac{1}{(2\pi)^{3/2}}(-ln\frac{\kappa}{2} + \psi(1))\|f\|^2 + \beta_s\|f\|^2$$

□

Now, similarly to Theorem 5.6 from [53], we are ready to prove the existence of at least one bound state.

Theorem 2.3.1. *The operator $-\Delta_{\alpha,\beta}$ has at least one isolated eigenvalue on $(-\infty, \xi_{1,\alpha})$.*

Proof. Adding the localized potential $\beta(s)$ can only change the discrete part of the spectrum, i.e. for the main operator, the part lying in $(-\infty, \xi_{1,\alpha})$ and for Q^κ, it belongs to (s_κ, ∞). Then, according to the lemma 2.3.1, there is at least one point of the discrete spectrum Q^κ, $\lambda(\kappa)$. By the lemma 2.3.2, $\lambda(\kappa)$ is continuous and $\lambda \to -\infty$ while $\kappa \to \infty$. Hence $\exists\kappa' > \left|\xi_{1,\alpha}\right|^{0.5} : \lambda(\kappa') = \alpha$. The point $-\kappa'^2$ is the pole of the resolvent (73), and hence the eigenvalue of the main operator. □

2.3.3 Upper bound for the number of linked states

We now use the Birman-Schwinger method (see [78]) to obtain an upper bound on the number of eigenvalues of the main operator.

We construct the Birman-Schwinger operator, which we will use to calculate

the eigenvalues.

$$Q^\kappa f - \alpha f = 0$$
$$T_\kappa f - \alpha f - \beta(s) f = 0$$
$$K_\kappa f \equiv (T_\kappa - \alpha)^{-1} \big(\beta(s) f\big) = f$$

Here, if f is the eigenvector of the operator Q^κ corresponding to the eigenvalue $\lambda_Q = \alpha$, then it is the eigenvector of the operator K_κ corresponding to the eigenvalue $\lambda_K = 1$. Also, note that the eigenvalues of the operator Q^κ are monotonically decreasing functions of κ, and therefore the eigenvalues of K_κ are also, so if we fix κ, for each point discrete spectrum of the main operator $-\Delta_{\alpha,\beta}$, there exists an eigenvalue of the operator Q^κ corresponding to it greater than α, and a corresponding eigenvalue of the operator K_κ greater than 1. summing all these eigenvalues of the operator K_κ, we obtain an upper bound on the number of eigenvalues $\lambda(Q^\kappa) > \alpha$ and, consequently, the number of points in the discrete spectrum of the operator $-\Delta_{\alpha,\beta}$ less than $-\kappa^2$. To cover the entire set $\sigma_{disc}(-\Delta_{\alpha,\beta})$, we approach the edge of the spectrum $\sigma_{ess}(-\Delta_{\alpha,\beta})$ and get the following bound:

Proposition 2.3.2. *The number of points in the discrete spectrum $\sigma_{disc}(-\Delta_{\alpha,\beta})$ has the following upper bound:*

$$\#\sigma_{disc}(-\Delta_{\alpha,\beta}) \leq$$
$$\lim_{-\kappa^2 \uparrow \xi_{1,\alpha}} \int_{\mathbb{R}^2} \left(\int \frac{e^{2\pi i (sp) w}}{-ln\sqrt{w^2+\kappa^2} + (-ln\frac{\kappa}{2} + \psi(1) - \alpha)\delta(w)} dw \; \beta(p) \right)^2 dsdp$$

2.3.4 Appendix: Transport characteristics of a system of two one-dimensional rings in $\mathbb{R}^3$

This section presents the results from our article [45]. We consider a system of one-dimensional quantum wires in $\mathbb{R}^3$ (in contrast to the previous paragraph, we are not talking about "quantum leaky wires"), under the action of an external magnetic field. The wires form two intersecting rings, and there is an incoming and outgoing channel.

Structures of this type can be found among macromolecules, for example, diphenyl molecules. A discrete model of diphenyl molecules was described in [80].

This molecule contains linked non-coplanar rings, as in our model. We are building a decidable continuous model in contrast to the discrete model in [80]. Our model simplifies the choice of system parameters for better control of e-transport.

Using the theory of quantum graphs, the transport properties of such a system, namely, the dependence of the transmission coefficient on the parameters of the system, are studied.

Theoretical model The figure 17 shows the proposed model of a quantum device consisting of two rings. One ring is in the ZOY plane and the other is in the XOY plane. These two rings are orthogonal to each other and have a point of intersection. The device also has an input wire that is connected to the first (left) ring. The second (right) ring is equipped with an output wire. The right ring can rotate around the Y axis, while the left ring is fixed, and the magnetic field vector is directed along the Z axis and does not change its direction. For quantum wires, a one-dimensional approximation is considered, based on the theory of quantum graphs and the scattering problem.

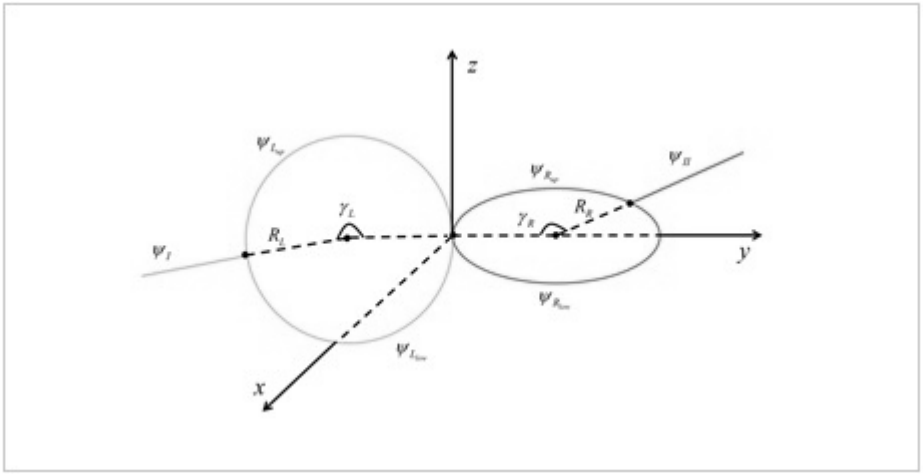

Figure 17 – Quantum graph with two semi-infinite channels (input and output quantum wires) and four segments that form two rings. $R_L(R_R)$ - ring radii, $\gamma_L(\gamma_R)$ - angles between input (output) wires and connection point.

The functions in the incoming and outgoing wires are denoted: $\psi_I(x_I), \psi_{II}(x_{II})$, and can be written as

$$\psi_I(x_I) = e^{ikx_I} + C_1 e^{-ikx_I}, \psi_{II}(x_{II}) = C_{10} e^{ikx_I}, \tag{75}$$

for the top and bottom of two identical rings:

$$\begin{aligned}
\psi_{L_{up}}(\gamma) &= C_2 e^{ikR_L\gamma} + C_3 e^{-ikR_L\gamma}, \\
\psi_{L_{low}}(\gamma) &= C_4 e^{ikR_L\gamma} + C_5 e^{-ikR_L\gamma}, \\
\psi_{R_{up}}(\gamma) &= C_6 e^{ikR_R\gamma} + C_7 e^{-ikR_R\gamma}, \\
\psi_{R_{low}}(\gamma) &= C_8 e^{ikR_R\gamma} + C_9 e^{-ikR_R\gamma},
\end{aligned} \tag{76}$$

where $R_L(R_R)$ is the radius of the left (right) ring, γ is the angle between the joints of the rings and wires, k is the wavenumber.

The Kirchhoff magnetic conditions at the vertices of the graph have the following form:

$$\begin{cases} e^{(-1)^\mu i\Phi_e(\gamma_e)}\psi_e(\gamma_e) = \psi_{e'}(\gamma_e)e^{(-1)^\mu i\Phi_{e'}(\gamma_e)} \\ \sum_e (-1)^{[e]}\partial\psi_e(\gamma_e)e^{(-1)^\mu i\Phi_e(\gamma_e)} = 0, \end{cases}, \tag{77}$$

where $[e] = 0$ for the output edge and $[e] = 1$ for the input edge, γ_e is the angle between the joints of the rings and wires. Since the orientations of the edges at some points will not match the parameters on the ring, we will take into account the negative sign in front of Φ_e, so μ is 0 or 1, depending on the orientation. Besides,

$$\Phi_e = \begin{cases} 0, \\ \int_{\gamma_e} a(\tau)d\tau, \end{cases}, \tag{78}$$

where 0 is at the beginning of the edge, $\int_{\gamma_e} a(\tau)d\tau$ is at the end.

As mentioned before, the magnetic field is assumed to be directed along the Z axis, so $\Phi_1(\gamma) = \frac{1}{2}BR_L^2\gamma\sin(\alpha), \Phi_2(\gamma) = \frac{1}{2}BR_R^2\gamma\cos(\alpha)$,where $\Phi_1(\gamma)$ belongs to the ring in the ZOY plane, $\Phi_2(\gamma)$ belongs to the ring in the XOY plane, α is the rotation angle around the Y axis.

Using Kirchhoff's magnetic conditions and expressions for channels, edges, and for $\Phi_1(\gamma), \Phi_2(\gamma)$, we obtain the following conditions for graph vertices:

$$\begin{aligned}
&\psi_I(0) = \psi_{L_{up}}(0) = \psi_{L_{low}}(2\pi)e^{i\Phi_1(2\pi)}, \\
&-\psi_I'(0) + \psi_{L_{up}}'(0) - \psi_{L_{low}}'(2\pi)e^{i\Phi_1(2\pi)} = 0,
\end{aligned}, \tag{79}$$

for the first vertex (the intersection point of the incoming wire and the left ring).

For the second vertex (the connection point of two rings), the equations look like:

$$\begin{aligned}
&\psi_{L_{up}}(\pi)e^{i\Phi_1(\pi)} = \ psi_{L_{low}}(\pi)e^{i\Phi_1(\pi)} = \psi_{R_{up}}(0) = \psi_{R_{low}}(2\pi)e^{i\Phi_2(2\pi)}, \\
&-\psi_{L_{up}}'(\pi)e^{i\Phi_1(\pi)} + \psi_{L_{low}}'(\pi)e^{i\Phi_1(\pi)} + \psi_{R_{up}}'(0) - \psi_{R_{low}}'(2\pi)e^{i\Phi_2(2\pi)} = 0.
\end{aligned}. \tag{80}$$

For the third vertex (connection point of the outgoing wire and the right ring), the equations look like:

$$\begin{array}{l} \psi_{R_{up}}(\pi)e^{i\Phi_2(\pi)} = \ psi_{R_{low}}(0) = \psi_{II}(0), \\ -\psi'_{R_{up}}(\pi)e^{i\Phi_2(\pi)} + \psi'_{R_{low}}(0) + \psi'_{II}(0) = 0. \end{array} . \tag{81}$$

Since the left ring is proposed to be fixed relative to the magnetic field, α for the left ring is equal to 0. This means that $\Phi_1(\gamma) = 0$ and the following system of equations takes place:

$$\begin{cases} 1 + C_1 - C_2 - C_3 = 0 \\ C_2 + C_3 - C_4 e^{ikR_L 2\pi} - C_5 e^{-ikR_L 2\pi} = 0, \\ -ik + ikC_1 + ikR_L C_2 - ikR_L C_3 - ikR_L C_4 e^{ikR_L 2\pi} + ikR_L C_5 e^{-ikR_L 2\pi} = 0 \\ C_2 e^{ikR_L\pi} + C_3 e^{-ikR_L\pi} - C_4 e^{ikR_L\pi} - C_5 e^{-ikR_L\pi} = 0 \\ C_4 e^{ikR_L\pi} + C_5 e^{-ikR_L\pi} - C_6 - C_7 = 0 \\ C_6 + C_7 - (C_8 e^{ikR_R 2\pi} + C_9 e^{-ikR_R 2\pi})e^{i\Phi_2(2\pi)} = 0 \\ -ikR_L C_2 e^{ikR_L\pi} + ikR_L C_3 e^{-ikR_L\pi} + ikR_L C_4 e^{ikR_L\pi} - ikR_L C_5 e^{-ikR_L\pi} + \\ +(ikR_R C_6 - ikR_R C_7) - (ikR_R C_8 e^{ikR_R 2\pi} - ikR_R C_9 e^{-ikR_R 2\pi})e^{i\Phi_2(2\pi)} = 0 \\ (C_6 e^{ikR_R\pi} + C_7 e^{-ikR_R\pi})e^{i\Phi_2(\pi)} - C_8 - C_9 = 0 \\ C_8 + C_9 - C_{10} = 0 \\ -(ikR_R C_6 e^{ikR_R\pi} - ikR_R C_7 e^{-ikR_R\pi})e^{i\Phi_2(\pi)} + (ikR_R C_8 - ikR_R C_9) + ikC_{10} = 0 \end{cases} \tag{82}$$

Further, using the Gauss method, we can get all unknown coefficients $C_1, C_2, \ldots C$ Finally, the reflection coefficient can be written as $R_{ref} = C_1 \cdot C_1^*$, the transmission coefficient: $T = C_{10} \cdot C_{10}^*$.

Numerical results In this section, we present a numerical study to illustrate some of the important characteristics of electron transport in the proposed device. The influence on the transmission coefficient of various system parameters, such as the angle of rotation α, ring radii R_L, R_R, wave number k, angles between channels and the attachment point of rings $\gamma_L = \gamma_R$ and magnetic induction B.

The figure 18 shows the electron transmission coefficient T and reflection coefficient R_{ref} as functions of the rotation angle α for the selected parameter values: $R_L = R_R = 1.14, k = 0.18, \gamma_L = \gamma_R = \pi$ in the figure 18 (left) and

$R_L = R_R = 1.2, k = 0.77, \gamma_L = \gamma_R = \pi$ in 18 (right). It can be seen that the transmission coefficient T and the reflection coefficient R_{ref} are not equal to zero. You can also find such values of the angle of rotation when $T = 1$ and $R_{ref} = 0$, which means that there is an ideal transmission (the wave passes completely in the output wire). In addition, there are ranges of α values when R_{ref} is close to 1 and T is close to 0, i.e. perfect reflection takes place.

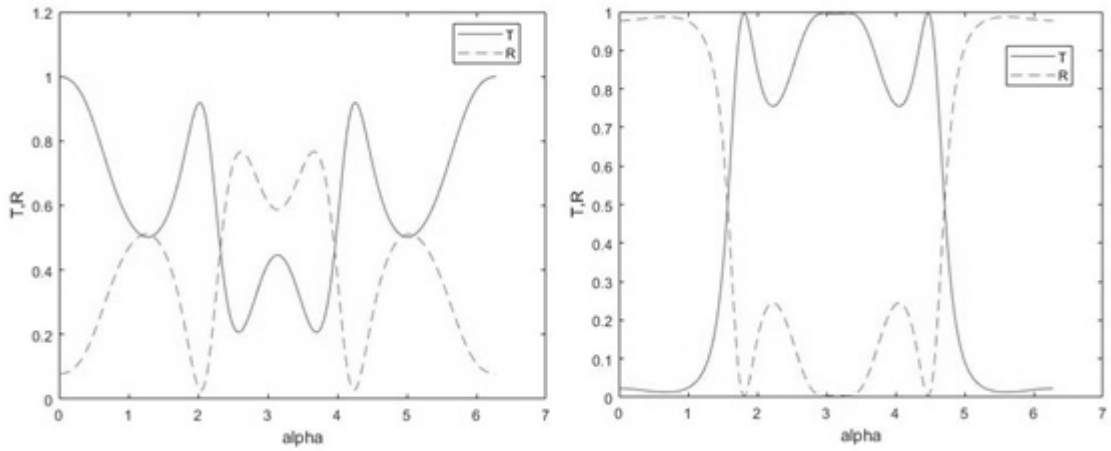

Figure 18 – Coefficient passing electrons T and coefficient reflection R_{ref} as functions corner rotation α, for $R_L = R_R = 1.14, k = 0.18, \gamma_L = \gamma_R = \pi$(left), $R_L = R_R = 1.2, k = 0.77, \gamma_L = \gamma_R = \pi$(right), α changes from 0 to 2π.

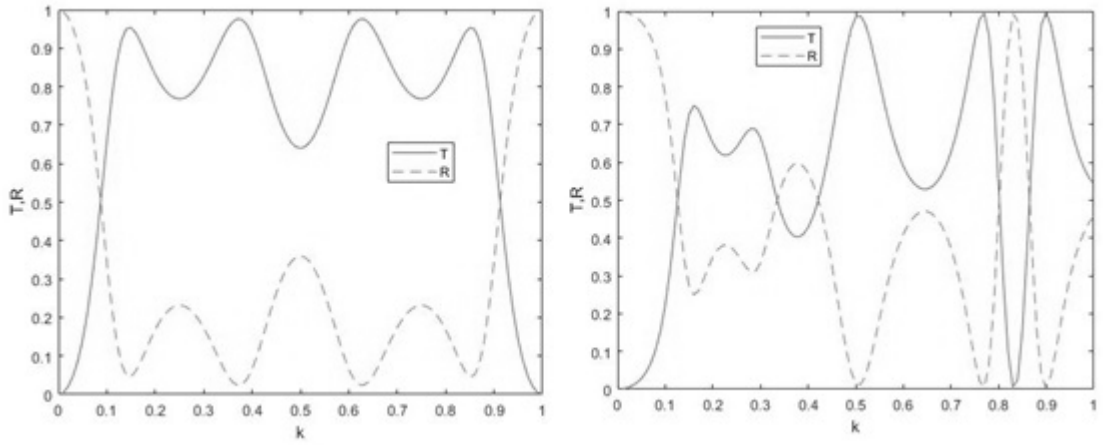

Figure 19 – Coefficient passing electrons T and coefficient reflection R_{ref} as functions wave numbers k for $\alpha = \pi, \gamma_L = \gamma_R = \pi$, $R_L = R_R = 1$,(left), $R_L = R_R = 1.2$(right).

On figure 19 shows addiction coefficient passing electrons T and coefficient reflections of R_{ref} from wave numbers k for selected values parameters :$R_L = R_R =$

$1, \alpha = \pi, \gamma_L = \gamma_R = \pi$ on figure 19 (left), $R_L = R_R = 1.2, \alpha = \pi, \gamma_L = \gamma_R = \pi$, on figure 19 (right). The behavior of the coefficients is similar to the picture 18. There are such values of the wave number at which ideal transmission (reflection) occurs.

When the rotation angle is $\alpha = \pi$, the rings are coplanar and there is a very high probability of perfect electron transfer. These results are supported by several [81] papers on spin filtering properties in two coupled Rashba quantum rings.

But changing the geometry of the model is not the best way to control electron transfer. The best way is magnetic flux.

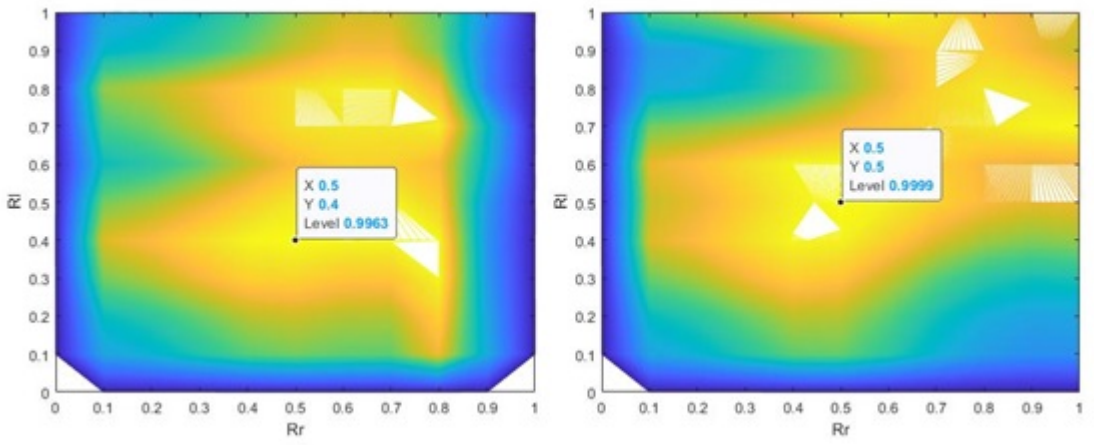

Figure 20 – Contour map of electron transmission coefficient T depending on ring radii for $k = 0.77, \gamma_L = \gamma_R = \pi$, $\alpha = 1.8\ \ rad$ (left), $\alpha = \pi$ (right).

The figure 21 shows the influence of the magnetic field on the transport properties. For the values 18 – 20 chosen from the figures 20 of the values of the rotation angle α, ring radii, wavenumber and transition angles, the electron transmission coefficient T and the reflection coefficient R_{ref}, are presented as functions of B. In the picture 21 you can see that the perfect transfer occurs when B becomes 0.31, 0.66.

In this section, the model of two quantum rings was considered and appropriate values of the wavenumber, rotation angle, ring radii, and angles between the junction points were presented for which the transmission coefficient T is close to 1, i.e. perfect electron transfer occurs. These results make it possible to

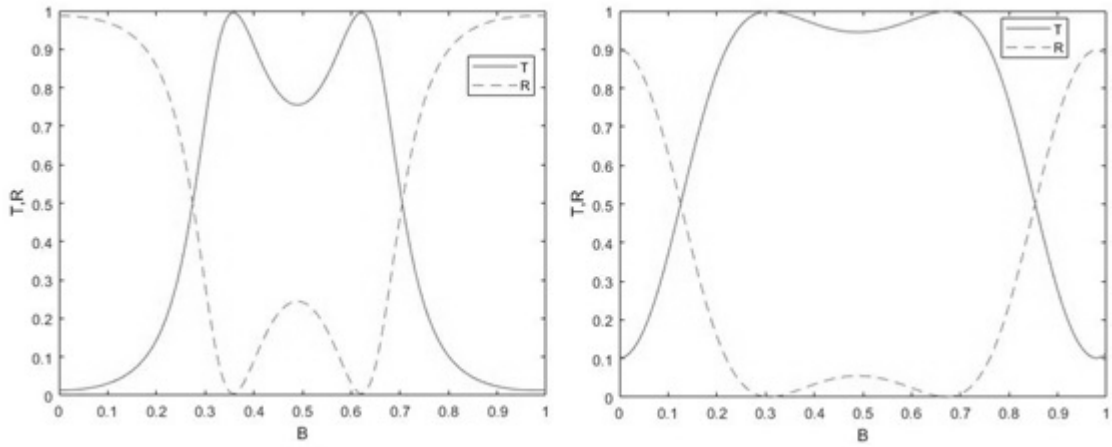

Figure 21 – Electron transmission coefficient T and reflection coefficient R_{ref} as functions of B for $R_L = R_R = 1.2, \alpha = 1.8 \;\; rad, \gamma_L = \gamma_R = \pi$, $k = 0.44$(left), $k = 0.51$(right).

design devices that use the variation of system parameters to control transport characteristics.

2.3.5 Conclusions

In the second chapter, systems with delta potentials on straight lines in two and three dimensions were considered. A number of theoretical results were proved for two types of system geometries, in particular, the existence of bound states was proved. Also, for the case of a two-dimensional system, an approach is proposed to study the spectrum using a certain test function. In the case of a three-dimensional system, a method was demonstrated for applying the Birman-Schwinger method to limit the number of bound states.

In the next chapter, we move on to consider another type of systems in three-dimensional space. In this case, the singular interaction will be caused by other particles.

Chapter 3. Two conducting layers in $\mathbb{R}^3$

In this chapter, we explore 3D quantum systems with complex geometries. More specifically, single-particle and multi-particle problems are considered, in which particles are enclosed within two conductive layers connected to each other through holes. In addition, an external electric field is applied. The question that interests us is the dependence of the spectrum (both discrete and continuous) of the operator on the parameters of the system. In the first section, we use the theory of operators to obtain some generalized analytical results, and then, in the second section, using numerical methods, we study in detail the influence of system parameters on the eigenvalues and propose some classification of the bound states of the system, according to the number and location of constant-sign domains.

3.1 A Pair of Conductive Layers: Analytical Results

In general, waveguides can be modeled by Laplacians with Dirichlet boundary conditions, in infinite flat strips and multidimensional layers. Their spectra have been the subject of much attention in recent decades. The problem is trivial as long as the strip or layer is straight, because then the method of separation of variables can be applied. However, already a local perturbation, such as bending, deformation, or a change in boundary conditions, can lead to the appearance of a non-empty discrete spectrum. As examples of possible perturbations, we indicate local deformation of the boundary conditions [85, 86], bending [87, 88, 89, 90] or twisting [91, 92] of the waveguide. A perturbation by adding a potential is considered in [87], a magnetic field in [93, 94], or a second-order differential operator, as in [95]. The type of systems of interest to us is two adjacent parallel waveguides connected by windows cut out in a common boundary. The two-dimensional case has been studied quite intensively, we refer to [96, 97, 98, 99, 100, 101, 102, 114, 112] (see also references therein). It has been shown that the perturbation by the window(s) is negative, i.e. leads to the pres-

ence of isolated bound states below the essential spectrum; the latter is invariant with respect to the window(s) presence. In the case of a single window, it was shown in [96, 98, 100] that expanding the window results in more and more isolated eigenvalues. They appear when the window length passes through certain critical values. This phenomenon has been studied in detail and asymptotic expansions for the resulting eigenvalues have been obtained, see [96, 98, 102]. In the three-dimensional case corresponding to layers with window connection, P. Exner and S. Vugalter showed that a small window generates one simple isolated eigenvalue that appears at the threshold of the essential spectrum [101]. They also obtained two-sided asymptotic estimates for this eigenvalue. An asymptotic extension for this eigenvalue was formally constructed in [103]. Another example of 3D waveguide coupling can be found in [113].

In this chapter, we consider a system of two parallel conducting layers in R^3 connected through holes in a common boundary. Such a system was studied in [104], where it is shown that the window generates eigenvalues that go beyond the threshold of the essential spectrum as the window passes through certain critical forms. Our system also contains an external electric field.

In the first section, we define the Hamiltonian of the system and present some analytical results. Further, in the following sections, we present a number of numerical results obtained using the finite element method. Graphs of the dependence of the system's own energies on its main parameters are plotted.

The last section explores the effect of window shape on bound states in more detail. We continuously change the shape of the window and consider the evolution of bound states for a fixed number and position of constant-sign domains. Questions about the number and position of constant-sign domains for Dirichlet Laplacians are the subject of active research. The first step was Courant's nodal theorem, and since then various cases have been explored, such as nodal domains for quantum graphs ([109],[110]) and on a sphere ([111]).

Also, within the framework of this geometry, we consider the case of two particles with different window shapes. We carry out numerical calculations using the Hartree-Fock estimation method (for the accuracy of the Hartree approximation, see [108]). For previous studies of many-particle problems in deformed waveguides, see, for example, [105, 106, 107]. We are interested in the following

two questions: how the energy of bound states and the number/position of nodal domains depend on the shape of the window, and what is the relationship between the one-particle and two-particle cases.

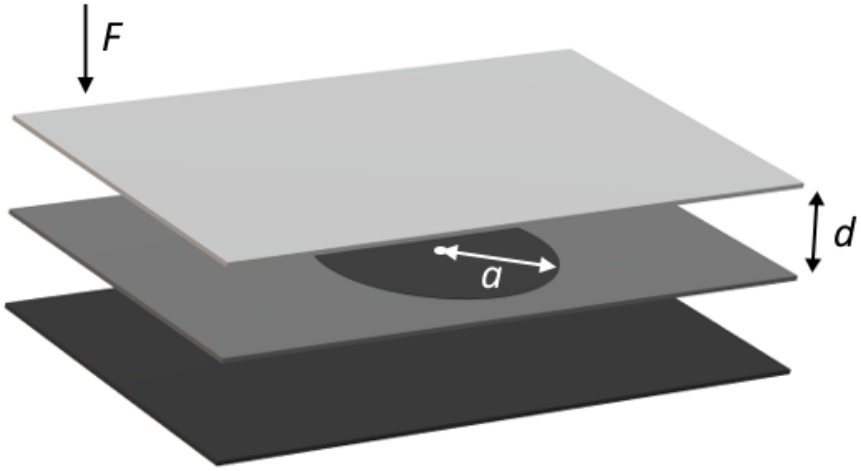

Figure 22 – Conductive layer, with two different boundary conditions and a family of windows on one of the boundaries. An orthogonal electric field F is applied.

3.1.1 Model description

The system we are going to study is shown in fig.22. We are considering a quantum particle enclosed within two parallel layers connected via window system. The Dirichlet condition is assumed at the layer boundaries. We model windows as areas on the border where Neumann boundary conditions are imposed. In this case it suffices to deal with the Hamiltonian $H(F)$ for one layer between the planes $z = 0$ and $z = d$. We will denote this configuration space via Ω,

$$\Omega = \mathbb{R}^2 \times [0, d].$$

We assume that the particle has a non-zero charge q. Also, it is under the influence of homogeneous electric field strength E, denote $F := Eq$. We assume that the electric field is directed along the Z axis. Without loss of generality, we put $F \geq 0$.

Let $(\gamma_i)_{1 \leq i \leq p}$ be a finite family of bounded and open sets lying on the boundary of Ω for $z = 0$. Since they are open sets, they contain a small disk of radius a, $a > 0$. Without loss of generality, we assume that the center of such a disk is at the point $(0, 0, 0)$.

Set $\Gamma = \partial\Omega \setminus (\cup_{i=1}^{p}\gamma_i)$. We consider the Dirichlet boundary conditions on Γ and the conditions Neumann on $\cup_{i=1}^{p}\gamma_i$. Black surfaces in figure 22 correspond to the Neumann boundary condition, while the gray surfaces correspond to the Dirichlet condition.

3.1.2 Construction of the Hamiltonian

We define a self-adjoint operator on $L^2(\Omega)$ corresponding to the Hamiltonian of the particle, $H(F)$. For this we use quadratic forms. Let $q(F)$ be quadratic form

$$q(F)[u,v] \;=\; \int_{\Omega} \big(\nabla u\overline{\nabla v} + Fzu\bar{v}\big)dxdydz, \quad u,v \in \mathcal{D}(q(F)), \tag{83}$$

where $\mathcal{D}(q(F)) := \big\{u \in \mathrm{H}^1(\Omega), u\lceil\Gamma = 0\big\}$, $\mathrm{H}^1(\Omega)$ is the standard Sobolev space and $u\lceil\Gamma$ is the trace of the function u on Γ. This implies that $q(F)$ is a densely defined, symmetric, positive and closed quadratic form [78]. We denote the only self-adjoint operator associated with $q(F)$ by $H(F)$ and its domain $\mathcal{D}$. This is the Hamiltonian describing our system (in appropriately scaled units and with atomic units $2m = h = q = 1$ to simplify the equation). From [78] (vol. 1, p. 276) and [78] (vol. 4, p. 263), it follows that the domain $\mathcal{D}$ has the following form:

$$\mathcal{D} \;=\; \big\{u \in \mathrm{H}^1(\Omega); \quad -\Delta u \in \mathrm{L}^2(\Omega), u\lceil\Gamma = 0, \frac{\partial u}{\partial z}\lceil\cup_{i=1}^{p}\gamma_i = 0\big\}, \tag{84}$$

and

$$H(F)u = (-\Delta + Fz)u, \quad \forall u \in \mathcal{D}. \tag{85}$$

3.1.3 Existence of discrete spectrum

In this subsection, we present two theorems without proof.

Using the property of the essential spectrum to be preserved under compact perturbations, one can prove its stability. Recall that the essential spectrum of the operator A, which we denote by $\sigma_{ess}(A)$, consists of points λ at which the set of values $\Re(\lambda I - A)$ is not closed, and eigenvalues of infinite multiplicity. A discrete spectrum is a set of isolated eigenvalues of finite multiplicity. It is denoted by $\sigma_{dis}(A)$. Denote by λ_0^1 the first eigenvalue of the transverse part (along the Z axis) of the main operator.

Theorem 3.1.1. *Let $H(F)$ be the operator given by* (85)*. Then,*

$$\sigma_{ess}\big(H(F)\big) = [\lambda_0^1, +\infty). \tag{86}$$

Further, based on this result and the principle of min-max [78], we conclude that if a discrete spectrum exists, then it lies below λ_0^1. The main result of the section is the following theorem:

Theorem 3.1.2. *For any $F \geq 0$ the operator $H(F)$ has at least one isolated eigenvalue below λ_0^1, i.e.*

$$\sigma_{dis}\big(H(F)\big) \neq \emptyset.$$

As noted earlier, the result differs from the result corresponding to two-dimensional waveguides. Indeed, in [115] the existence of a discrete spectrum depends on the values of F.

It is important to note that the electric and magnetic fields affect the spectrum of our system in different ways. Indeed, in [116] it was proved that in the case of a magnetic field, the discrete spectrum exists only when the window radius passes some critical value.

3.2 Pair of conductive layers: Numerical calculations

As shown in the previous section, the eigenvalue below essential spectrum appears for any window radius a. As the hole radius increases, more isolated eigenvalues appear. We use numerical calculations based on the finite element method to study this issue. In addition, we consider the existence of bound states for many-particle systems using the Hartree-Fock approach (which is described in more detail, for example, in [117]). In all calculations we use arbitrary units, with $\hbar = e = 1$, $m = 0.5$ (e, m are the electron charge and mass, respectively).

To build our own functions, we use the finite element method, specifically, the **FreeFem++** package. Some examples of single-particle bound states, in a cut through the hole plane, are shown in Fig. 23.

Let's start with a description of the Hartree-Fock method, which we will use to consider many-particle problems in the following sections, as well as an iterative

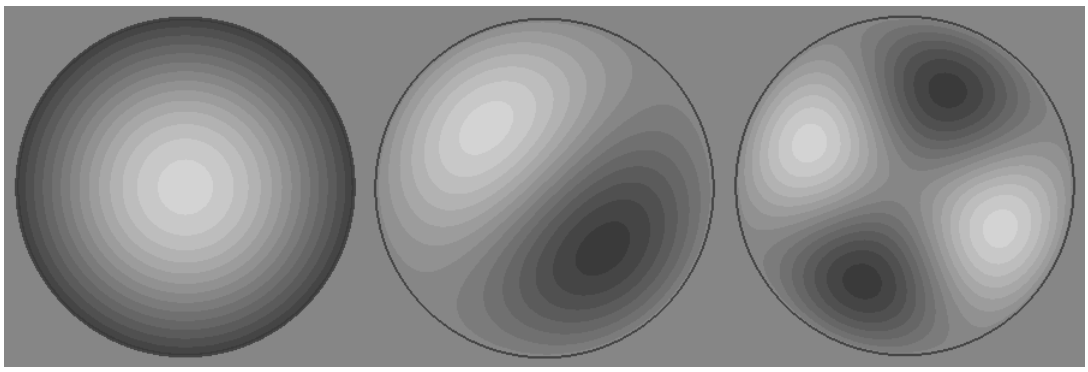

Figure 23 – Examples of one-particle bound states.

procedure created on the basis of the method, the result of which converges to many-particle eigenstates.

3.2.1 Hartree-Fock method

Let us describe the Hartree-Fock model and the algorithm.

Let's start with the Hamiltonian

$$\hat{H} = \sum_k (-\Delta_k + U_k) + \frac{1}{2} \sum_{\substack{j,k \\ j \neq k}} V_{jk} = \sum_k \hat{H}_k + \frac{1}{2} \sum_{\substack{j,k \\ j \neq k}} V_{jk}, \tag{87}$$

where $\Delta_k = \frac{\partial^2}{\partial {x_k}^2}$ are the Laplace operators acting on the coordinates x_k particles with number k, U_k - external field potential, $V_{j,k}$ - particle interaction potential, $\hat{H}_k = (-\Delta_k + U_k)$.

We can then use the Slater determinant to approximate the multiparticle wave function:

$$\Psi(x_1, x_2, \ldots, x_n) = \frac{1}{\sqrt{n!}} \begin{vmatrix} \psi_1(x_1) & \ldots & \psi_n(x_1) \\ \ldots & \ldots & \ldots \\ \psi_1(x_n) & \ldots & \psi_n(x_n) \end{vmatrix}, \tag{88}$$

where ψ_k are single-particle wave functions and $x_k = (r_k, s_k)$, where r_k and s_k are spatial and spin coordinates of the kth particle.

Following the Hartree-Fock method, we insert (88) into (87) and use a vari-

ation of the energy functional $\left\langle \Psi \left| \hat{H}\psi \right. \right\rangle$ to obtain the Hartree-Fock equations:

$$\left[\hat{H}_k + \sum_{j,j \neq k} \int \psi_j^* \left(x_j\right) V_{jk} \psi_j \left(x_j\right) dx_j \right] \psi_k \left(x_k\right) - \sum_{j,j \neq k} \left(\int \psi_j^* \left(x_j\right) V_{jk} \psi_k \left(x_j\right) dx_j \right) \psi_j \left(x_k\right) = E_k \psi_k \left(x_k\right). \tag{89}$$

Now we must take into account the spin of the particles. We ignore spin-orbit interaction. Let $n^{\uparrow}$ be a number particles with spin 0.5 and $n^{\downarrow}$-particles with spin -0.5. The wave functions of these particles are equal to $\psi_k^{\uparrow}$ and $\psi_k^{\downarrow}$. Then, due to independence of V_{jk} from the spin variable, we have

$$\int \psi_j^*(x_j) V_{jk} \psi_k(x_j) dx_j = \delta_{s_j s_k} \int \psi_j^{*s_j}(r_j) V_{jk} \psi_k^{s_k}(r_j) dr_j, \tag{90}$$

where $\delta_{s_j s_k}$ is the Kronecker symbol, indices s_j, s_k take the values $\uparrow, \downarrow$.

We use the delta potential as the interaction potential: $V_{jk} = U\delta(r_j - r_k)$, where U is a constant. Using delta potential and (90), from (89) we get the following system:

$$\begin{aligned} &H_k \psi_j^{\uparrow}(r_k) + U \sum_j^{n\downarrow} \left(\left| \psi_j^{\downarrow}(r_k) \right|^2 \psi_k^{\uparrow}(r_k) \right) = E_k^{\uparrow} \psi_k^{\uparrow}(r_k), \quad (k = 1, ..., n^{\uparrow}), \\ &H_k \psi_j^{\downarrow}(r_k) + U \sum_j^{n\uparrow} \left(\left| \psi_j^{\uparrow}(r_k) \right|^2 \psi_k^{\downarrow}(r_k) \right) = E_k^{\downarrow} \psi_k^{\downarrow}(r_k), \quad (k = 1, ..., n^{\downarrow}). \end{aligned} \tag{91}$$

To solve the system, we used the following iterative algorithm:

1. Find one-particle stationary solutions for the case potential $U_k = Fz_k$ and arbitrarily choose N solutions as initial guesses for $\psi_i\left(x_i\right)$.

2. For each particle, calculate the potential $P_i = U \sum\limits_j \left| \psi_j \left(x_j\right) \right|^2$, where the sum includes particles with opposite spins, and then use it to calculate a set of solutions.

3. For each of the N sets, select the associated state. (Here we can use arbitrary additional criteria to speed up the process).

4. Check if the new solutions are close enough to the previous ones. If not, return to step 2.

A positive result of this algorithm is sufficient (with a given accuracy), but not a necessary condition for the existence solutions. In step 2, we choose a solution from the set that minimizes the functional $L_i(u) = \int\limits_{\Omega} \left| u(x)\, \psi_i^{prev}(x) \right|^2 dx$, i.e. closest to the previous one. The sizes of the sets are arbitrary. This method prone to looping between two sets of features that complement each other. To avoid this kind of fluctuation, the step 2 formula can be changed: $U_i = \alpha U_i^{prev} + (1-\alpha)\, U \sum\limits_j \left| \psi_j\left(x_j\right) \right|^2$, where U_i^{prev} is the value of the potential at the previous iteration, and $\alpha \cong 0.1$.

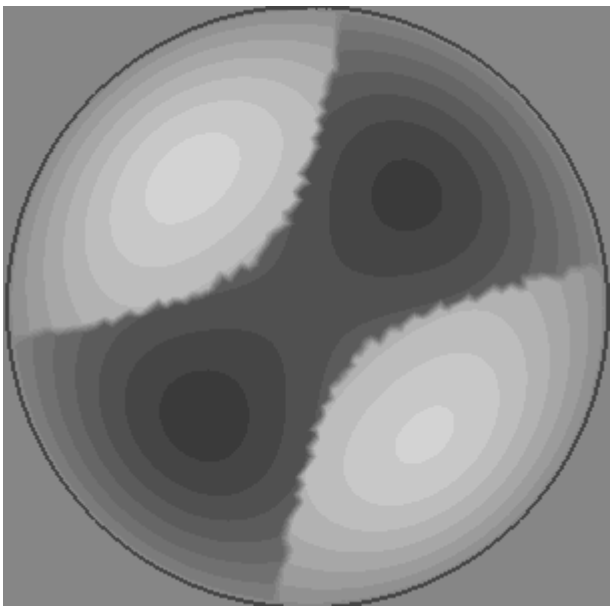

Figure 24 – Two-particle bound state in a cut through the hole plane

As a result, we can get many-particle bound states. Fig. 24 shows a two-dimensional cut of the bound state of two particles with different spins. Here one particle is dark and the other one is light.

3.2.2 Main results

The results of this section are published in [82, 83].

In this section, we begin a numerical study of the dependence of the discrete spectrum on the main parameters of the system. The geometry of the system is described at the beginning of the chapter, but it should be noted that the electric

field F here, in contrast to the analytical part, is not symmetrical with respect to the common boundary of two layers, but has a more physically correct form: it is directed downward for both layers. We consider the case of one circular window, with varying area (and an elliptical window for the last result). In all calculations we use arbitrary units, with $\hbar = e = 1$, $m = 0.5$ (e, m are the charge and mass of the electron, respectively). Energy level colors are consistent across all charts in this section. On all plots, the black line (top one on each plot) represents the lower end of the essential spectrum.

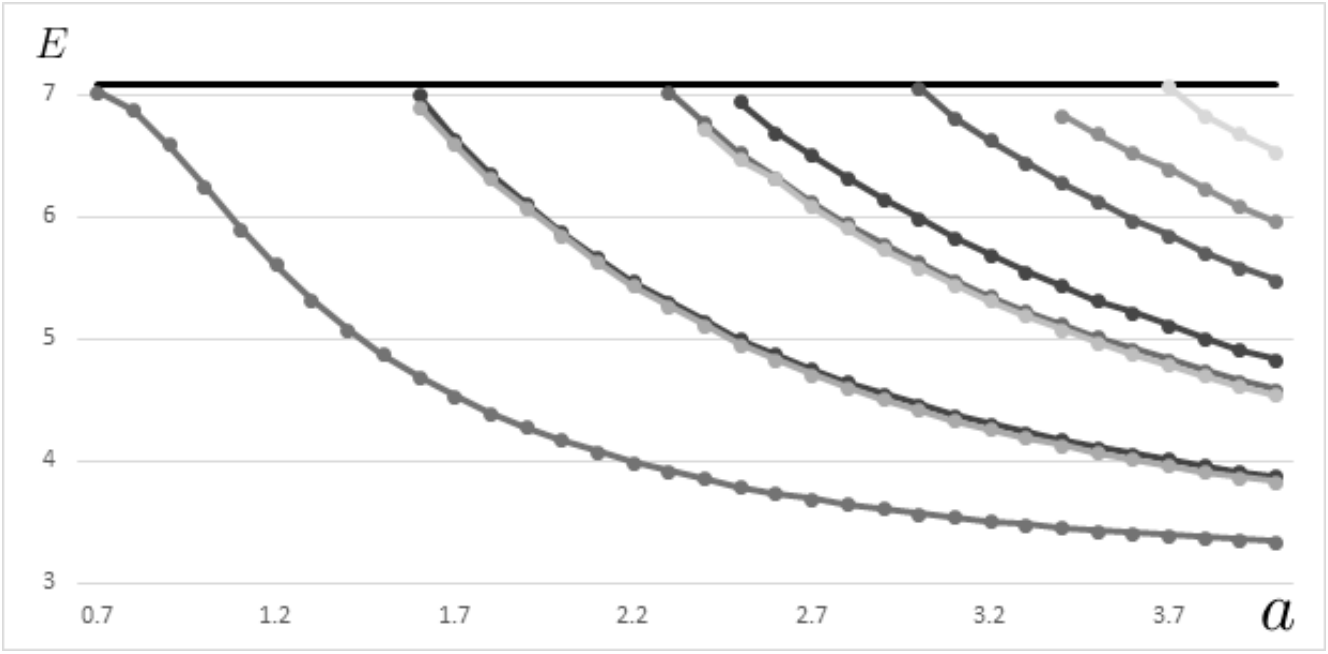

Figure 25 – Energies of bound states as a function of the window radius a. The electric field strength is fixed $F = 5$.

First, we examine the dependence of the discrete spectrum on the area of the window, shown in Fig.25. Here the field strength is fixed, $F = 5$ (which corresponds to the maximum value of F on the graph 26). The essential spectrum does not depend on the window parameters (theorem 3.1.1). Each bound state decreases monotonically as a function of the window area, while the number of bound states increases. In accordance with the main theorem, the first boundary state is below the boundary of the essential spectrum for all positive values of the radius and merges with the boundary of the essential spectrum when the radius decreases to zero.

Now let's examine the dependence of the spectrum on the electric field strength (Fig. 26). The window radius is fixed, $a = 4$ (this is the maximum radius

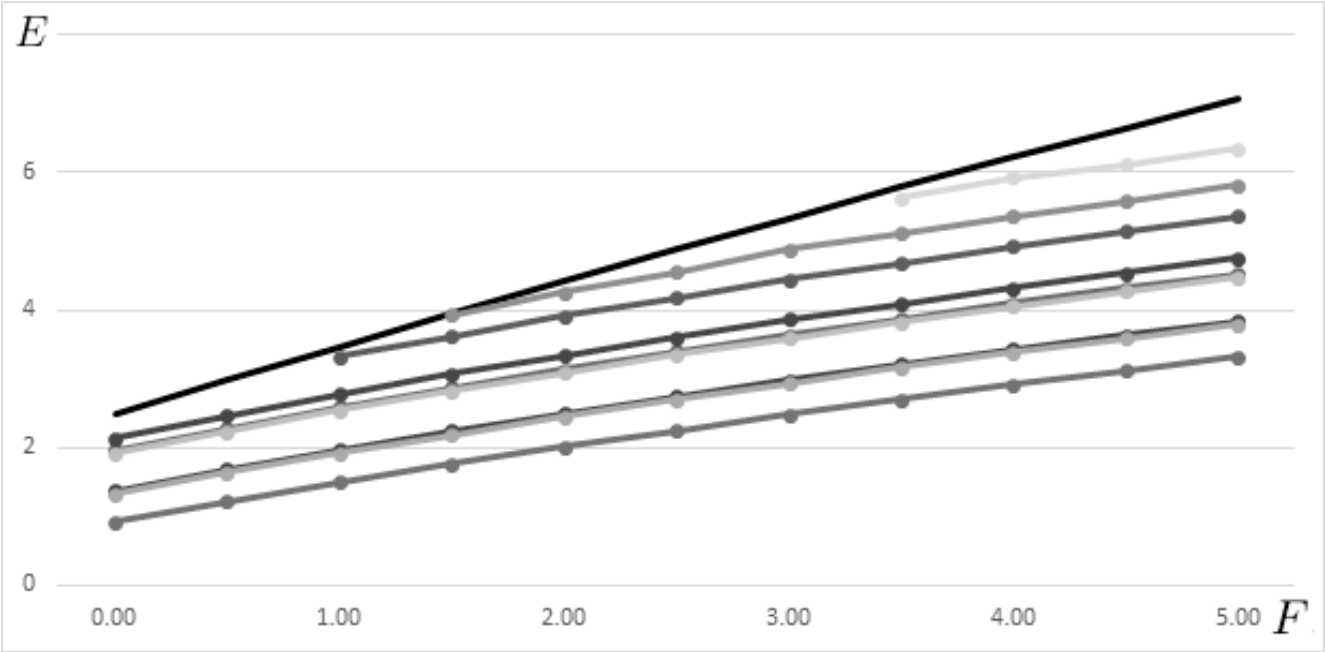

Figure 26 – Energies of bound states as a function of the electric field strength F. The window radius is fixed $a = 4$.

from fig.25). The electric field is not a local perturbation of the system; therefore, it changes both the essential spectrum and the discrete one. Both spectra are increasing functions of F, but the edge of the essential spectrum grows faster, allowing more bound states to occur as the field strength increases.

Note that on the plots 25 and 26, the values of the parameters a and F coincide on the right border of both plots, that is, the points in the rightmost column of each of them correspond to one and the same eigenstates of the system (in particular, their energies are equal).

Naturally, the question arises which window parameters are important. In particular, how the discrete spectrum depends on the area, perimeter, and shape of the window. These issues are considered in more detail for a similar system (the same geometry, but there is no uniform electric field) in the 3.3 section. Here we consider the influence of the window shape, in particular, we change the eccentricity of the elliptical window by tracking various related states, see fig.27. The area is fixed and corresponds to the area of the circle with $a = 4$. The field strength is fixed, $F = 5$. Here we see different dynamics for different types of bound states (for more information about classification, see the 3.3 section).

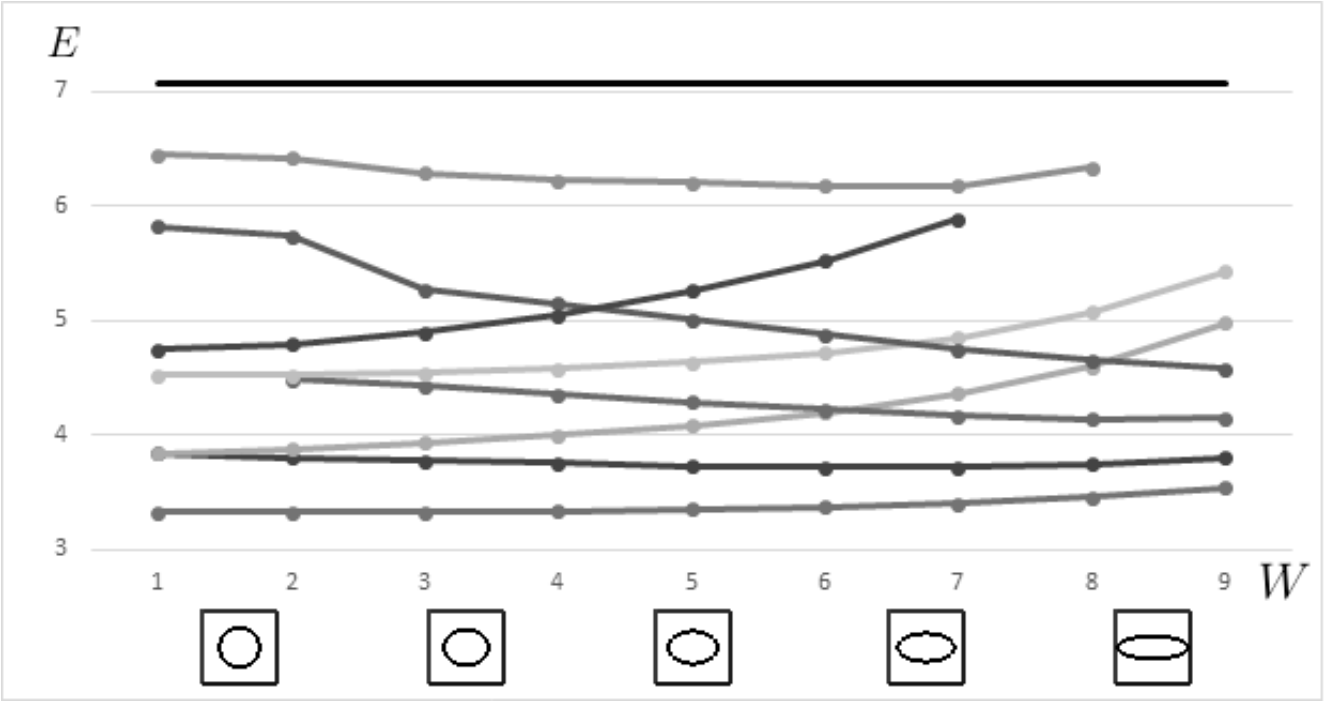

Figure 27 – Bound state energies as a function of the distance between the foci of an elliptical window. The window area is constant ($S = 16\pi$), the electric field strength is fixed $F = 5$.

3.2.3 Additional results

In this subsection, the study of conducting layers continues. Unlike the previous paragraph, in this one, the external electric field is not uniform with respect to both layers, but is symmetrical relative to the plane, i.e. for both the upper and lower layers, at a positive intensity, it is directed in different directions, away from their common border. Just such a field is obtained if the second layer is modeled using the Neumann conditions on the lower boundary of the first one, as was done in the first part of the chapter.

First, we plot the shift of the lower bound of the essential spectrum as a function of the strength of the applied electric field. These calculations are carried out for the case without a window. This is sufficient due to the well-known theorem that a local perturbation, such as a window, does not change the essential spectrum. The results are shown in fig. 28. In the absence of an electric field, $F = 0$, the lower limit of the essential spectrum is equal to π^2. When a field is applied, the spectrum shifts almost linearly with F.

Then we perform calculations for various values of the electric field strength F

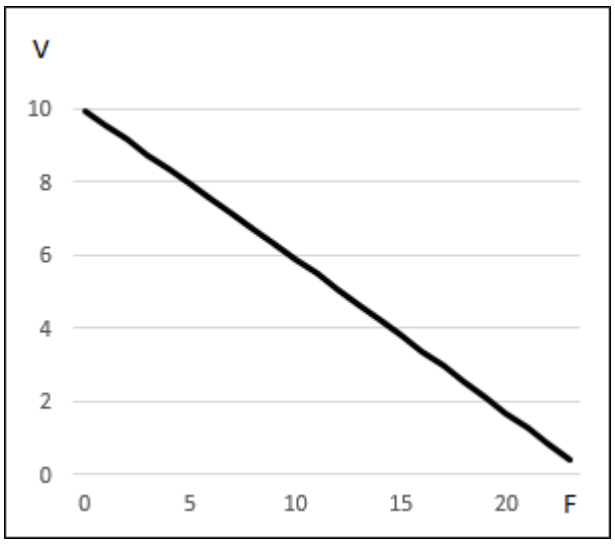

Figure 28 – Lower bound of the essential spectrum for a one-particle bound state, in arbitrary units.

and the window radius a and compare the eigenvalues with the threshold value for the essential spectrum. Eigenvalues below the threshold value correspond to the discrete spectrum. The number of possible bound states depends on both the field intensity and the window radius. In the plot shown (Fig. 29), the minimum window radius allowing 2, 3, 4, or 5 bound states is shown as a function of the electric field strength. As F increases, the particle is repelled from the window interface, and bound states that were stable without an electric field can be destroyed.

Now we can calculate the minimum radii for which bound states still exist (fig. 30). In the figure, different graphs correspond to different interaction forces U, which increases linearly from graph to graph.

Similar graphs can be drawn for particles with the same spin, but, as (91) shows, with delta interaction they will not contribute to each other's potentials and simply occupy different levels of the system of one particle, from Fig.29, for example, the minimum radii for a three-particle state with the same spin, corresponds to the $N = 3$ line in Fig.29.

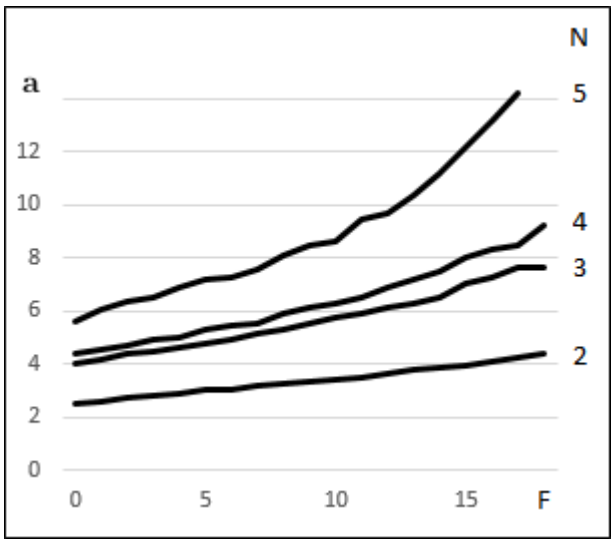

Figure 29 – Plots of minimum radii for which there are still N discrete levels below the essential spectrum, for a single-particle bound state. The graph number, N, corresponds to the number of levels below the main spectrum: 2, 3, 4 and 5

3.3 Classification of coupled states of conductive layers

3.3.1 Constructions

This section presents the results of our article [84]. We continue to study a system of two conductive layers connected through windows in a common boundary. Now, unlike the previous sections, there is no electric field $F = 0$, and attention is focused on the shape of the windows.

We consider the dependence between the shape of the window and the energy levels of the eigenstates of the system, as well as the number of constant-sign domains of the eigenfunctions. In accordance with the obtained energy levels and the shape of the numerically obtained bound states, a classification of these functions is proposed according to the number and location of constant-sign domains. A feature of the selected classes is a stable and unique for each class dependence of the energy level on specific parameters of the hole shape.

We are looking at two types of windows: elliptical windows and Cassini oval windows (peanut shaped) that transition into two separate round windows. We show the dependence of the bound state energy E on the parameter W, which in

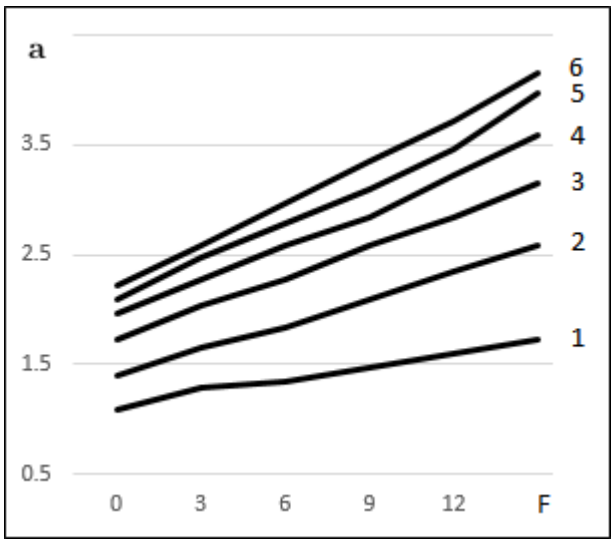

Figure 30 – Boundary radii for which the two-particle (particles have different spins) bound state still exists as a function of F. Different graphs correspond to different strength of interaction between particles U, from 1 to 6 in arbitrary units

the case of Cassini ovals is the distance between the foci of the ovals, and for two holes, the distance between their centers. The ellipses are chosen to match the width of the Cassini ovals. All windows have the same area.

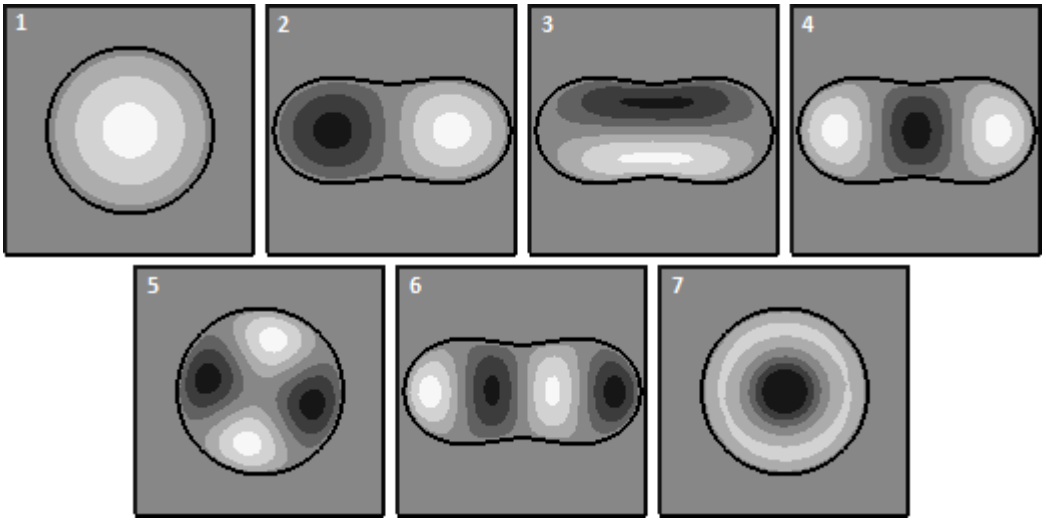

Figure 31 – Examples of types of bound states, as a two-dimensional slice along the plane of the window. Tags: 1-one, 2-two, 3-cross two, 4-three, 5-square four, 6-four in a row, 7-ring.

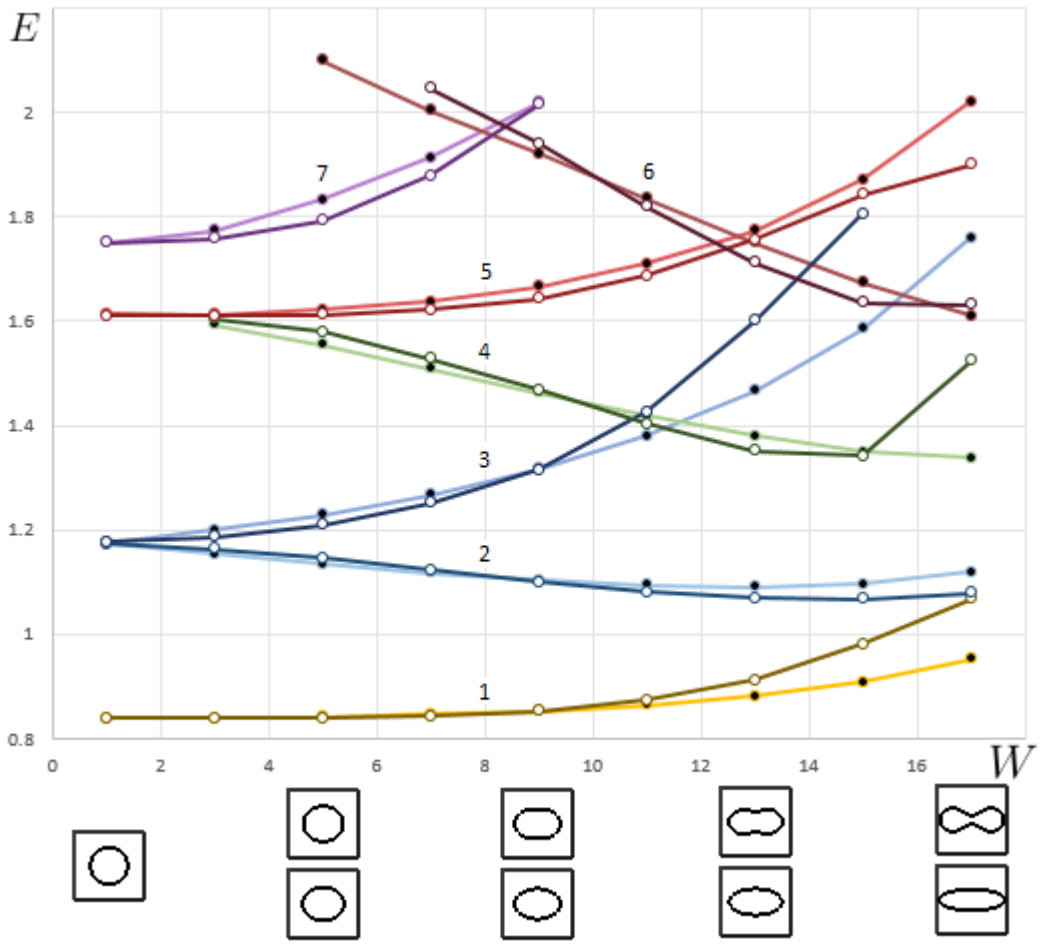

Figure 32 – Energies of various one-particle types of states as a function of the distance between the centers of the Cassini ovals. The dim lines following the main lines represent the energies of states of the same type, but for an elliptical window (the same width as the corresponding elliptical window). All windows have the same area. Types are designated according to the classes shown in fig.31. Window shapes are shown below the W axis.

We first consider the case of a single particle. If we consider a two-dimensional slice of eigenfunctions through the window plane, we can distinguish several stable types of solutions classified by the number and position of nodal domains. Courant's nodal theorem states that for the Dirichlet Laplacian, the number of nodal domains cannot exceed the state index in the list of all states sorted by ascending eigenvalues. In our case, we will stick with the first seven types, which are shown in fig.31. These types of bound states, with a change in the parameter W, exhibit stable behavior, and their energies change differently, depending on the geometry of the type (elliptic or Cassini). The results for the cases of an

elliptical window and a window in the form of Cassini ovals are shown in fig.32.

As we can see, for most types, the energy levels tend in a positive direction with increasing deformation of the round window, but for some types, on the contrary, there is a decrease in the energy level. Let's note some features. The first two states for Cassini ovals converge to the same energy, since the first state turns into a copy of the second, but with both peaks pointing in the same direction. The transverse pair (3) and triple (4) types are most affected by the change in the Cassini ovals at the end (the energy of the transverse pair for the latter type of holes is too high and falls out of the given range), because their constant sign zone is in the center and is deformed by closing gap. With further closing of the "bridge", type (4) will approach type (6), but, in accordance with the Courant theorem, will not exceed it.

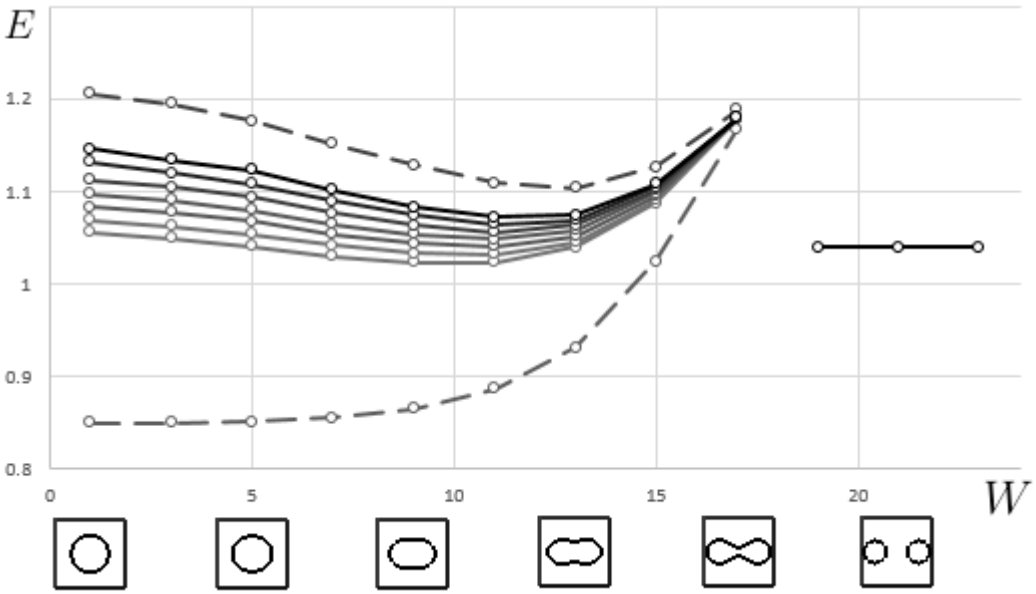

Figure 33 – Energy of the first bound state for the case of two particles. The dotted plots show the first two single particle types for Cassini windows from fig.32, for comparison. (They differ slightly from those shown in the other graph due to the difference in the given calculation accuracy.) The gray lines represent the energies of each particle in the first two-particle bound states, each line corresponding to a different strength of the delta interaction. Powers used: 30, 50, 85, 140, 250, 500, 1000 from the lowest to the highest line respectively. For the case of two separate circular holes, all forces naturally have very close energies plotted on the right side of the graph (the last three points).

For a two-particle system, we consider the Cassini window, and look at the lowest bound state energy level, for various delta interaction forces (see fig.33), and compare it with the first two levels from fig.32. We also extended the window deformation by adding three states with two round windows at the end. For the case of two holes, the different forces have levels that are indistinguishable on our scale. The graph shows that with an increase in the strength of interaction, the joint states of a pair of particles tend from the first to the second type. The energy for two holes is almost independent of the distance between them (recall that the geometry of the system still implies interaction between particles in this last case - in the upper and lower layers, but not in the plane between them).

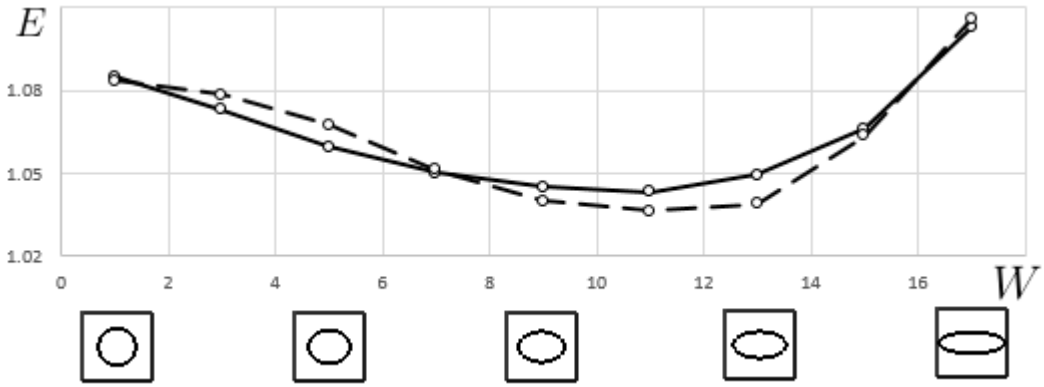

Figure 34 – Comparison of the energies of the bound states of a pair of particles for the elliptical window (solid line) with the corresponding levels for the Cassini window (dashed line).

In Fig.34 we compare the energies of elliptical bound states with the Cassini energies for the same interaction strength. Plots for different interaction forces U between particles, show the same relationships and therefore are omitted.

3.3.2 Conclusions

So, we have considered a quantum system of parallel 3D layers of the same width, connected through one or more windows in a bounded area, with a symmetrical external electric field (Fig.22). For such a system, the stability of the continuous spectrum and the existence of at least one isolated eigenvalue below the essential spectrum were proved for any window size.

Then, numerically, we examined in more detail a number of bound states,

and their specific dependence on the area of the window, various intensities of the external field, and the shape of the window. The results show a monotonic increase in the number of bound states with increasing area or field strength, for a round window. For the case of window shape deformation, bound states form several different types, with stable and predictable behavior.

Further, the study focused on the shape of the window, and a classification of the bound states of the system was obtained according to the number and location of constant-sign domains. The derived classes have a unique response to changes in the shape of the holes, for example, for the types of states in which the zone is located at the center of symmetry of the window, the energy increases sharply when the window is deformed, which reduces the available area around the center of the hole, while the effect of such a deformation on the energies of "even " types is negligible.

The results suggest, as possible directions for further research, the creation of more formal ways of describing the proposed types of bound states and a more rigorous analysis of the dependence of the energy levels of different types on specific window shape parameters.

3.4 Conclusion

In the present work, a number of systems of various geometries with singular interactions were studied. We start with corrugated 2D systems with delta-like interactions caused by purely geometric perturbations. Then we pass to the real two-dimensional delta potential on straight lines, continue with the delta potential on a straight line in three-dimensional space, and, finally, we present a numerical study of three-dimensional layers with delta interaction between particles.

The results of the work are interesting from a mathematical point of view, and contain a set of statements that extend the theory of linear operators. The considered systems are also used as models of a number of physical systems in various fields of physics: in acoustics, nanoelectronics, molecular biology, and so on. We consider the most important characteristic for such models - the spectrum and eigenstates of the system, and hope that the results will become one of the steps in the development of scientific thought in these areas.

References

[1] Vorobiev, A. M. On formal asymptotic expansion of resonance for quantum waveguide with perforated semitransparent barrier [Text] / A.M. Vorobiev, A.S. Bagmutov, A.I. Popov // Nanosys Phys Chem Math. - 2019. - Vol.10(4). - P. 415–419.

[2] Багмутов, А.С. Вольт-амперные характеристики для двух систем квантовых волноводов с присоединенными квантовыми резонаторами [Текст] / А.С. Багмутов, И.Ю. Попов // Научно-технический вестник информационных технологий, механики и оптики - 2016. - Т. 16. - № 4(104). - С. 725-730.

[3] Багмутов, А.С. Спектр лапласиана в области с границей и барьером, составленными из малых резонаторов [Текст] / А.С. Багмутов, И.Ю. Попов // Математическая физика и компьютерное моделирование - 2022. - Т. 25. - № 4. - С. 29-43.

[4] Asymptotic Expansions of Resonances for Waveguides Coupled through Converging Windows [Text] / Трифанова Е.С., Багмутов А.С., Катасонов В.Г., Попов И.Ю. // Челябинский физико-математический журнал [Chelyabinsk Physical and Mathematical Journal] - 2023. - Т. 8. - № 1. - С. 72-82

[5] Trifanova, E.S. Resonator with a Corrugated Boundary: Numerical Results [Text] / E.S. Trifanova, A.S. Bagmutov, I.Yu. Popov // Physics of Particles and Nuclei Letters - 2023, Vol. 20, No. 2, P. 96-99

[6] Courant, R. Methods of Mathematical Physics [Text] / R. Courant, D. Hilbert .- Vol. 1: Wiley-Interscience, New York, 1953.

[7] Arrieta, J.M. Eigenvalue problems for non-smoothly perturbed domains [Text] / J.M. Arrieta, J.K. Hale, Q. Han // J. Differential Equations - 1991. - Vol.91. - P. 24–52.

[8] Sanchez-Palencia, E. Nonhomogeneous Media and Vibration Theory [Text] / E. Sanchez-Palencia - Springer-Verlag, Berlin - New York, 1980.

[9] Cardone, G. Neumann spectral problem in a domain with very corrugated boundary [Text] / Cardone G., Khrabustovskyi A. // J Differential Equations - 2015. - Vol.259(6). - P. 2333–2367.

[10] Popov, I.Yu. A model of a boundary composed of the Helmholtz resonators [Text] / I.Yu. Popov, I. V. Blinova, A. I. Popov. // Complex Var. Elliptic Equ. - 2021. - Vol.66(8). - P. 1256-1263.

[11] Borisov, D. Quantum waveguides with small periodic perturbations: gaps and edges of Brillouin zones [Text] / Borisov D., Pankrashkin K. // J Phys A. - 2013. - Vol.46(18). - P. 235203.

[12] Cardone, G. A gap in the essential spectrum of a cylindrical waveguide with a periodic perturbation of the surface [Text] / Cardone G., Nazarov S., Perugia C. // Math Nachr. - 2010. - Vol.283. - P. 1222–1244.

[13] On boundary value problem with singular inhomogeneity concentrated on the boundary [Text] / Chechkin G. A., Cioranescu D., Damlamian A. et al. // J Math Pures Appl. - 2012. - Vol.98. - P. 115–138.

[14] Hempel, R. The essential spectrum of Neumann Laplacians on some bounded singular domains [Text] / Hempel R, Seco L, Simon B. // J Funct Anal. - 1991. - Vol.102. - P. 448–483.

[15] Pavlov, B.S. Extensions theory and explicitly solvable models [Text] / Pavlov B.S. // Russian Math Surveys. - 1987. - Vol.42(6). - P. 127–168.

[16] Popov, I.Yu. The extension theory and localization of resonances for the domain of trap type [Text] / Popov I.Yu. // Matematicheskii sbornik. - 1990. - Vol.181(10). - P. 1366-1390.

[17] Popov, IYu. The resonator with narrow slit and the model based on the operator extensions theory [Text] / Popov IYu. // J Math Phys. - 1992. - Vol.33(11). - P. 3794–3801.

[18] Popov, I.Yu. The extension theory and resonances for a quantum waveguide [Text] / Popov I.Yu., Popova S.L. // Phys Lett A. - 1993. - Vol.173. - P. 484–488.

[19] Popov, I.Yu. Zero-width slit model and resonances in mesoscopic systems [Text] / Popov I.Yu., Popova S.L. // Europhys Lett. - 1993. - Vol.24(5). - P. 373–377.

[20] Popov, I.Yu. Eigenvalues and bands imbedded in the continuous spectrum for a system of resonators and a waveguide: solvable model [Text] / Popov I.Yu., Popova S.L. // Phys Lett A. - 1996. - Vol.222. - P. 286–290.

[21] Gugel, Yu.V. Hydrotron: creep and slip [Text] / Gugel Yu.V., Popov I.Yu., Popova S.L. // Fluid Dynam Res. - 1996. - Vol.18(4). - P. 199–210.

[22] Melikhova A.S. Spectral problem for solvable model of bent nanopeapod [Text] / Melikhova A.S., Popov I.Y. // Appl Anal. - 2017. - Vol.96(2). - P. 215–224.

[23] Gadyl'shin, R. R. Existence and asymptotics of poles with small imaginary part for the Helmholtz resonator [Text] / R. R. Gadyl'shin // Russian Mathematical Surveys - 1997. - Vol.52(1). - P. 1–72.

[24] А.М.Ильин, Согласование асимптотических разложений решений краевых задач [Текст] / А.М.Ильин - М.: Наука - 1989. 336 с.

[25] Trifanova, E.S. Resonance phenomena in curved quantum waveguides coupled via windows [Text] / E.S. Trifanova // Techn. Phys. Lett. - 2009. - Vol.35(2). - P. 180-182.

[26] Borisov, D. Distant perturbation asymptotics in window-coupled waveguides. I. The nonthreshold case [Text] / D. Borisov, P. Exner. // J. Math. Phys. - 2006. - Vol.47(11). - P. 113502(1-24).

[27] Khrabustovskyi, A. Homogenization of eigenvalue problem for Laplace-Beltrami operator on Riemannian manifold with complicated "bubble-like"microstructure [Text] / A. Khrabustovskyi // Math. Methods Appl. Sci. - 2009. - Vol.32. - P. 2123–2137.

[28] Zangeneh-Nejad, F. Active times for acoustic metamaterials [Text] / Zangeneh-Nejad F., Fleury R. // Rev Phys. - 2019. - Vol.4. - P. 100031.

[29] Mahesh, K. Helmholtz resonator based metamaterials for sound manipulation [Text] / K. Mahesh, R. S. Mini // J. Phys.: Conf. Ser. - 2019. - Vol.1355. - P. 012031.

[30] Acoustic perfect absorbers via Helmholtz resonators with embedded apertures [Text] / S. Huang, X. Fang, X. Wang, et.al. // The Journal of the Acoustical Society of America - 2019. - Vol.145. - P. 254;

[31] McCann, R.C. Highly Accurate Approximations of Green's and Neumann Functions on Rectangular Domains [Text] / R.C. McCann, R.D. Hazlett, D.K. Babu. // Proc. R. Soc. Lond. A - 2001. - Vol.457. - P. 767-772.

[32] Birman, M.S. Spectral theory of self-adjoint operators in Hilbert space [Text] / Birman M.S., Solomyak M.Z. - Dordrecht: D. Reidel Publishing Company - 1986.

[33] Behrndt, J. Elliptic boundary value problems with k-dependent boundary conditions [Text] / Behrndt J. // J Differential Equations. - 2010. - Vol.249. - P. 2663–2687.

[34] Exner, P. Waveguides coupled through a semitransparent barrier: a Birman-Schwinger analysis [Text] / Exner P., Kreicirik D. // Rev. Math. Phys. - 2001. - Vol.13. - P. 307-334.

[35] Behrndt, J. Boundary triples for Schrödinger operators with singular interactions on hypersurface[Text] / Behrndt J., Langer M., Lotoreichik V. // Nanosystems: Phys. Chem. Math. - 2016. - Vol.7(2). - P. 290-302.

[36] Mantile, A. Laplacians with singular perturbations supported on hypersurfaces [Text] / Mantile A., Posilicano A. // Nanosystems: Phys. Chem. Math. - 2016. - Vol.7(2). - P. 315-323.

[37] Exner, P. Asymptotics of the bound state induced by delta-interaction supported on a weakly deformed plane [Text] / Exner P., Kondej S., Lotoreichik V. // J. Math. Phys. - 2018. - Vol.59. - P. 013051.

[38] Approximation of Schroedinger operators with delta-interactions supported on hypersurfaces [Text] / Behrndt J., Exner P., et.al. // Math. Nachr. - 2017. - Vol.290. - P. 12151248.

[39] Popov, I.Yu. The operator extension theory, semitransparent surface and short range potential [Text] / Popov I.Yu. // Math. Proc. Cambridge Phil. Soc. - 1995. - Vol.118. - P. 555-563.

[40] Tikhonov, A.N. Equations of Mathematical Physics [Текст] / Tikhonov A.N., Samarskii A.A. - M.: Science - 1972. - P. 531.

[41] Frolov, S.V. Resonances for laterally coupled quantum waveguides [Text] / Frolov S.V., Popov I.Yu. // J. Math. Phys. - 2000. - Vol.41. - P. 4391-4405.

[42] Gadyl'shin, R.R. Surface potentials and the method of matching asymptotic expansions in the Helmholtz resonator problem [Text] / Gadyl'shin R.R. // Algebra i Analiz, 1992, 4(2), P. 88–115; translation in St. Petersburg Math. J. - 1993. - Vol.4(2). - P. 273-296.

[43] Bagmutov, A.S. Bound states for laplacian perturbed by varying potential supportedby line in R3 [Text] / Bagmutov A.S. // Наносистемы: Физика, химия, математика = Nanosystems: Physics, Chemistry, Mathematics - 2021. - Vol. 12, No. 5. - P. 549-552.

[44] Bagmutov, A.S. Bound states for two delta potentials supported on parallel lines on the plane [Text] / Bagmutov A.S., Popov I.Y. // Physics of Complex Systems - 2022, Vol. 3, No. 1, P. 37-42.

[45] The electron transmission properties in a non-planar system of two chained rings [Text] / Smolkina M.O., Popov I.Y., Bagmutov A.S., Blinova I.V. // Journal of Physics: Conference Series - 2021, - Vol. 2086, No. 1. - P. 012211.

[46] Approximation of Schroedinger operators with delta-interactions supported on hypersurfaces [Text] / Behrndt, J., Exner, P., Holzmann, M., Lotoreichik, V. // Mathematische Nachrichten - 2017. - Vol.290 (8–9). - P. 1215–1248.

[47] Spectral theory for Schroedinger operators with δ-interactions supported on curves in R^3 [Text] / J. Behrndt, R.L. Frank, Ch. Kuhn, V. Lotoreichik, J. Rohleder // Ann. H. Poincar'e - 2017. - Vol.18. - P.1305–1347.

[48] Behrndt, J. Boundary triples for Schrodinger operators with singular interactions on hypersurfaces [Text] / J. Behrndt, M. Langer, V. Lotoreichik, // Nanosystems: Physics, Chemistry, Mathematics - 2016. - Vol.7 (2). - P. 290–302.

[49] Schroedinger operator with singular interactions [Text] / Brasche J., Exner P., Kuperin Yu. A., Seba P. // Journal of Mathematical Analysis and Applications - 1994. - Vol.184 (1). - P. 112–139.

[50] Brasche, J. Spectral analysis and scattering theory for Schrodinger operators with an interaction supported by a regular curve [Text] / Brasche, J., Teta, A. // Ideas and Methods in Quantum and Statistical Physics - 1992. Cambridge: Cambridge University Press. - P. 197–211.

[51] Exner, P. Geometrically induced spectrum in curved leaky wires [Text] / P. Exner, T. Ichinose // Journal of Physics A: Mathematical and General - 2001. - Vol.34 (7). - P. 1439–1450.

[52] Exner, P. Spectral asymptotics of a strong δ' interaction on a planar loop [Text] / P. Exner, M. Jex // Journal of Physics A: Mathematical and Theoretical - 2013. - Vol.46 (34). - P. 345201.

[53] Exner, P. Curvature-induced bound states for a δ interaction supported by a curve in R3 [Text] / P. Exner, S. Kondej // Annales Henri Poincaré - 2002. - Vol.3 (5). - P. 967–981.

[54] Exner, P. Strong-coupling asymptotic expansion for Schroedinger operators with a singular interaction supported by a curve in R3 [Text] / P. Exner, S. Kondej // Reviews in Mathematical Physics - 2004. - Vol.16 (5). - P. 559–582.

[55] Exner, P. Scattering by local deformations of a straight leaky wire [Text] / P. Exner, S. Kondej // Journal of Physics A: Mathematical and General - 2005. - Vol.38 (22). - P. 4865–4874.

[56] Exner, P. Gap asymptotics in a weakly bent leaky quantum wire [Text] / P. Exner, S. Kondej // Journal of Physics A: Mathematical and Theoretical - 2015. - Vol.48 (49). - P. 495301.

[57] Exner, P. Asymptotics of the bound state induced by δ-interaction supported on a weakly deformed plane [Text] / P. Exner, S. Kondej, V. Lotoreichik // Journal of Mathematical Physics - 2018. - Vol.59 (1). - P. 013051.

[58] Exner, P. Strong coupling asymptotics for a singular Schrodinger operator with an interaction supported by an open arc [Text] / P. Exner, K. Pankrashkin // Communications in Partial Differential Equations - 2014. - Vol.39 (2). - P. 193–212.

[59] Exner, P. On the existence of bound states in asymmetric leaky wires [Text] / P. Exner, S. Vugalter // Journal of Mathematical Physics - 2016. - Vol.57 (2). - P. 022104.

[60] Exner, P. Asymptotics of eigenvalues of the Schroedinger operator with a strong delta-interaction on a loop [Text] / P. Exner, K. Yoshitomi // Journal of Geometry and Physics - 2002. - Vol.41 (4). - P. 344–358.

[61] Li, F. Structure, function, and evolution of coronavirus spike proteins [Text] / F. Li // Annual Review of Virology - 2016. - Vol.3. - P. 237–261.

[62] Popov, I. Yu. The helmholtz resonator and the theory of operator extensions in a space with indefinite metric [Text] / I. Yu. Popov // Russian Academy of Sciences. Sbornik Mathematics - 1993. - Vol.75 (2). - P. 285–315.

[63] Popov, I. Yu. The extension theory and the opening in semitransparent surface [Text] / I. Yu. Popov // Journal of Mathematical Physics - 1992. - Vol.33 (5). - P. 1685–1689.

[64] Posilicano, A. A Krein-like formula for singular perturbations of self-adjoint operators and applications [Text] / A. Posilicano // Journal of Functional Analysis - 2001. - Vol.183 (1). - P. 109–147.

[65] Posilicano, A. Boundary triples and weyl functions for singular perturbations of self-adjoint operators [Text] / A. Posilicano // Methods of Functional Analysis and Topology - 2004. - Vol.10 (2). - P. 57–63.

[66] Structure of mouse coronavirus spike protein complexed with receptor reveals mechanism for viral entry [Text] / Shang, J., Wan, Y., Liu, C. et al. // PLOS Pathogens - 2020. - Vol.16 (3). - P. e1008392.

[67] Vorobiev, A. M. Resonance asymptotics for a pair quantum waveguides with common semitransparent perforated wall [Text] / A. M. Vorobiev, E. S. Trifanova, I. Yu. Popov // Nanosystems: Physics, Chemistry, Mathematics - 2020. - Vol.11 (6). - P. 619–627.

[68] Solvable Models in Quantum Mechanics [Text] / S. Albeverio, F. Gesztesy, R. Høegh-Krohn, H. Holden.- Springer, Heidelberg - 1988.

[69] Shondin, Yu. On the semiboundedness of delta-perturbations of the Laplacian on curves with angular points [Text] / Yu. Shondin // Theor. Math. Phys. - 1995. - Vol.105. - P. 1189–1200.

[70] Behrndt, J. Boundary value problems for elliptic partial differentialoperators on bounded domains [Text] / J. Behrndt, M. Langer // J. Funct. Anal. - 2007. - Vol.243. - P. 536–565.

[71] Behrndt, J. Schroedinger operators with δ and δ'-potentials supported on hypersurfaces [Text] / J. Behrndt, M. Langer, V. Lotoreichik // Ann. Henri Poincar'e - 2013. - Vol.14. - P. 385–423.

[72] Exner, P. Leaky quantum graphs: a review [Text] / P. Exner // Analysis on Graphs and its Applications, Proc. Symp. Pure Math. - 2008. - Vol.77. - P. 523–564.

[73] Exner, P. Spectra of soft ring graphs [Text] / P. Exner, M. Tater // Waves Random Media - 2003. - Vol.14. - P. S47-S60.

[74] Exner, P. Hiatus perturbation for a singular Schrödinger operator with an interaction supported by a curve in $\mathbb{R}^3$ [Text] / P. Exner, S. Kondej // J. Math. Phys. - 2008. - Vol.49. - P. 032111.

[75] Exner, P. Strong coupling asymptotics for Schrodinger operators with an interaction supported by an open arc in three dimensions [Text] / P. Exner, S. Kondej // Rep. Math. Phys. - 2016. - Vol.77. - P. 1–17.

[76] Kurylev, Ya. Boundary conditions on curves for the three-dimensional Laplace operator [Text] / Ya. Kurylev // Journal of Soviet Mathematics - 1983. - Vol.22(1). - P. 1072-1082.

[77] Blagovescenskii, A.S. A three-dimensional Laplace operator with a boundary condition on the real line [Text] / A.S.Blagovescenskii, K.K.Lavrent'ev // Vestn.Leningr.Univ., Math. Mekh. Astron. - 1977. No 1. - P. 9-15.

[78] Reed, M. Methods of Modern Mathematical Physics.- Vol. IV. / M. Reed, B. Simon .- Analysis of Operators - Academic Press, New York - 1978.

[79] Pavlov, B. S. Model of diffraction on an infinitely-narrow slit and the theory of extensions [Text] / B. S. Pavlov, I.Y. Popov // Vestnik Leningrad. Univ. Ser. Mat., Mekh., Astr. - 1983. No 4. - P. 36-44.

[80] Transport properties of a biphenyl-based molecular junction system the electrode metal dependence [Text] / H. Kondo, J. Nara, H. Kino, N. Ohno // J. Phys.: Condens. Matter - 2009. - Vol. 21. - P. 064220

[81] Smolkina, M. O. The spin-filtering properties in two coupled Rashba quantum rings [Text] / M. O. Smolkina, I. Y. Popov, I. V. Blinova // Journal of Physics: Conference Series - 2020. - Vol. 1697. - P. 012198

[82] On the discrete spectrum of a quantum waveguide with Neumann windows in presence of exterior field [Text] / Bagmutov A.S., Najar H., Melikhov I.F., Popov I.Y. // Наносистемы: Физика, химия, математика = Nanosystems: Physics, Chemistry, Mathematics - 2022. - Vol. 13, No. 2. - P. 156-164

[83] Numerical analysis of multi-particle states in coupled nano-layers in electric field [Text] / Popov I.Y., Bagmutov A.S., Melikhov I.F., Najar H. // AIP Conference Proceedings - 2020, - Vol. 2293. - P. 360006

[84] Bagmutov, A.S. Window-coupled nanolayers: window shape influence on one-particle and two-particle eigenstates [Text] / A.S. Bagmutov, I.Y. Popov

// Наносистемы: Физика, химия, математика = Nanosystems: Physics, Chemistry, Mathematics - 2020. - Vol. 11, No. 6. - P. 636-641

[85] Bound states in weakly deformed strips and layers [Text] / D. Borisov, P. Exner, R. Gadyl'shin, D. Krejcirik // Annales Henri Poincare - 2001. - Vol.2, No. 3. - P. 553–572.

[86] Bulla, W. Existence of bound states in quantum waveguides under weak conditions [Text] / W. Bulla, W. Renger // Lett. Math. Phys. - 1995. - Vol.35, No.1. - P. 1–12.

[87] Duclos, P. Curvature-induced bound state in quantum waveguides in two and three dimensions [Text] / P. Duclos, P. Exner // Rev. Math. Phys. - 1995. - Vol.7, No. 1. - P. 73–102.

[88] Duclos, P. Curvature-induced resonances in a two-dimensional Dirichlet tube [Text] / P. Duclos, P. Exner, P. Stovicek// Annales Henri Poincare - 1995. - Vol.62, No.1. - P. 81–101.

[89] Chenaud, B. Geometrically induced discrete spectrum in curved tubes [Text] / B. Chenaud, P. Duclos, P. Freitas, D. Krejcirik // Diff. Geom. Appl. - 2005. - Vol.23, No. 2. - P. 95–105.

[90] Exner, P. Bound States in a Locally Deformed Waveguide: The Critical Case [Text] / P. Exner, S. A. Vugalter // Lett. Math. Phys. - 1997. - Vol.39, No. 1. - P. 59–68.

[91] Briet, Ph. Eigenvalue asymptotics in a twisted waveguide [Text] / Ph. Briet, H. Kovarik, G. Raikov, E. Soccorsi // Comm. PDE - 2009. - Vol. 34, No. 8. - P. 818–836.

[92] Ekholm, T. A Hardy inequality in twisted waveguides [Text] / T. Ekholm, H. Kovarik, D. Krejcirik // Arch. Rat. Mech. Anal. - 2008. - Vol.188, No. 2. - P. 245–264.

[93] Borisov, D. Spectrum of the magnetic Schrodinger operator in a waveguide with combined boundary conditions [Text] / D. Borisov, T. Ekholm, H. Kovarik // Annales Henri Poincare - 2005. - Vol.6, No. 2. - P. 327–342.

[94] Ekholm, T. Stability of the magnetic Schrodinger operator in a waveguide [Text] / T. Ekholm, H. Kovarik // Comm. PDE - 2005. - Vol.30, No. 4. - P. 539–565.

[95] Grushin, V. V. On the eigenvalues of finitely perturbed laplace operators in infinite cylindrical domains [Text] / V. V. Grushin // Math. Notes - 2004. - Vol.75, No. 3. - P. 331–340.

[96] Borisov, D. Discrete spectrum of a pair of non-symmetric waveguides coupled by a window [Text] / D. Borisov // Sbornik Mathematics - 2006. - Vol. 197. No. 4. - P. 475-504.

[97] Borisov, D. Distant perturbation asymptotics in window-coupled waveguides. I. The non-threshold case [Text] / D. Borisov, P. Exner // J. Math. Phys. - 2006. - Vol.47, No. 11. - P. 113502-1 – 113502-24.

[98] Borisov, D. Geometric coupling thresholds in a two-dimensional strip [Text] / D. Borisov, P. Exner, R. Gadyl'shin // Journal of Mathematical Physics. - 2002. - Vol.43, No. 12. - P. 6265-6278.

[99] Weakly coupled bound states in quantum waveguides [Text] / W. Bulla, F. Gesztesy, W. Renger, B. Simon // Proc. Amer. Math. Soc. - 1997. - Vol.125, No. 5. - P. 1487-1495.

[100] Bound states and scattering in quantum waveguides coupled laterally through a boundary window [Text] / P. Exner, P.Seba, M. Tater, D. Vanek // J. Math. Phys. - 1996. - Vol.37, No. 10. - P. 4867-4887.

[101] Exner, P. Bound-state asymptotic estimate for window-coupled Dirichlet strips and layers [Text] / P. Exner, S. Vugalter // J. Phys. A. - 1997. - Vol.30, No. 22. - P. 7863-7878.

[102] Gadyl'shin, R. On regular and singular perturbation of acoustic and quantum waveguides [Text] / R. Gadyl'shin // Comptes Rendus Mechanique. - 2004. - Vol.332, No. 8. - P. 647-652.

[103] Popov, I. Yu. Asymptotics of bound states and bands for laterally coupled waveguides and layers [Text] / I. Yu. Popov // J. Math. Phys. - 2002. - Vol. 43, No. 1. - P. 215-234.

[104] Borisov, D. On the spectrum of two quantum layers coupled by a window [Text] / D. Borisov // J. Phys. A: Math. Theor. - 2007. - Vol.40, No. 19. - P. 5045–5066.

[105] Linde, H. Geometrically induced two-particle binding in a waveguide [Text] / H. Linde // J. Phys. A: Math. Gen. - 2006. - Vol.39 (18). - P. 5105-5114.

[106] Popov, S. I. Two interacting particles in deformed nanolayer: discrete spectrum and particle storage [Text] / S. I. Popov, M. I. Gavrilov, and I. Yu. Popov // Phys. Scripta. - 2012. - Vol.86(3). - P. 035003.

[107] Melikhov, I. F. Hartree-Fock approximation for the problem of particle storage in deformed nanolayer [Text] / I. F. Melikhov, I. Yu. Popov // Nanosystems: Physics, Chemistry, Mathematics - 2013. - Vol.4(4). - P. 559-563.

[108] Calogero, F. Comparison between the exact and Hartree solutions of a one-dimensional many-body problem [Text] / F. Calogero, A. Degasperis // Phys. Rev. A - 1975. - Vol.11(1). - P. 265-269.

[109] The Number of Nodal Domains on Quantum Graphs as a Stability Index of Graph Partitions [Text] / Band, R., Berkolaiko, G., Raz, H. et al. // Commun. Math. Phys. - 2012. - Vol.311. - P. 815–838. https://doi.org/10.1007/s00220-011-1384-9

[110] Band, R. Nodal domains on graphs—how to count them and why? In Analysis on graphs and its applications [Text] / R. Band, I. Oren, U. Smilansky // volume 77 of Proc. Sympos. Pure Math., Providence, RI: Amer. Math. Soc. - 2008. - P. 5–27

[111] Helffer, B. On nodal domains in Euclidean balls [Text] / B. Helffer, M. - P. Sundqvist, // Proc. Amer. Math. Soc. - 2016. - Vol.144(11). - P. 4777–4791

[112] Melikhov, I. F. Multi-Particle Bound States in Window-Coupled 2D Quantum Waveguides [Text] / I. F. Melikhov, I. Yu. Popov // Chin. J. Phys. - 2015. - Vol.53. - P. 060802.

[113] Popov, I. Yu. Asymptotics of bound states and bands for laterally coupled three-dimensional waveguides [Text] / I. Yu. Popov // Rep. on Math. Phys. - 2001. - Vol.48(3). - P. 277-288.

[114] Popov, I. Yu. Asymptotics of bound state for laterally coupled waveguides [Text] / I. Yu. Popov // Rep. on Math. Phys. - 1999. - Vol.43(3). - P. 427-437.

[115] Exner, P. A Quantum Pipette [Text] / P. Exner // J. Phys A: Math and General - 1995. - Vol.28, No. 18. - P. 5323-5330.

[116] Najar, H. A quantum waveguide with Aharonov-Bohm Magnetic Field [Text] / H. Najar and M. Raissi // Math. Meth. App. Sci - 2016. - Vol.39, No. 1. - P. 92-103.

[117] Messiah, A., Quantum Mechanics [Text] .- V. 2. / A. Messiah : North Holland Publishing Company, Amsterdam - 1965.